Development of an Innovative Insulation Fire Resistant Façade from the Construction and Demolition Waste

DEFEAT

INTEGRATED/0918/0052

DELIVERABLE D5.1

REPORT ON THE FIRE AND INSULATION DESIGN

Table of Contents

LIST OF FIGURES

LIST OF TABLES

1. PREAMBLE

Our planet is facing crises in form of climate change, i.e., the long-standing moves in weather patterns and temperatures; degradation of natural restricted resources; profuse waste generation; etc., which are the most significant since it directly impacts the global environment, economy, and human health. The most key challenges and pressing crises the world is facing today can be addressed through improved global strategies with the help of technologies. What is more to add, the incidents of catastrophic fires are increasingly common across the globe because they are undeniable part of our future. Although fire is an inherent feature of the Earth system and lots of ecosystems as well as it is an essential part of human civilization for the development of human society. However, deadly fire incidents turned out to be a titanic challenge when it acts as fire disasters constituting a momentous threat and big losses to not only infrastructures and properties but also lots of casualties and even human deaths [1,2]. That means, the role of fire can change very swiftly and can act as a horrifying one. For illustration, it may be tremendously risky at sites, viz., tunnels, sky-scrapping towers, pressure vessels, nuclear reactor plants, gasification and liquation vessels, and storage tanks for flammable fuels, etc. [3]. When during their service lives, the conventional concrete structures enclosing Ordinary Portland Cement (OPC) are being subjected to accidental cataclysmic fires or elevated temperatures, they can withstand up to ordinary fires only and the spalling of the concrete initiate at very higher temperatures finally leading to structural failure.

Thus, the concrete thermal instability is monitored to appear in the initial period of fire exposure which can seriously jeopardize its stability due to mechanical and chemical changes. The damage from ruinous fires can be crucial in concrete structures and, hence, the safeguarding of people and property is highly indispensable. Despite the use of all the measures and technological advancements to prevent fire incidents, there remains a constant risk of a fire breakout. Sorry to list a few incidents of deadly fire incidents such as fire arising from the 9/11 attack on World Trade Centre, U.S.A.; the Windsor tower fire; the fire in Mont Blanc and Channel tunnels, etc., that caused heavy losses of not merely assets but also human lives. In aftermath of cataclysmic fires that took place in different corners of the world during the 20th century, especially in Europe, a great apprehension was experienced by concrete technologists to explore much more competent heat and fire-resistant edifice materials in order to protect the referred failure of structures on account of the setback of conventional

concrete spalling at lofty temperatures. The said spalling of concrete causes a quick layered loss with regard to the cover of concrete, prospectively escorting to the exposure of the core reinforcements within the concrete. For that reason, the resistance to fire is a crucial parameter in Reinforced Concrete (RC) structures which are commonly employed in high-rise towers. The data of preceding research studies on the topic of fire indicate that the OPC-system experiences far-reaching smash up at very high temperatures because of physical and chemical changes causing deterioration with regard to mechanical characteristics [1-4]. As we know, concrete is a heterogeneous building material; therefore, a boost in temperature influences the aggregates and the cement paste as well [5-7]. Furthermore, the behavior of concrete at higher temperatures relies upon its chemistry besides its component characteristics. At high-ceilinged temperatures, the mechanical properties and rigidity of concrete reduce severely ensuing in a loss in strength of the concrete. In particular, these molecular modifications associated with micro-structural stresses pilot to lose the mechanical attributes such as the material's compressive strength. The said deteriorating of the strength is found through the $Ca(OH)_2$-dihydroxylation varying in range from 400°-500°C and a constant Calcium-Silica-Hydrate (C-S-H) – dehydration at 105°C in a matrix of OPC cement-concrete takes place. In fact, the differentiation with respect to heat expansion or contraction among the binder matrix of cement paste and the aggregates of OPC-concrete causes stresses at the interface that leads to cracking which in turn, results in the reduction in the mechanical strengths and stiffness of the concrete. What's more, the thermal gradient of OPC-concrete is accountable for its poor performance when subjected to soaring temperatures. The hydration product of OPC, i.e., calcium hydroxide $(CaOH)_2$, decomposes in the region of 400 °C into calcium oxide (CaO) and water (H_2O). When the temperature goes more than 400°C up, an absolute loss of strength is reported due to this dehydration of calcium hydroxide and rehydration of calcium oxide [6,8]. On exposure at 400–500 °C, the strength loss in the OPC paste is found beyond 50% because of the dehydroxylation of hydroxide and continuous dehydration of calcium silicate hydrate (CSH) starting at 105°C [8]. That means the phase transformations, pore pressure effects and limited thermal conductivity of OPC-concrete are collectively answerable for the strength to get affected adversely at elevated temperatures [5]. This has forced world researchers to search the likelihood of tweaking the chemistry and constituents of concrete. Consequently, the novel researches with regard to the safety of structures against inferno are of paramount significance and vital since it will bring a reduction in losses. For this reason, all concrete structures, especially the liner of tunnels,

must offer enough resistance against fire. The bitter experiences of violent tunnel fires in the last couple of decades have twisted the arm of concrete technologists to concentrate on novel fire-resisting facades to construct such gigantic structures.

The Table 1 [9] gives an idea of the expenditure amount of repairing as well as losses of revenue, and the number of human victims in a few nightmarish incidences of great fires.

Table 1. Statistics of damage and loss caused by tunnel fires in the past [9].

Year	Tunnel	Number of Victims	Repairing Cost (M€)	Loss of Revenue (M€)
1996	Eurotunnel Channel	2 injured	49	203
1999	Mont Blanc	41 deaths	189	203
1999	Tauern	12 deaths	8.5	20
2005	Frejus	2 deaths	2	3

When a severe tunnel fire takes place, there found an express boost in the air temperature within the starting few minutes of fire ensuing in substantial concrete spalling, which ultimately damage the tunnel lining. As a result, the time has come to think for limiting the occurrence of calamitous fires and consequential situations as well as to search for inventive sustainable, durable, fire-resistant concrete to protect structures from failure due to spalling. The buildings are emphasized as one of the chief sectors addressed in the Roadmap to a Resource Efficient Europe elaborated through the EC, i.e., European Commission (2011) [10] and the brand-new European agenda for sustainable development [11].

On the other hand, the generation of diverse plenty of wastes of dissimilar origins is cropping as a new challenge since their landfills are causing pollution threats to environments, soils, and waters and also carrying health hazards. One such waste generated from ongoing construction sites and demolition of old concrete structures, i.e., CDW, is accountable for over 35% of the total waste generation in the European Union. Not only have that, but the European construction sector is also liable for 5–12% of total Greenhouse Gas (GHG) emissions [11] and 42% of energy consumption. More to add, construction sector can save as much as 30% of water in some of the regions [12] and improved material competence can mitigate 80% of these emissions [11]. Truly speaking, the traditional construction sector as conventionally envisaged is one of the least sustainable activities on the earth. Under these circumstances, the development of new-fangled alternative building materials using waste

emerges as a crucial strategy for slimming down the environmental impact and energy as well as Carbon footprint linked to their productions. That's why; the implementation of the circular economy in the construction and infrastructure industries call for the consumption of the Construction and Demolition Waste (CDW) in the world in general and European Union in particular. Moreover, the systematic CDW waste recycling and its organized disposal is equally essential in order to succeed the "Zero waste" concept, etc., to save restricted natural geo-resources and bring down the cost of production. In harmony with the European Commission (2018) data, the CDW reported representing more or less one third (1/3) of the total waste generated in the EU figuring roughly 860 million tonnes of CDW generation in 2014. For this reason, the EU has set an objective of 70% recovery of the CDW, however, the heterogeneous composition of varied materials created a hindrance to touching the goal. The development of higher value-added materials and novel business models from CDW is a challenge to be considered within the short term because a majority of management plants for CDW focusing merely on their physical classification and transformation as a key target to obtain recycled aggregates (RA) for civil engineering works and constructions [13], which is not enough to deal with this titanic quandary. Interestingly, from the scientific point of view based on published different research studies, the most modern route to consume the landfills of these copious wastes of CDW has been found reported in form of their use as precursors for the process of Geopolymerization to produce innovative construction composites. This is possible since the CDW encloses largely (nearly 87%) the remains of minerals (European Commission, 2018) like concrete and ceramic debris, etc., bearing components enclosing silica and alumina and mostly enriched in calcium making it fit to serve the purpose [14-17]. Expectantly, a better future financial feasibility for a potential industrial scaling of these materials is anticipated. As a consequence of urban development, millions of older buildings close to the end of their service lives are being demolished to offer space for newer ones. However, the huge CDW resulting from this demolition work is creating a problem of its management and turning to be a topic of universal debate. Therefore, the generation of CDW is an international concern found nearly everywhere in the world [18, 19]. In the majority of the cases, the CDW is transported to fill open spaces otherwise useful for good causes and forms landfills which are not only costly but also create pollutions and health hazards in a variety of ways [20]. On the most part, the facilities to handle CDW correctly vary considerably in each country and on the whole, restricted to operate with out-of-date methods, namely, direct crushing, road base/sub-base filling, etc. A necessity to develop

pioneering and effective routes to cope up with piles of CDW is looked-for particularly in developing and underdeveloped nations. The most competitive line of attack to get rid of these plentiful wastes is to employ them for the production of novel geopolymeric composites for construction. Also, the earlier accessible literature on the research studies throwing light on the development of Geopolymeric building materials supports the concept of the use of CDW based precursors like CDW-concrete waste, CDW-bricks waste, CDW-tiles waste, CDW-ceramics waste, CDW-glass waste, etc.

Analogously, one more colossal world concern is of rising global temperatures resulting in a gigantic dilemma of earth-heating, i.e. global warming, the swift mitigation in emissions of Green House Gases [GHG], particularly, Carbon Dioxide (CO_2) – a primary GHG, to relieve the earth from heating is the pressing need of the hour. Predominantly, the emission of CO_2 is generating more or less 7% of the total world CO_2 emissions annually as reported from the contemporary Ordinary Portland Cement industry [21-23]. So far construction and infrastructure industry is concerned, Geopolymer concrete technology is attracting more and more engineers and researchers owing not only to display approximately nine-time lower emissions of CO_2 but also for about six-fold lesser operational energy as compared to conventional one [21-23]. That means, eco-constructions are possible with this brand-new technology and it seems that the days of "higher energy and higher temperature reactions" are the talks of the past. This is because the process of production of Geopolymer (GP) products coined as "Geopolymerization" is possible even at as low as room temperature and atmospheric pressure only. On top of those, the end-products ensuing through the application of this novel innovative concept are found with brilliant attributes especially resistances against chemicals, thermal and fire as well as the incorporation of diverse wastes to produce an assortment of construction of Geopolymer composites is possible which also offers a methodical solution to their management. For these central reasons, the world concrete researchers are attracted and working more and more with full concentrations and attention on a variety of Geopolymer composites using this earth-shattering revolution in construction and infrastructure industries to address the above said global predicaments.

Characteristically, the 'Geopolymers' – as the first-named and developed by French material scientist Joseph Davidovits in 1978, are ceramic-like inorganic three-dimensional amorphous alumina-silicate binders, which form covalent bonding [22]. They can be produced through alkali activation of precursors rich in alumina and silica in an alkali medium at low

temperature by means of exothermic reaction kinetics of "Geopolymerization" exhibiting low carbon footprints and lower energy consumption. The dissolution of alumina-silicates occurs in the presence of an alkaline silicate activator that is regulated by poly-condensation and polymerization reactions whereby the setting time varies from one hour to 48 hours, accordingly, they are condensed polymers based upon silicates and aluminates. At the outset, the ensuing structures were classified as sialates, sialate-siloxo and sialate-disiloxo by Davidovits [22]. Geopolymers are not the only user and eco-friendly end-products but also found demonstrating other outstanding properties viz., high early strength; thermal and fire-resistance; strength and mechanical; durability and freeze-thaw conditions; etc. For these reasons, they emerged as the most modern promising green binders with eco-sustainability [24, 25]. A variety of geopolymer construction materials lends a hand to the circular economy of the particular nation since they consume plenty of waste in integration during their production reducing the manufacturing prices. Thus, a methodical solution of copious and various wastes can be achieved through this ground-breaking novel technology otherwise filling the useful land spaces creating contaminations of environments, soils, water supplies and sub-surface waters. As a result, geopolymer building materials are a versatile solution to meet potential structural materials requisites.

Geopolymer building materials are found fit to serve the purpose as fire-resistant material since they do not undergo decomposition of the binder phase on exposure at elevated temperatures as generally met with in the case of OPC-system. This is assigned to their brilliant and exceptional chemical stability. Admirably, the inorganic framework of geopolymers is intrinsically found fire-resistant with extraordinary thermal stability having only minor degradation of gel structure up to 700° to 800°C [26]. It is most worth mentioning the advantage of geopolymers over OPC-system because the OPC-concrete gets deteriorated owing to the dehydration of content of hydrates while the Geopolymers provided evidence of being chiefly chemically stable when undergoing exposure to sky-scrapping temperatures [26-30].

The present study is a part of the research project titled "Development of an Innovative Insulation Fire Resistant Façade from the Construction and Demolition Wastes" (Contract Number: INTEGRATED/0918/0052), funded by the Cyprus Research & Innovation Foundation (RIF) and the European Regional Development Fund. The key objective of this project is to produce an Innovative Insulation Fire-Resistant geopolymer Façade based 100%

upon the CDW, using novel 3D printing technology. This research report includes the preliminary information which would be useful to obtain our potential goal to manufacture the 3D printed CDW based fire-resistant geopolymer façade. In the present research study, geopolymers based entirely on CDW are tested under elevated temperature conditions with a prime focus on properties such as rheology, strength, density, visual appearance and mass loss. Therefore, the present research does not only have a novel approach of the application of CDW-based components to produce geopolymers at elevated temperatures, but also it offers the benefits of sustainable, green material development, together with waste upcycling and decreased call for raw materials, demonstrating trouble-free and quick producibility with plunge in the production cost. The 100% enclosure of CDW-wastes of bricks and wastes of ceramics are employed as precursors and dissimilar alkaline activators such as potassium hydroxide (KOH) and sodium silicate (Na_2SiO_3) are utilized as alkali activators to manufacture CDW-based geopolymers. The authors believe, to the best of their knowledge, that the current research study is quite a new-fangled one in the geopolymeric construction field to investigate primary data to develop purely CDW based fire-resistant geopolymer façade and offers a strong groundwork to carry out potential advance investigations in the future.

2. LITERATURE REVIEW

The past literature on the "Geopolymerisation" reaction kinetics [31, 32] using CDW offers a valuable approach to recycling, which can form a significant step in the direction of CDW waste management. The appropriateness of wastes of CDW-brick and CDW-concrete as source materials for the synthesis of geopolymer cement has already been tested with regard to their mechanical characteristics by Allahverdi and Kani [33] and accounted that the prepared geopolymer specimens are suitable for utilization on an industrial scale. They carried out examinations on the wastes of CDW-concrete and CDW-bricks using geopolymer concrete technology. Further, they reported that paste prepared from CDW-bricks waste exposed to definite curing conditions obtained compressive strength of up to 40 MPa on the 28th day, whereas the case of CDW-concrete waste is not as efficient. One more study by Reig et al. [34] on the manufacturing of geopolymer mortars based on CDW-ceramic waste has examined the strength property. They concluded that the compressive strength is found ranging between 22 and 41 MPa for mortars when cured at 65°C for one week relying upon the sodium (Na) concentration of the alkali activator and ratio of water-to-binder (w/b). On the other hand, Komnitsas et al. [35] developed geopolymers based on CDW-concrete waste, CDW-tile waste and CDW-brick waste using sodium hydroxide (NaOH) and sodium silicate (Na_2SiO_3) solutions as alkali activators. They conducted tests on the compressive strength of these referred geopolymers using varying activator ratios under dissimilar curing conditions and recorded the compressive strength on the 7th day as 13.0, 49.5 and 57.8 MPa, for CDW-concrete waste-based GP, CDW-brick waste-based GP and CDW-tiles waste-based GP, respectively. The use of CDW-fire clay brick waste as a precursor was made by Silva et al. [36] to produce geopolymers by proposing dissimilar conditions of geopolymerization reaction kinetics. The outcomes unveiled that when fitting conditions, i.e., silica modulus of 0.60, Na_2O amounting to 8%, keeping a water-to-binder ratio of 0.27 and oven curing for one week using 65° to 80°C temperature, the compressive strength recorded as 37 MPa. Also, researchers attempted to employ waste glass as a precursor to develop GP composites (Ulugol¨ et al. [31], Xiao et al. [37], Torres-Carrasco and Puertas [38], Cyr et al. [39] and Vafaei and Allahverdi [40]). Also, Robayo-Salazar et al. [41] utilized red clay brick waste, concrete waste and glass waste individually, or as Portland cement-substitution, as precursors for producing GP-materials for the construction and infrastructure industry. Their study revealed that by employing the CDW-based wastes as constituents resulted to acceptable

Ευρωπαϊκή Ένωση
Ευρωπαϊκό Ταμείο
Περιφερειακής Ανάπτυξης

Κυπριακή Δημοκρατία

Διαρθρωτικά Ταμεία
της Ευρωπαϊκής Ένωσης στην Κύπρο

mechanical attributes. Quite recently, an article is discussed well about GP-systems produced consuming ingredients of CDW as precursors single-handedly or in grouping with conventional mineral admixtures [42]. All the above referred recent research studies convinced that CDW are quite successful precursors for geopolymerization and hence, the wastes from CDW can be used for GP-production successfully. However, still, this concept necessitates further attention to advanced researches in order to have comprehensive data on the development of novel innovative CDW-based geopolymer systems.

Numerous investigations have been conducted on the studies of durability and mechanical characteristics of geopolymers, especially considering the influence of very high temperatures, but they mostly carried upon dissimilar geopolymers, synthesized with diverse kinds of precursors and activators. For illustration, the combinations used were of fly ash and Na-activators or fly ash and sodium plus potassium activators or fly ash together with slag and Na-activator or metakaolin and mixed Na plus K containing activators, etc. [43-50]. However, the class F type fly ash is giftedly abundant in alumina, as well as silica, having an inferior quantity of low oxide of calcium permits its superior stability at a lofty temperature in the cases of fire than others amongst all the above-referred precursors. Not merely have that, it is cost-effective with ease of access as compared to other raw materials. It was revealed that geopolymers based on fly ash underwent little damage, on comparing to their metakaolin counterparts, because of contained huge quantities of interconnected pores that permitted moisture to flee on elevated temperature exposure [44]. In the event of geopolymers based on metakaolin, thermal shrinkage, as well as phase stability with high ceiling temperatures, are affected in the choice of the alkaline cation either Na, K or a combination of both for geopolymer mixture [28]. The referred inorganic nature indicates its utilization in thermal applications like fire-resistant products [51-53]. This fire-resistant potential of geopolymers is the key property of geopolymeric composites particularly of fly ash based is highly significant. The researches have been conducted to develop Geopolymeric materials as heat resistant [54-58], cement and concrete, escorting to facilitate their applications as fire-proof panels, refractory materials for lower temperature [59], tooling for the foundries, as thermal insulators [60-68], thermal energy storing GPCs, as in aeroplanes as well as ships [69], etc. Commonly, Gradual heating levels and prolonged periods at temperature are imposed on the refractory products, whilst fire resistance is intended to experience rapid initial temperature acceleration for a relatively short time. The applications of geopolymer concrete as fire-resistant building material necessitate examining

its thermal performances at a micro, i.e., micro-structural or chemical stability, meso, as well as macro-scales of the material when exposed to an elevated temperature. Subsequent to the fire breaking out, the cooling cycle must essentially be quick on account of vast amounts of water trying to extinguish it or a sluggish reduction if the fire is permitted to be put out owing to fuel exhaustion. Since the geopolymers possess enhanced pore volume connectivity in comparison with OPC, they remarkably boost the transportation of water from the binder with accompanied mitigated spalling through higher temperature exposure. Generally speaking, the diverse Geopolymer concretes synthesized with various source materials and activators are exhibiting exceptional resistance against fire and thermal at elevated temperature, however, they should be re-viewed systematically for this excellence in order to make them viable and acceptable for such kind of infrastructures and constructions whereby the risk of fire incidences and towering thermal impacts are likely to crop up.

The bulk of related studies has thrown light on the residual compressive strength of geopolymers following the very high temperatures exposure ranging from 600° to 800°C. There exist copious of research works were conducted concerning geopolymer composites through employing diverse raw materials such as metakaolin, rice husk ash, blast furnace slag, fly ash and amalgamation of diverse source materials at a higher temperature. The alumina silicate polymer has demonstrated the higher intrinsic thermal resistance however the loss in strength on exposure at higher temperatures relies upon a variety of factors. The chief factors influencing the residual strength of geopolymers are the kinds of source material and alkali cation present in activators, diverse content of calcium enclosing raw materials, temperatures for curing and the ratio of activator/binders [70]. While the interstitial water in geopolymeric frameworks is exposed to high-temperature applications such as 350-400°C, could cause stress, thereby cracks propagates and eventually trim down the strength. For that reason, one of the solutions to mitigate cracks and enhance thermal attributes is to prepare the sans pore in the geopolymer matrix, which in turn, extend higher mechanical strength [71-73]. The strength impacting mechanisms at high temperatures have been investigated in the context of the effects of pore pressure, as well as phase transformations. The residual compressive strength of geopolymers was monitored to be greater than the initial compressive strength when examined prior to the exposure of thermal.

Nevertheless, the supplement of aggregates mitigated the compressive strength of geopolymer concrete subsequent to exposure at 800°C [74]. This is assigned to the fact that

the compressive strength performance is affected by thermal incompatibility besides chemical changes and pore pressure. This thermal incompatibility takes place at higher temperatures due to the heterogeneous distribution of temperature and the variations in the coefficient of multiphase materials for thermal expansion of the components. Concerning multiphase material, whilst the inconsistent thermal distortion obtained from the non-uniform distortion amongst components of the phase cannot be maintained through the sample, degradation of strength is found to take place because of the commencement and propagation of cracks. The impact of thermal discordancy on compressive strength is affected by the degree to which samples could be deformed with no development of fracture, that is, the ductility or decreased brittleness of the material.

Also, preceding works have demonstrated that geopolymers exhibit exceptional thermal steadiness at the microscale [75]. The resistance capability of material against change in volume and crack development due to thermal effect as well as to keep hold of its compressive strength even at towering temperatures are the meso- and macro-scale thermal stability, correspondingly. An earlier investigation on the influence of soaring temperature on weight loss, thermal shrinkage, and chemistry of metakaolin based geopolymers was carried out. Furthermore, Bernal et al. [75] have examined the influence of temperature on compressive strength of geopolymers based on metakaolin plus Ground Granulated Blast Furnace Slag (GGBS), but the investigations were made by using merely a single Si/Al molar ratio. The earlier research works pilots to understand that Si/Al ratio influences greatly not merely the microstructure but also the mechanical attributes of the geopolymer manufactured at ambient temperature [76, 77]. Therefore, the factor of Si/Al molar ratio is possibly to impact crucially the presentation of mechanical and micro-structure types of geopolymeric materials as well when exposed to greater temperatures. Also, the past researches to figure out the thermo-chemistry and thermal properties had thought out geopolymers based on fly ash with a target for ratios of amorphous Si/Al of higher than two. The amorphous content present in fly ash, Si/Al ratio commanded the response to exposure of thermal, with elevated ratios providing enhanced response when subjected up to 1000 temperature. The application of a lower ratio of Si/Al to manufacture geopolymers for increased resistance against thermal is evaluated. A past study was performed by Kong et al. [70] exploring the impacts of several factors like temperature of calcination of kaolin, as well as ratios of activator/metakaolin and Si/Al on compressive strength, i.e., macro-scale; of geopolymers synthesized with metakaolin on subjecting to very high temperatures. Hitherto, the basic

mechanisms controlling the compressive strength performance at the macro-scale are not comprehended. Rickard et al. [44] had tested five dissimilar fly ashes based geopolymers at targeted ratios of Si/Al for 2.0, 2.5 and 3.0 and revealed that diminishing the quantity of aluminate or silicate supplemented through the activator solutions provided strength enhancements or retaining subsequent to the exposure of thermal. Geopolymer with lower Si/Al ratio amorphous fly ash exhibited brilliant early compressive strength, which diminished swiftly following thermal exposure. The thermo-explosion or degradation of material over a controlled temperature system by the thermo-analytical technique of dilatometry for measurement of geopolymerically synthesized materials with this fly ash showed immense expansion events which, due to unreacted residue silicate materials, were assigned to the expansion. The application of filler materials considered thermally stable is commonly found placed in other materials technology for minimizing thermal shrinkage or expansion, e.g., the adding up of inorganic type fillers is well-known to alter the attributes for thermal extension of polymers of organic nature. Several researchers have assessed the influence of the supplement of fillers and aggregates on the thermal characteristics of geopolymer. The totaling of granite and quartz aggregates to geopolymer mortars produced with metakaolin whereby the addition of 20 wt.% aggregate to the said mortar had mitigated the shrinkage by almost 50% in the range of 23 to 500 [78] have studied. More decline in the context of shrinkage was attained by escalating the quantity of aggregate to 40 wt.%. A supplement of up to 30 wt.% of alumina to metakaolin based geopolymers produced by using potassium silicate as an activator [79]. The measurement of thermal volume shrinkage of samples after being subjected to higher temperature have also been taken by them and they monitored momentous mitigations concerning shrinkage figures beyond 20 wt.% additions of alumina. In particular, this was recorded above 800 , escorting to conclude that the existence of alumina was valuable for dropping thermal shrinkage and accelerates the crystallization at a set temperature, as well as the extent of crystallization fillers, together with Al plus K containing geopolymer based on metakaolin. The inorganic type fillers were found absent in the micro-structure, maybe owing to either a geopolymer gel coating or the particles of filler reacting in the geopolymerisation kinetics, making them indistinguishable [80]. Metakaolin based geopolymers were activated with potassium-containing activators which were filled with alumina or fine quartz to estimate the thermal characteristics of the blends. The best possible shrinkage of the controlled geopolymer was found was 17% at 1000 which was reduced to 12% and 13% by the adding up of the alumina and quartz respectively. Naturally

occurring mineral fibres of wollastonite are used to reinforce metakaolin-geopolymer [81]. Its stiffness was found to augment as a volume of fibre, accelerated to 5 vol.% of wollastonite is well-matched with the higher level of pH used in the formation of geopolymer paste [81]. Accordingly, fillers such as wollastonite and alumina, which are thermally stable, can be incorporated with the geopolymeric mixture to enhance the resistance against thermal, through minimizing shrinkage throughout the heating process. The factors influencing the resistance against thermal of geopolymer based on metakaolin as confirmed through dilatometric technique are the alkaline cation employed and the molar ratio for Si/Al. Duxson et al. [26] have analyzed several geopolymer formations through dilatometry contrary to thermal, with diverse alkaline cations, as well as molar ratios for Si/Al. In this case, four diverse steps are met with like, firstly, the enclosed water in the micro-pores evaporates up to 100°C without causing shrinkage. Secondly, free water is removed over 200°C, in the third step, a degree of restructuring takes place between 300°-600°C, while the fourth step involves the appearance of a significant shrinkage owing to the viscous flow monitored beyond 600°C. Particularly, the ratio of Si/Al molar ratio is answerable for the appearance of viscous flow; especially, superior is the ratio of Si/Al, the more is the enhance in the quantity of the viscous flow. The same phenomenon was also observed by other studies in the thermal resistance analysis carried out on metakaolin based geopolymers synthesized with potassium or sodium-containing activators [82, 83]. Similarly, also witnessed similar mechanisms on formations of fly ash-based geopolymers. The accumulation of reinforcements in geopolymer mixes enhances mechanical characteristics and resistance against thermal at high temperatures. Basalt, glass as well as carbon type fibers can be incorporated into the geopolymers to provide fire-resistant materials. The dissimilar specimens up-held 50% of the value of flexural strength subsequent to a thermal exposure period of 600°C for 1 hour and 1000°C for the glass, carbon and basalt fibers. A good quality adhesion has been reported among the matrix of the geopolymer, as well as the pre- and post- the thermal exposure of fibers at 600°C temperature. The viscous flow appearance alters the behavior of geopolymer and the observance among the matrix, as well as fibers relies upon the different dilatometric coefficients, while the temperature attains 1000°C. Accordingly, the mechanical characteristics and resistance against geopolymers elevated heat can be enhanced through the adding up of reinforcements in the matrix. The basalt and carbon fibers had the best outcome. For the most part, the shrinkage of geopolymer is estimated during the action of the heat at 1000°C [26]. Merely few illustrations for the research on the shrinkage performance of the

geopolymers at a lower temperature is found. The drying shrinkage property of geopolymer concrete is found with declining when slag content augments and sodium silicate to sodium hydroxide ratio trims down. What is more, the hydration sphere, total cation and stability of aluminium species are stated to be key factors affecting the sensitivity of geopolymers with a metakaolin dependent ambient temperature drying shrinkage. The supplement of a minute quantity of up to 1.6% ammonium molybdate slims down of shrinkage at higher temperatures [84]. Geopolymers manufactured by sand do not found pursue the predictable tendency concerning shrinkage, as well as a supplement of around 10% sand does not allow the disintegration of specimens upon when subjected to thermal action at 110°C [85]. Sprinkling, pouring as well as extrusion are the key techniques for the shaping of ceramic materials that involve employing slurries that diverge as to the viscosity of slurry, necessitated to perform the shaping course of action. In the context of the spraying method, the viscosity of the mixture has to be lower; accordingly, allowing the alteration in the little drops, as well as a spray gun is required for the deposition process. Whereas in the case of the extrusion method, the screw forces to the slurry with the help of dye and the material ought to be viscous sufficient to safeguard its shape. These techniques engrossed dissimilar values of viscosity that are scarcely appropriate for geopolymer manufacturing. The technique of pouring could be employed even for higher viscosity. Nevertheless, the eloquence of the mix must be higher, adequate to fill up the voids of the moulds. Geopolymers exhibit modifications in the context of viscosity by the setting kinetics. Therefore, shaping by the technique of pouring is most likely the most apposite process for geopolymers. On the other hand, Duan et al. [86] have delved into durability and microstructural attributes of metakaolin and fly ash-based geopolymer and summed up that the said materials displayed superior durability and denser microstructure in comparison with OPC counterparts on subjecting them to soaring temperatures. A drop concerning mechanical attributes of diverse formations following the thermal process at 200°C, irrespective of the kinds of fibers employed as strengthening materials like carbon, basalt as well as glass monitored [87]. Geopolymers, when freshly manufactured are in form of liquid with poles apart viscosity values; for this reason, it is necessary to employ shaping techniques alike ceramic solutions and suspensions. Ranjbar et al. [45] have concentrated on the study of the impacts and adaptability of POFA as a substitution material in geopolymer mortar prepared with fly ash. Their findings piloted them to achieve early high compressive strength in the context of geopolymer prepared with fly ash, in comparison with POFA incorporated geopolymer. Sarker et al. [88] have

experimented on the towering temperature effect of exposure of fly ash-based GPC and its OPC-counterpart up to 1000°C and their findings concluded that GPC samples were observed to undergo lesser damage than the counterpart samples of OPC concrete subsequent to elevated temperature exposure. Passive fire protection (PFP) is a measure to safeguard structures and industrial paraphernalia against fortuitous incidences of fire. The materials which are competent enough for fireproofing stay away from sudden heating of the structures and mitigate the deterioration of the mechanical attributes of the structural parts [89]. Nowadays, a trend to apply cementitious aggregates mixed with light inorganic elements possessing appropriate thermal characteristics, viz., vermiculite, are usually employed for the thermal insulation of fixed installations [90]. Quite recently, based on a small number of considerations, PFP-systems had emerged out as possible utilizations of geopolymers for elevated thermal resistance due to their intrinsic structure having inorganic nature [91], absence of ignition or discharge of smoke even subsequent to ex-tended heat flux exposure, and high-quality fortification during rigorous fire resistance examinations. What's more, the diversity of parameters entailed in the geopolymerization such as precursors, activator solutions and conditions for curing permits for the couture of the attributes of the mixture to fireproofing uses. Novel components viz., perlite or hydrogen peroxide can be supplemented to trim down material's thermal conductivity ahead. The impacts of time of exposure and cooling rates on the residual compressive strength of the concrete after exposure [92, 93]. The time for exposure of one to two hours was found sufficient for the temperature to break through the cubic specimens and grounds for the majority of the loss with regard to compressive strength. The influence of elevated temperature mitigated the time necessitated to cause strength losses, which is linked to the augment of thermal conductivity at lofty temperatures. Subsequent to the exposure for one hour, 80%, 70%, 60%, 30% for 200 , 400°C, 600°C and 800°C the residual strength was found respectively. Cooling rates and rates for heating have displayed no impact on the concrete's residual compressive strength when subjected to 600°C and ahead of, excluding little influences at inferior temperatures, probably on account of the building up of pore-pressure. Also, the impacts of diverse cooling rates on concrete were experimented by Khoury [94]. The shrinkage or cooling strain was depending on the interaction among aggregate and cement developing cracks and was not associated with age of concrete, early presence of moisture or rate of heating. Moreover, the influence of elevated temperature strain rate and heat on the residual compressive strength of blended concrete enclosing silica fumes plus fly ash [95]. The noteworthy loss concerning

strength was recorded after 400   temperature. In addition, Kong and Sanjayan [96] have accounted for a 25% drop in the context of compressive strength of the cubic specimen of metakaolin incorporating geopolymer paste following the exposure at 800   for 10 minutes. A standard and elevated strength concrete with pozzolans. Metakaolin based concrete had been found with enhanced strength till 200°C temperature exposure and upheld superior strengths till 400°C than concrete with fly ash, silica fume incorporating concrete and usual conventional OPC concrete. Following 400°C, the higher strength concretes swiftly get deteriorated. The concrete-based on metakaolin had demonstrated the minimum ultimate residual strength in spite of exhibiting improved initial strength gain, signaling that it is, in particular, vulnerable to a definite higher range of temperature. The disparities in the concrete performance containing pozzolanic materials at elevated temperature exposure are widespread. The good stability and higher initial strength gains among 200 - 400°C followed by express deterioration and lower ultimate compressive strength than reference concrete is generally accounted [97, 98]. Ductility is notably influenced the residual compressive resistance of geopolymer mortars following the exposure at 800°C [99]. Following the middle-of-the-road literature published to date, the said materials achieve their crucial point at around 600° to 800°C. The dimensional stability of the materials is seriously influenced gravelly and bending strength is also significantly get affected in this temperature range, whereas the compressive strength was found enhanced. The referred impact is assigned to the partial sintering which occurred at those range of heating or somewhat at elevated temperatures. In accordance with the proposal of Khoury [100], the disassociation of $Ca(OH)_2$ at a temperature of 300-400°C, as well as gigantic and abrupt creep, are more often than not the root cause of failure at 600°C, at 700°C dissociation of $CaCO_3$, ceramic binding as well as absolute water losses at 800°C along with melting point at 1200°C to 1350°C. Wang et al. [101] have monitored the temperature of 900°C as an imperative transition temperature concerning metakaolin incorporating geopolymers, whereby the geopolymer partly melts and coagulates in the vicinity. Still, significant interspaces were found present at 900°C temperature which distinct the melted structures. Several researchers have tested the thermal attributes of fly ash-based geopolymer subjected to uniform heating regimes through a furnace. The striking thermal characteristics of geopolymers have put forward their appropriateness to employ them in fireproofing applications whereby the prerequisite for the material would be to withstand against fluctuating temperature heating with superior heat rates. The past studies have thrown lights on the geopolymer manufactured with diverse

source materials viz., metakaolin, rice husk ash, blast furnace slag, fly ash, etc. at lofty temperature range [102]. Even though inorganic alumino-silicate geopolymers integrally exhibit the higher resistance against thermal, the strength loss is found to occur at towering temperatures relying on a variety of factors like nature of precursor, alkali activator solution as well as interstitial water present in the structures of geopolymers and its evaporation when subjected to higher temperatures of 350° to 400°C, that could create stress thereby resulting in the initiation of cracks eventually escorting to the strength loss. Consequently, one of the solutions to minimize the development of cracks and enhance the thermal attributes is to manufacture the sans pore geopolymer mixture, which will extend improved mechanical strength. The fly ash-based geopolymers have demonstrated better fire resistance in comparison with fly ash mixed with supplementary materials. Zhang et al., [103] have accounted that during thermal exposure of geopolymer based on fly ash as well as metakaolin at towering temperature, the degradation concerning bending as well as tensile strength was found advanced, but it was observed inferior concerning bonding and compressive strength in comparison with OPC-system. This kind of analysis published outcomes and demonstrating excellent resistance against thermal, sustainable mechanical performance, etc. are the core reasons why the geopolymer with fly ash has drawn further attention amid researchers [104]. Fan et al. [105] have studied the thermo-mechanical attributes and micro-structure modifications previous to and following the heating process as well as the cooling process of geopolymers based on fly ash at 500°C and 800°C under dissimilar reaction kinetics situations. On the other hand, Duan et al. [86] have examined the microstructure and durability of metakaolin as well as geopolymer with fly ash and determined that geopolymer represents superior durability attributes and has denser microstructure to OPC system, while subjected to not only very high temperatures but also under the chemical environment of the aggressive type. Demirel et al. [106] have revealed the influence of lofty temperature on mechanical characteristics of concrete manufactured with silica fume and finely ground pumice. The outcomes have displayed that the addition of the mineral materials to concrete had diminished both, i.e., compressive strength as well as unit weight. Not merely have that, escalating the temperature beyond 600°C has influenced the compressive strength on account of losses in concrete samples weight was more boosted for concrete mixes having both silica fume and fly ash. Duan et al. [86] have investigated the impact of silica fume (0-30%) substitution on thermal resistance examinations of geopolymer paste with fly ash and monitored that the compressive performance is escalating with the addition of silica fume.

Sarker et al. [88] have experimented at an elevated temperature at 1000°C in the case of both, geopolymer based on fly ash and counterpart OPC-concrete. They monitored that the former has suffered lesser damage than the specimens of the OPC system. Table 2 indicating the previous literature on the impact of fire on geopolymers.

Table 2. Previous literature on the impact of fire on geopolymers.

Reference	Observations
Zhang et al. [103]	The geopolymer mortar manifests higher bending and tensile strength temperature degradation than OPC mortar, but inferior degradation in compressive and bond strength.
Hosan et al. [107]	The compressive strength is significantly improved with the $Na_2SiO_3/NaOH$ ratio 3, where the residual compressive resistance is raised to 600°C.
Duan et al. [108]	The compressive resistance of geopolymers diminished during thermal cycles. The losses in mass and compressive strength amplified with a temperature rise.
Zhang et al. [109]	The geopolymer samples prepared with metakaolin and fly ash display analogous bending and compressive performance, both at ambient temperatures and after exposure to high temperatures as for OPC specimens. In practical building applications, geopolymers based on metakaolin and fly ash, therefore, deliver a viable alternative to traditional OPC.
Lahoti et al [110]	The geopolymer with potassium was substantially amended (30%–40%) as well as the geopolymer made with sodium was declined (10%) and after exposure to elevated temperatures, the strength of mixed sodium and potassium geopolymer remained unaffected.
Kong and Sanjayan [48]	The research designates the two major features for geopolymer activity at a high temperature (800°C) i.e. specimen and aggregate sizes. The size of aggregates greater than 10 mm leads to healthier strength at low and high temperatures. The thermal instability between the geopolymer matrix and aggregates is the outcome of a heavy loss of geopolymer concrete at elevated temperatures.
Samal [111]	The geopolymers had a significant effect on thermal shrinkage decline as Si / Al ratios amplified due to trim down in porosity during the process of dehydroxylation as well as sintering.
Sarker et al. [88]	Following the fire exposures, less harm was observed to the geopolymer concrete samples as regards cracking than to the OPC concrete specimens. There was considerable spalling in the concrete cylinders of the OPC for exposures between 800 and 1000 though geopolymer concrete samples were not spalled. In particular, the samples of geopolymer concrete maintained higher strength than the specimens of OPC.
Pan et al. [112]	The strength of geopolymer was up by 192% at 550°C in contrast to the original strength value, while the strength of OPC pastes changed slightly. The percentage residual strength of both geopolymer and OPC concrete after exposure to 550 ° C was nevertheless close.
Lahoti et al. [113]	Upon high-temperature exposure to 900°C, all the geopolymer specimens experienced reduced compressive strength. While the geopolymer mixes disclosed strong chemical stability on a microscale, their volumes at mesoscale were poorly stable and thermal shrinking was extremely high.
Mathew and Joseph [114]	At ambient temperature, the deformation attributes of geopolymer concrete beams are identical to those of reinforced cement beams. The strain compatibility method, therefore, underestimates the deformation behaviour of strengthened geopolymer concrete beams when exposed to high temperatures.
Kljajević et al. [115]	Cross-linking of polymer changes in geopolymer samples at 600°C reduces the number of bonding of Si-O-Na. Thermal action at 900°C declines oxygen and articulated sodium significantly, following major morphological changes, i.e. the creation of a complex pore structure.
Sivasakthi et al. [116]	The geopolymer paste and mortar's linear dimensional stability remnants unchanged until 800°C. 10% of the addition of micro silica has a more filling effect, thus growing compressive strength by damaging

Reference	Observations
	the integrity of the bulk specimen of geopolymer composites.
Luhar et al. [21]	The rubberized geopolymer concrete, loss of strength at elevated temperatures is only somewhat more than the control geopolymer concrete, due to the possible inconsistencies of the integral materials coefficients of thermal expansion.

3. MATERIALS CHARACTERIZATIONS AND EXPERIMENTAL METHODS

The precursors derived from wastes of CDW-bricks and wastes of CDW-ceramic tiles are employed for manufacturing the geopolymers. The CDW materials are provided by the industrial partner PA2 of the project, i.e. *Resource Recovery Cyprus (RRC),* which is a key local player in the collection, separation and management of CDW. Subsequently, the CDW is loaded separately into a crusher that applied the primary crushing to slim down the size. After the crushing process, the oxide compositions are represented in Table 3, while the distributions of particle size are depicted in Figures 1 and 2. The elemental and oxide analysis results of precursors are verified by means of X-Ray Fluorescence (XRF) analysis, as well as laser diffraction technique, correspondingly (Figures 3 and 4). The XRD analysis is shown in Figures 5 and 6. Previous to ultimate milling, it is assumed that different CDW precursors would have less than 150-micron sizes. The combination of sodium silicate (Na_2SiO_3) plus potassium hydroxide (KOH) is employed similarly in all the mixes as, 1.6:1.0 for alkali activation of CDW precursors. The selection was based on preliminary trials. The KOH-potassium hydroxide and Na_2SiO_3 - sodium silicate, used here are in pellet form and as solution, correspondingly.
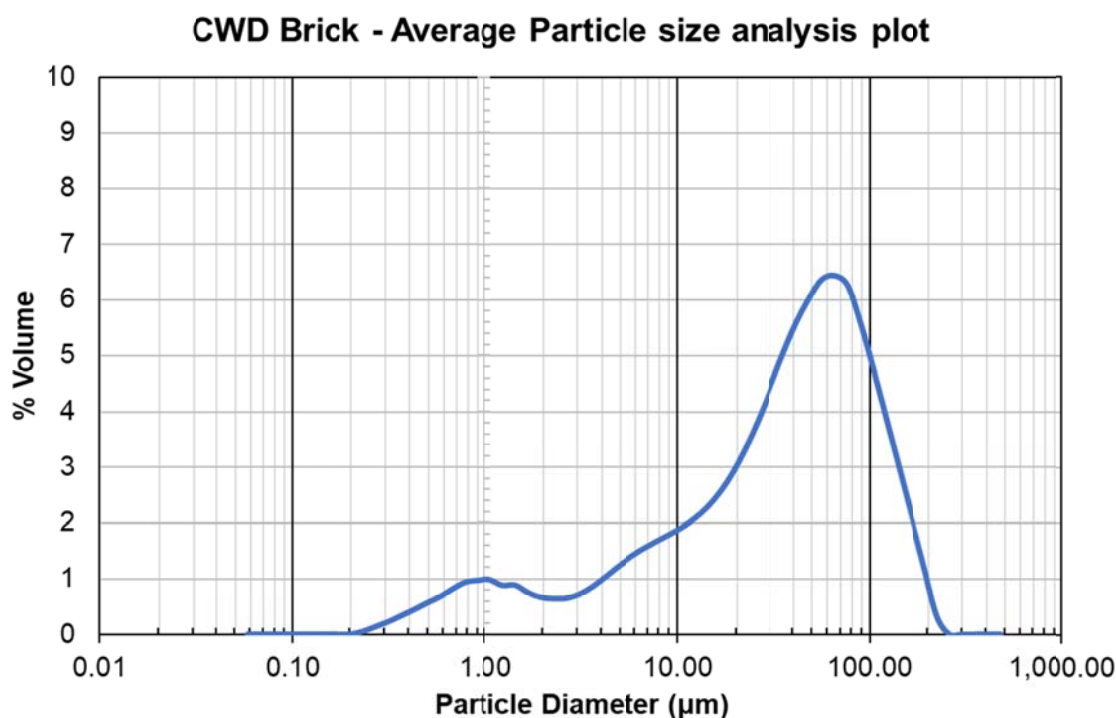

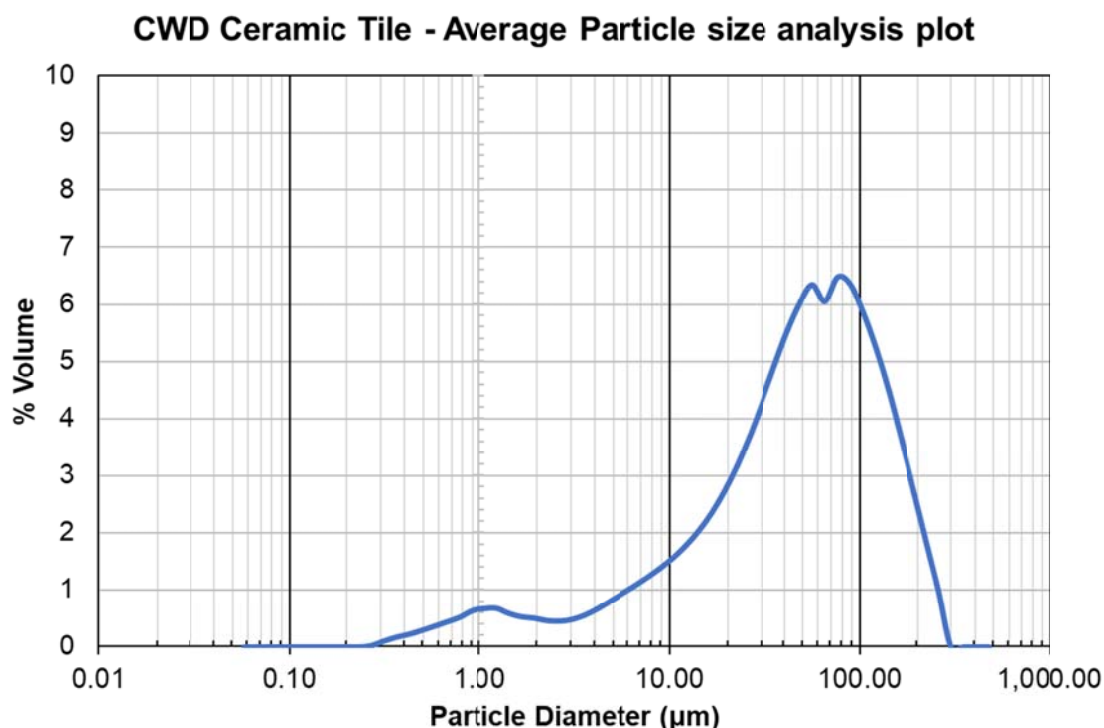**Figure 1**. Particle size analysis of waste brick material.

Figure 2. Particle size analysis of waste tile material.

Figures 1 and 2 show the particle size analyses and distributions for the examined CDW materials. In the predominant measurement runs, it was monitored that the percentage volume of the samples reached its peak value more or less within the range of 60-80 microns. A slight increase of volume at 1-micron size occurred followed by a 0.5% volume reduction at the regime between 2 and 3 microns. Past the peak, the volume fraction was thereon decreased in the samples reaching zero at around 200-300 microns. The particular pattern was evident in almost all investigated CDW incorporated samples, i.e. waste of CDW-bricks and wastes of CDW-ceramic tiles. This was assigned to the consistent and identical sieving technique that was applied to all samples, which was utilised for the purposes of reproducibility, consistency, repeatability and validity in the sample examinations. It should be noted that the specific particle size analysis technique provides useful regimes of volume distributions across a range of diameters for the as-received samples, however, it is not possible to ascertain any information on the physical and chemical as well as mineralogical composition of the materials through the specific analysis.
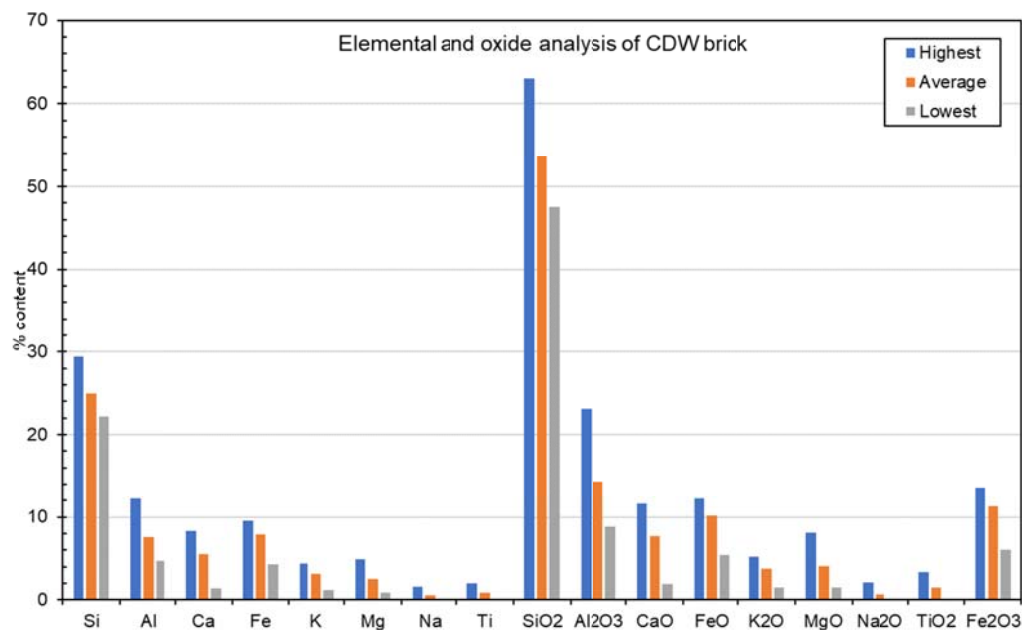
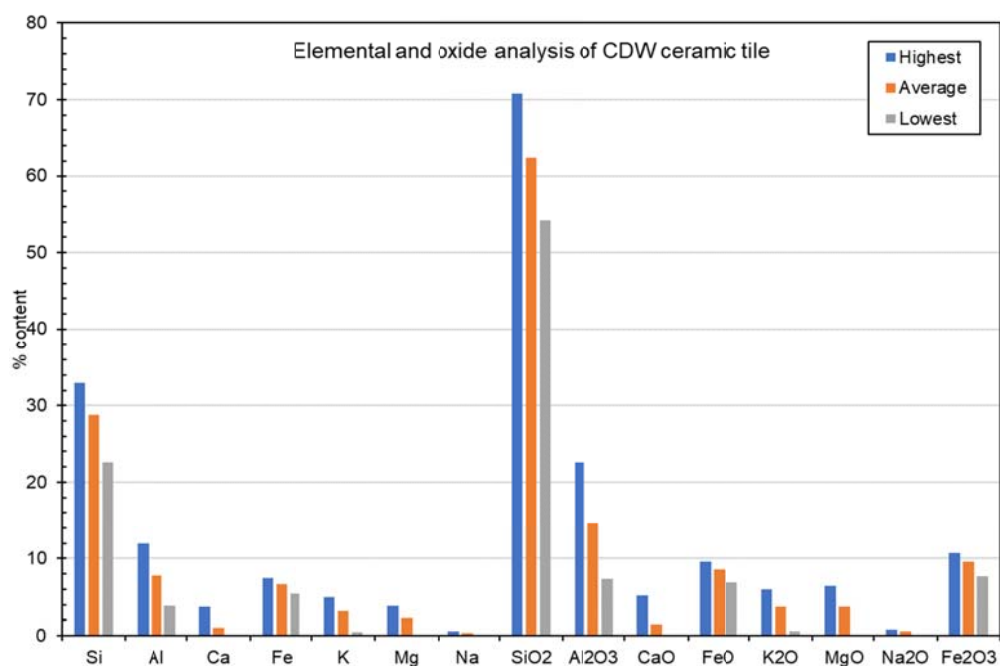**Figure 3**. Elemental and oxide analysis for waste brick material.

Figure 4. Elemental and oxide analysis for waste ceramic material.

Table 3. Summary of elemental and oxide content analysis for the wastes of CDW materials.

	BRICK				CERAMIC TILE			
	Highest %	Lowest %	δ max %	Average %	Highest %	Lowest %	δ max %	Average %
Si	29.43	22.18	7.25	25.00	33.01	22.57	10.44	28.73
Al	12.21	4.69	7.52	7.59	11.95	3.87	8.08	7.77
Ca	8.29	1.32	6.97	5.51	3.70	0.04	3.66	1.05
Fe	9.49	4.23	5.26	7.92	7.47	5.37	2.10	6.68
K	4.34	1.19	3.15	3.10	4.94	0.44	4.50	3.12
Mg	4.89	0.89	4.00	2.45	3.89	0.02	3.87	2.22
Na	1.55	0.06	1.49	0.49	0.56	0.11	0.45	0.39
Ti	1.98	0.09	1.89	0.87	-	-	-	-
SiO_2	63.06	47.53	15.53	53.57	70.74	54.16	16.58	62.40
Al_2O_3	23.07	8.86	14.21	14.33	22.57	7.30	15.27	14.68
CaO	11.60	1.85	9.75	7.71	5.18	0.06	5.12	1.48
FeO	12.20	5.44	6.76	10.19	9.60	6.90	2.70	8.58
K_2O	5.23	1.43	3.80	3.74	5.95	0.53	5.42	3.76
MgO	8.11	1.48	6.63	4.07	6.45	0.03	6.42	3.68
Na_2O	2.09	0.08	2.01	0.66	0.75	0.15	0.60	0.52
TiO_2	3.30	0.16	3.14	1.46	-	-	-	-
Fe_2O_3	13.55	6.05	7.50	11.32	10.67	7.67	3.00	9.54

Elemental and oxide analysis results for all two CDW materials are demonstrated in Figures 3 and 4 and

Table **3.** Summary of elemental and oxide content analysis for the wastes of CDW materials
The measurements for CDW bricks and CDW ceramic tiles have expectedly displayed predominant alumina-silicates content within their chemical composition. The highest amounts of silica reached almost 30.00% for CDW bricks samples and 33.01% for CDW ceramic tiles, whereas their corresponding lowest reached 22.18% and 25.27%, respectively. Similar variations in aluminium contents were observed, with the highest contents for Sample 1 and Sample 3, reaching an interesting 12.21 % and 11.95%, respectively. It was observed, however, that such high Al contents occurred only in isolated runs for both samples, whereas the predominance of analysis results was indicating towards the range of approximately 9-9.5% contents for the samples.
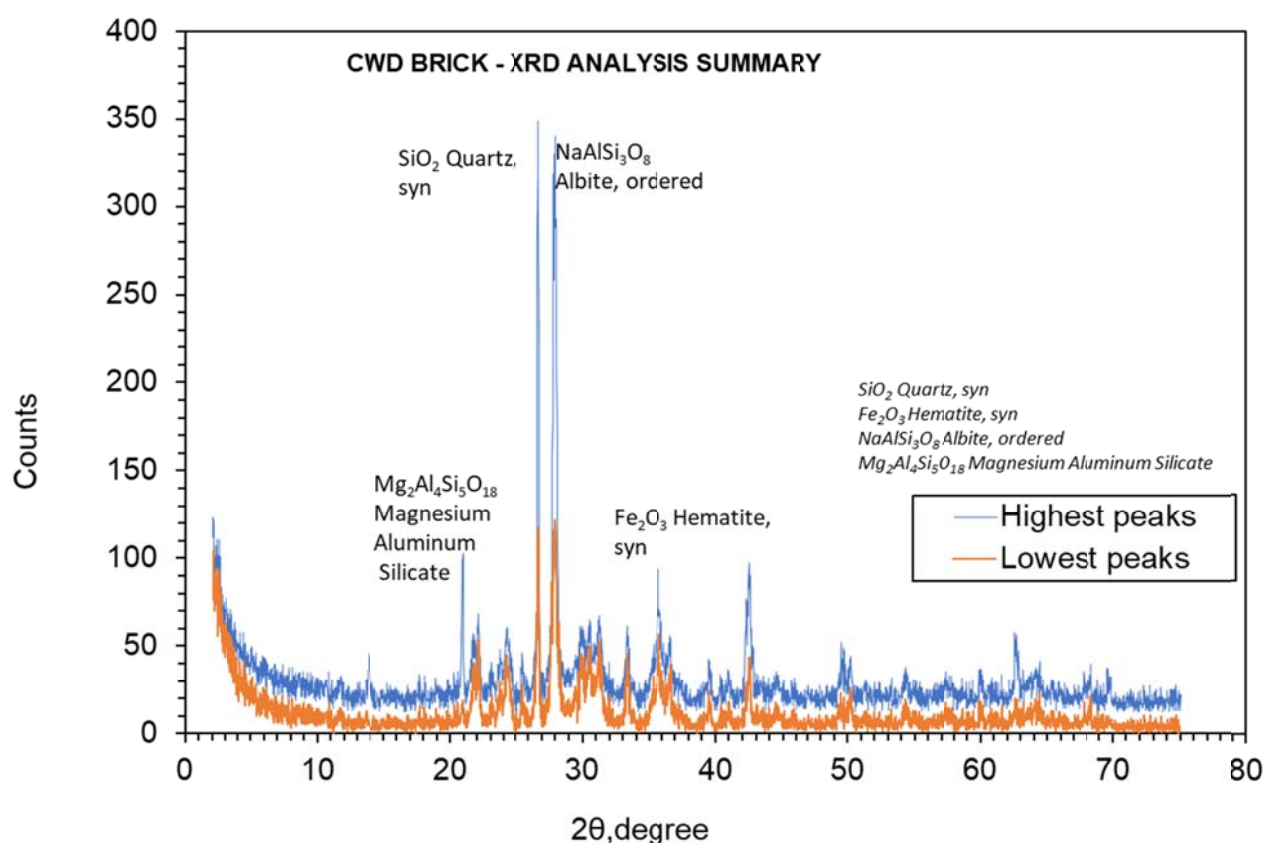

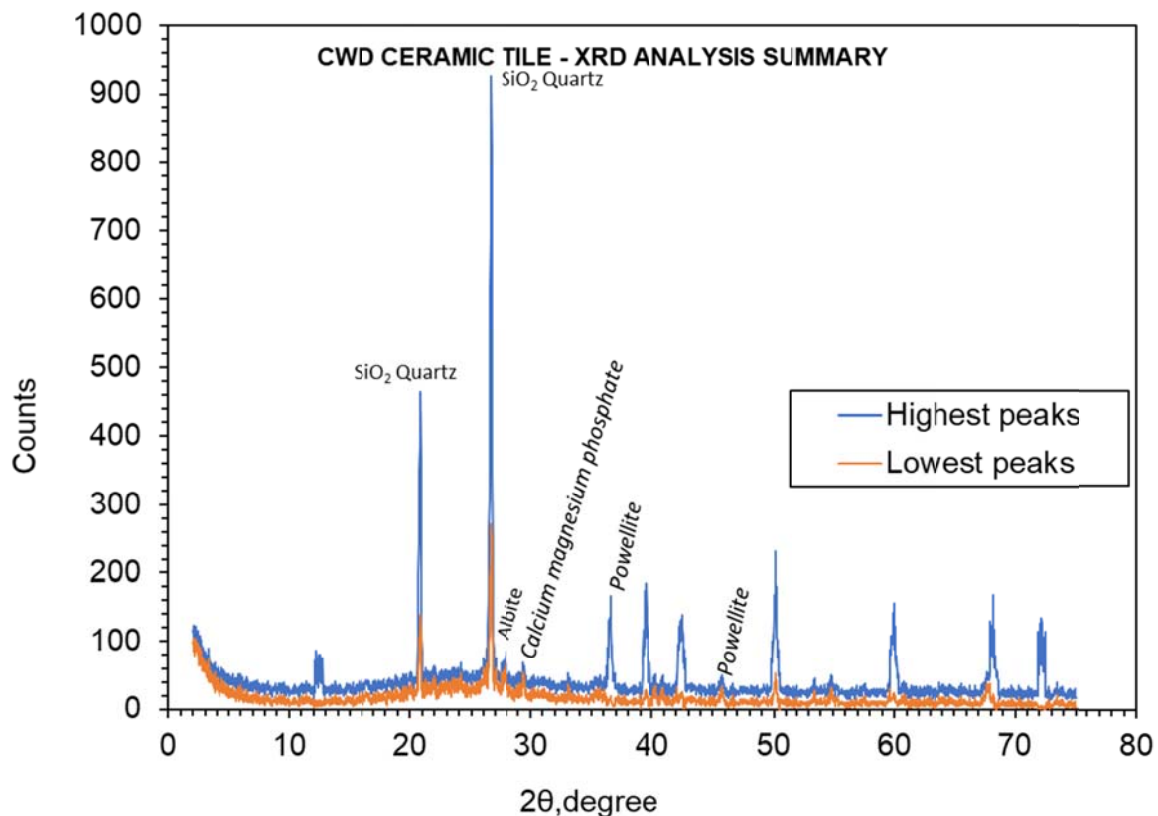**Figure 5**. XRD analysis of waste brick materials.

Figure 6. XRD analysis of waste tile materials.

Figures 5 and 6 illustrate the summary of XRD diffractograms for the CDW materials. In both types of samples (i.e., CDW bricks and CDW ceramic tiles) there was, expectedly, a strong presence of SiO_2 peaks detected at a 2 theta of approximately 26.5^o, with some brick samples exhibiting albite peaks at 27.5^o of similar intensity, or even higher than that of the quartz. In both materials, relatively strong peaks of magnesium aluminium silicates were detected at approximately 20.5^o, however, these seemed to appear weaker in the samples of waste of CDW-ceramic tiles (roughly 100 counts inferior to those detected in waste of CDW-brick samples). Generally, in both samples, there was a presence of aluminosilicate-based phases as expected, which were additionally embodying certain salts or minerals, e.g. Na (in the form of albite) or Mg. The high intensity of albite peaks in some of the brick samples indicates a slightly stronger presence of sodium minerals bound in aluminosilicate-based phases. In such a scenario, possible air transportation of sodium-based minerals on the former CDW structure may have increased the content of sodium in the existing elements of the structure to reflect such amounts by means of a more intense peak. Other peaks commonly detected in both CDW ceramic tile and CDW brick samples were those reflecting ferrite-based phases, such as hematite (Fe_2O_3). The intensity of the particular phase was varying in both samples and at different 2-theta angles (higher than 40°), denoting the different ambient

conditions of the formerly CDW structures and the different locations of the sources. Slightly more complicated crystalline phases were detected in concrete samples, with the predominant ones being calcium sulfoferrites, calcium carbonates and to a lesser intensity calcium hydroxide, ettringite, calcium silicates (possibly anhydrous) as well as calcium alumino-silicates. As hydrated C-S-H are associated with an amorphous micro-structure, it would not be possible to evidence their presence in the diffractograms.

3.1. Mixture proportions

The diverse mix proportions (Table 4) are applied with the objective to get significant workability, mechanical and rheological properties. In context to all the mixes prepared, the ratio of precursor to liquid is kept constant as 2.5, and there is no supplement of chemical admixtures in order to examine better the sole effect of alkali activators on the reaction kinetics of geopolymerization process. Afterwards, the effects of definite proportions on the rheological characteristics, density and compressive strength of the mixes are studied. However, the present study outputs revealed that 8 M, S/L ratio of 2.5 for CDW-brick waste and 3.4 for CDW- ceramic tiles waste, curing temperature 50°C, curing time of 7 days, Na_2SiO_3 to KOH ratio as 1.6:1.0 have resulted in sufficient rheological and flowability attributes for both types of CDW waste materials. Figures 7 and 8 represent the methodology of the experimental work for fire-resistant tests and raw materials, respectively.

Table 4. Materials and mix proportions.

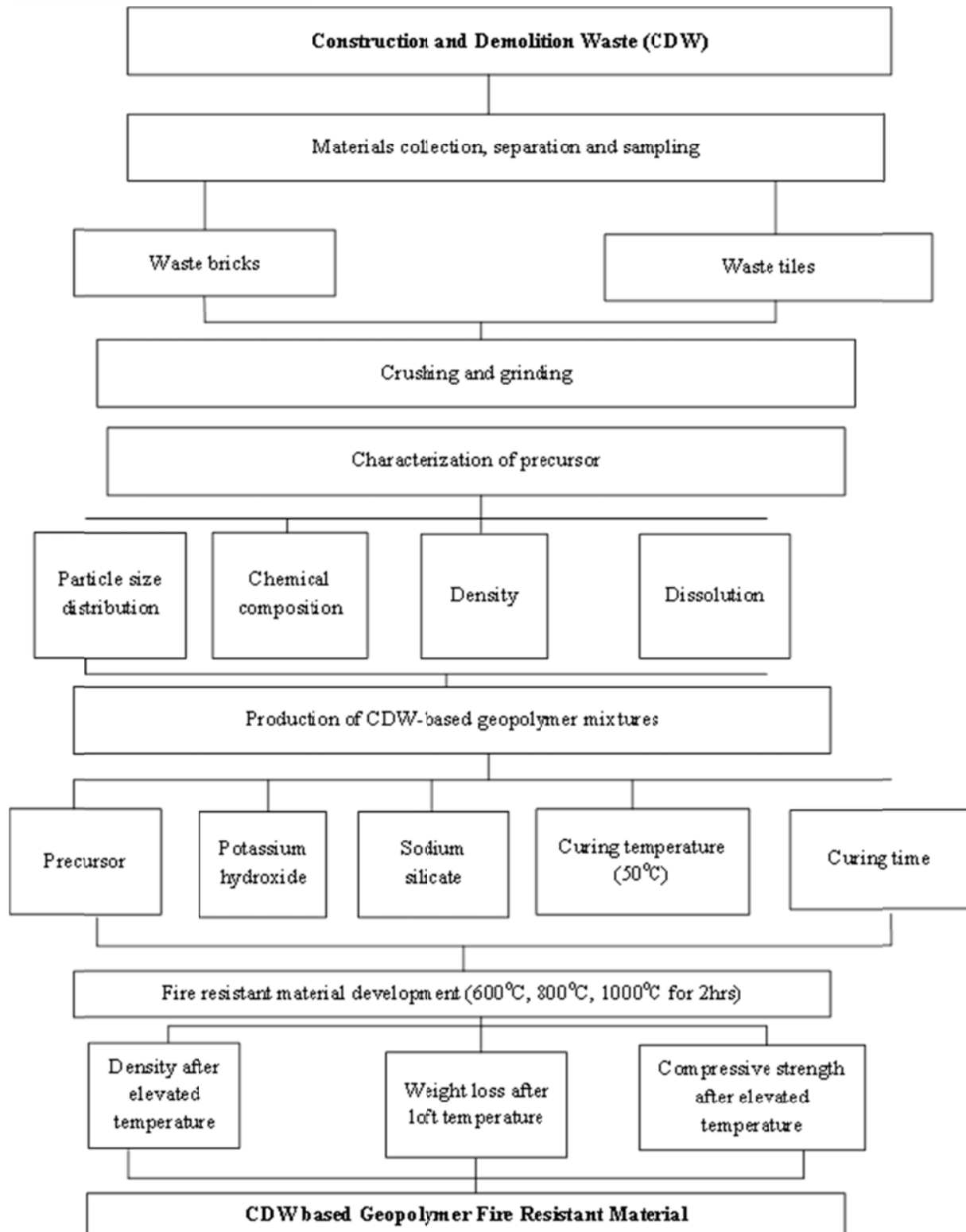| Material Type	Precursor (g)	S/L	8M of KOH (ml)	Na_2SiO_3 (ml)	Remark
M1	5520	2.5	849	1359	Specimens were prepared at room temperature of 27^0C and relative humidity of 38%.
M2	5000	3.4	566	904	

M1= Ground waste bricks

M2= Ground waste tile

Figure 7. Structure of experimental work.

Waste bricks	Waste tiles

Figure 8. Raw materials from CDW.

3.2   Experimental methods

3.2.1   Compressive strength test

With a view to determining the compressive strength of the studied formulations, geopolymer specimens of size 100 mm x 100 mm x 100 mm are cast and examined (3 samples of each formulation). The specimens are tested on a 2000 KN electro-hydraulic mechanical testing machine.

3.2.2. Elevated temperature exposure

The specimens were heated in a muffle furnace designed for a maximum temperature of 1200 °C. The specimens were treated at 600°C, 800 °C and 1000 °C and the rate of heating was 4.4 °C/min, beginning from the room temperature. The specimens were placed in the furnace for approximately 2hrs after the desired treatment temperature was achieved. The specimens were then allowed to cool in open air or atmosphere at room temperature and analyzed for weight loss, compressive strength and density.

3.2.3   Rheological properties

The rheology measurements are carried out by means of the rotational rheometer shown in Figure 9. Each specimen is examined only once to avoid the material from having an, unlike shear history. Every time, there are 3 specimens tested, piloting to a total of 24 samples. The temperature is maintained at 27° C ± 2 °C all through the testing. The fresh material will only flow while exposed to stresses greater than its static yield stress. Once it completes, the relationship among the shear rate and shear stress will be linear via a constant known as plastic viscosity (Figures 10 and 11). Rheological properties of the GP mixture from CDW bricks and CDW ceramic tiles are shown in Tables 5 and 6.
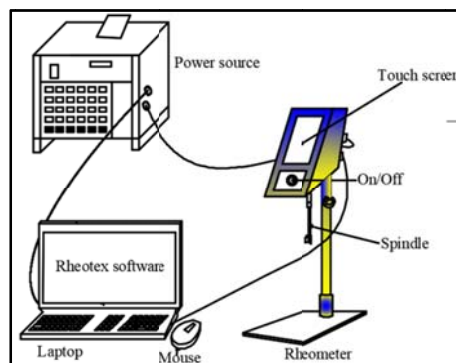

Figure 9. Reheometer setup.

Table 5. Rheological properties of the GP mixture from waste bricks.

No	Time (s)	Temperature (∘C)	Shear Rate (s⁻¹)	Shear Stress (Pa)	Viscosity (Pa.s)	Torque (mN.m)	Speed (rpm)
				AVERAGE VALUES FOR M1 (BRICKS)			
1	4	23	100	38424	384	5	100
2	9	23	100	32964	330	4	100
3	14	23	100	31830	318	4	100
4	18	23	100	32055	321	4	100
5	24	23	100	32154	322	4	100
6	29	23	100	31805	318	4	100
7	34	23	100	31425	314	4	100
8	41	23	100	30888	309	4	100
9	48	23	100	30164	302	4	100
10	54	23	100	29606	296	4	100
11	58	23	100	29252	293	4	100

Table 6. Rheological properties of the GP mixture from a waste ceramic tiles.

| No	Time (s)	Temperature (∘C)	Shear Rate (s⁻¹)	Shear Stress (Pa)	Viscosity (Pa.s)	Torque (mN.m)	Speed (rpm)
				AVERAGE VALUES FOR M2(TILES)			
1	4	25	200	123906	620	16	200
2	9	26	200	105385	527	13	200
3	14	26	200	95642	478	12	200
4	18	26	200	91412	457	12	200
5	24	26	200	89435	447	11	200
6	29	26	200	87819	439	11	200
7	34	26	200	86459	432	11	200
8	41	26	200	84345	422	11	200
9	48	26	200	82242	411	10	200
10	54	26	200	80983	405	10	200
11	58	26	200	80140	401	10	200
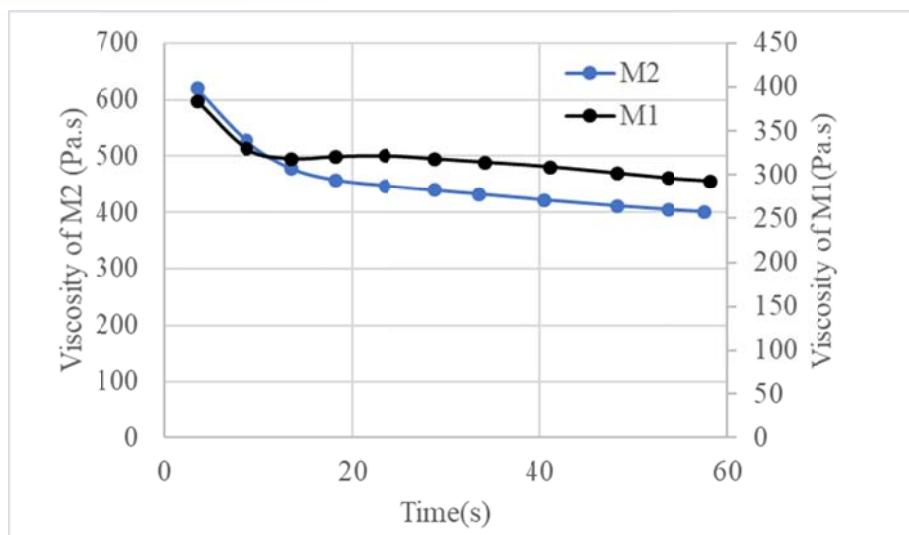
Figure 10. Viscosity of CDW bricks (M1) and CDW ceramic tiles (M2) mixtures.
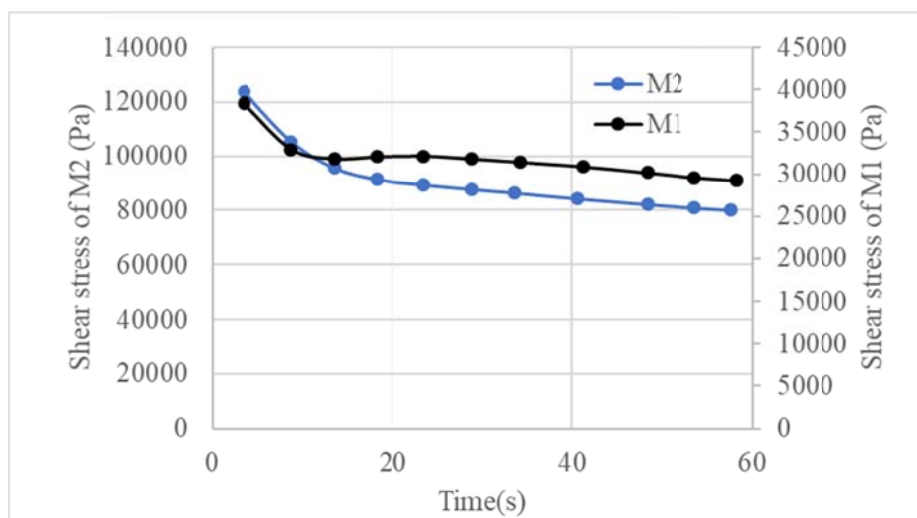
Figure 11. Shear stress of CDW bricks(M1) and CDW ceramic tiles (M2) mixtures.

4. RESULT AND DISCUSSIONS

4.1. Visual surface appearance subsequent to exposure to elevated temperature:

The alterations taking place during the heating course of action include moisture loss, evaporation and decomposition of chemical structure. Consequently, the hairline cracks were found to develop in both types of geopolymer paste, i.e., CDW brick-based geopolymer and CDW tile-based geopolymer at 800°C temperature exposures. The cracks did not appear in geopolymer paste at elevated at 600°C temperature. Conversely, larger size cracks were found to appear at 1000°C temperature for both types of geopolymer concrete as depicted in the Figure 12-15.

Tile waste-based geopolymer samples before elevated exposure	Tile waste-based geopolymer samples after elevated exposure
Brick waste-based geopolymer samples before elevated exposure	**Brick waste-based geopolymer samples after elevated exposure**

Figure 12. Visual appearance of geopolymer samples (100x100x100 mm) before and after temperature exposure.

(a) Tile waste-based specimens at different temperature regimes		
600°C	800°C	1000°C

(b) Brick waste-based Specimens at different temperature regimes		
600°C	800°C	1000°C
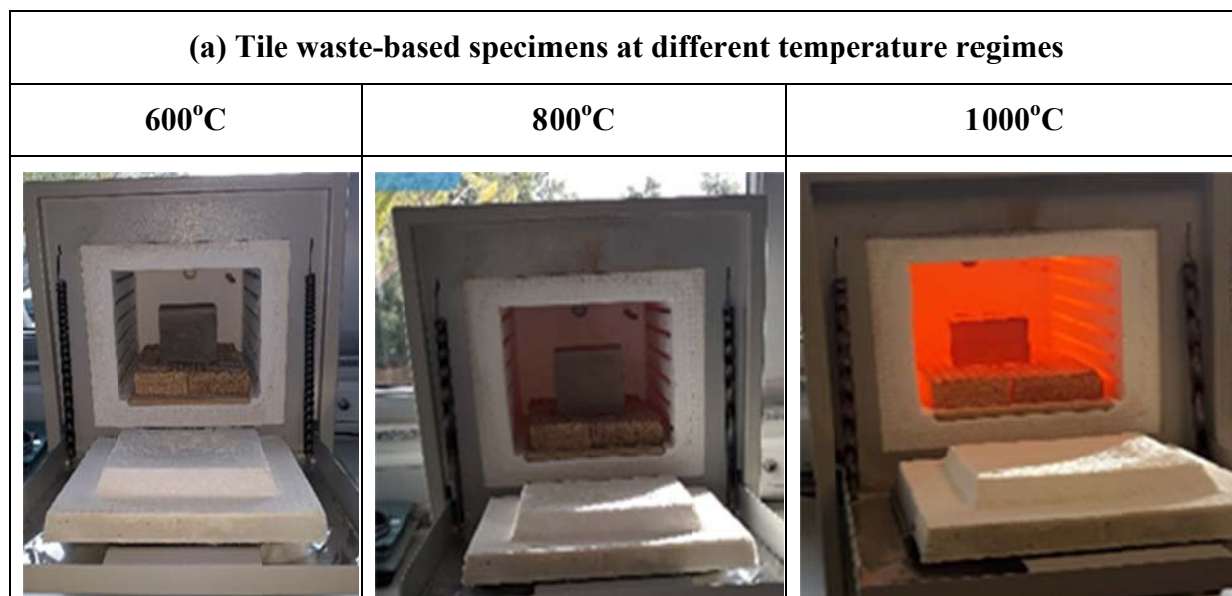
Figure 13. Samples (100x100x100 mm) at different temperature exposure.

Specimen from the tile before fire test	Specimens from tile after the fire test

Specimen from brick before fire test	Specimens from bricks after the fire test

Figure 14. Visual appearance of geopolymer samples (50x50x50 mm) before and after exposure.

(a) Tile waste-based Specimens at different temperature regimes		
600°C	**800°C**	**1000°C**

(b) Brick waste-based Specimens at different temperature regimes		
600°C	**800°C**	**1000°C**

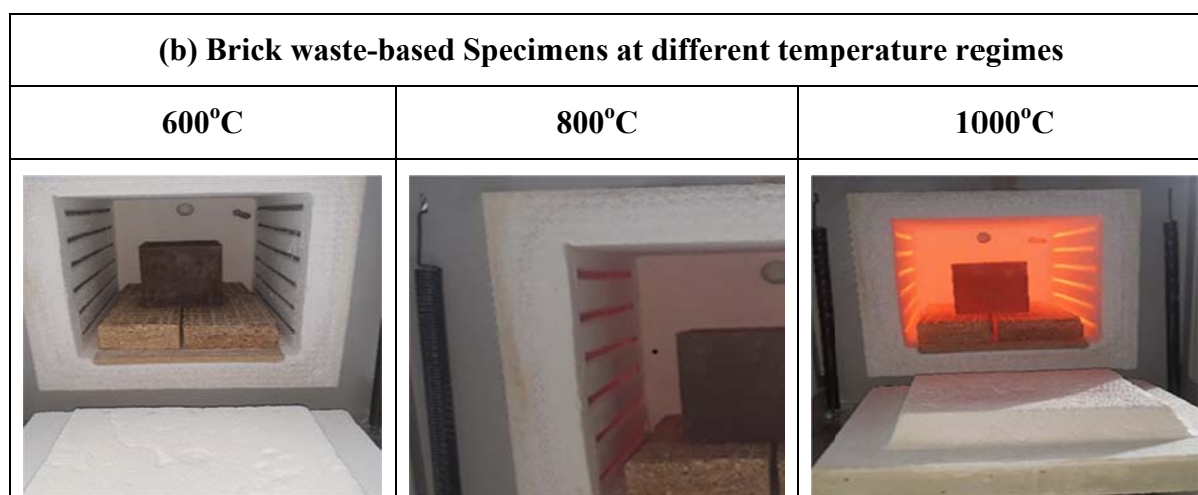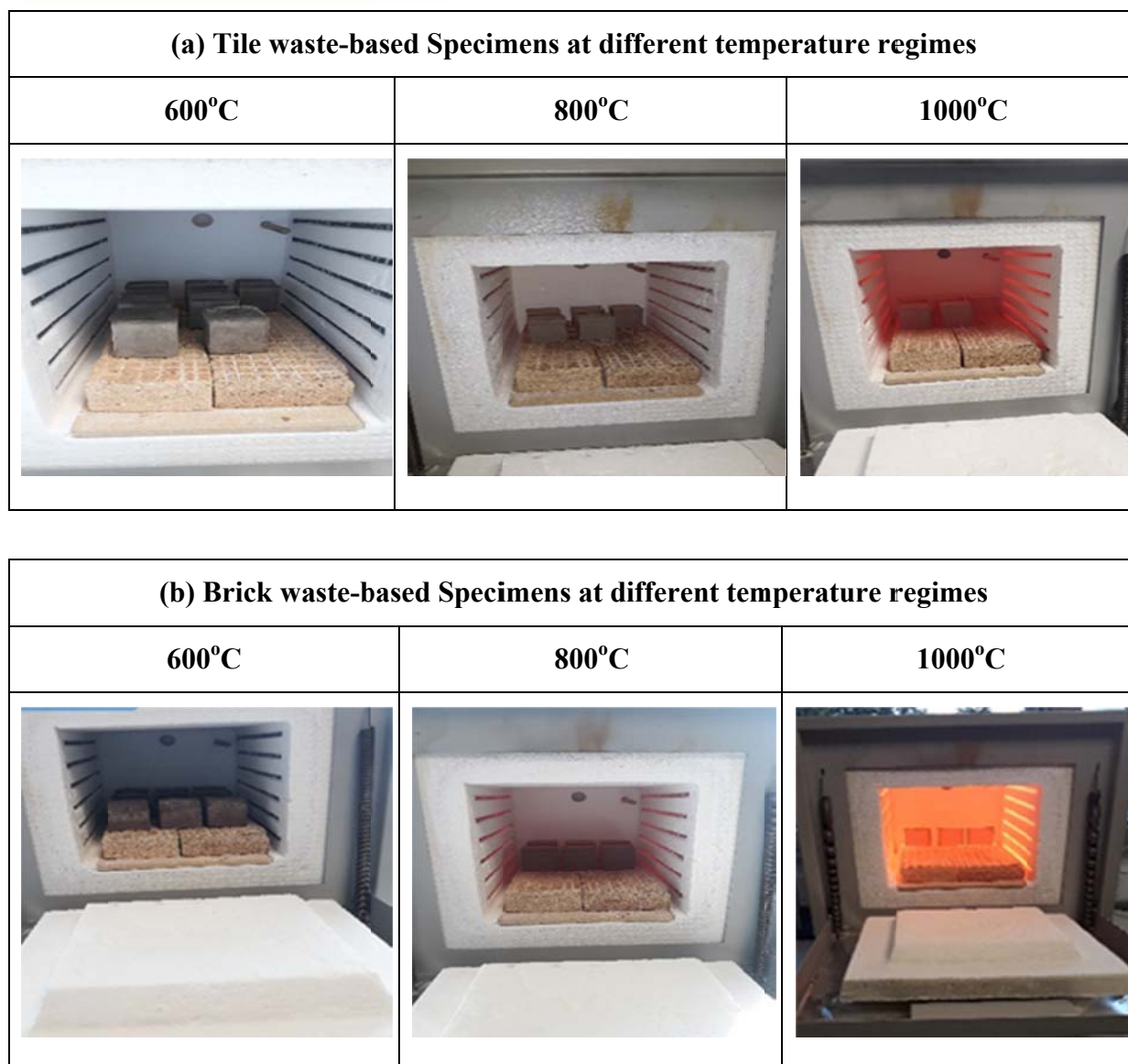**Figure 15**. Samples (50x50x50 mm) at different temperature exposures.

4.2. Mass loss

The weight loss of specimens occurred on account of the exposure to elevated temperature during the heating process. The weight of both CDW tile-based and CDW brick-based geopolymer specimens decreased with an increase in temperature, as shown in the Figures16-18 and Table 7. At all the elevated temperatures examined in this case, the mass loss of CDW brick-based geopolymer concrete was recorded lesser than that of CDW tile-based geopolymer. Specifically, Figures 16 to18 put on display that at 800°C temperature, the mass

loss for CDW wastes of brick-based and CDW wastes of tile-based geopolymer were reported 7.5% and 7.9%, as well as 9.9% and 10.4 % on 7th and 28th days, respectively.

Table 7. Density, weight loss and compressive strength at various temperature regime.

| Temperature (^{0}C)	Density (kg/m^3)		Weight Loss (%)		Compressive Strength (MPa)	
	7 Days	28 Days	7 Days	28 Days	7 Days	28 Days
Brick waste based geopolymer						
50	1554	1556	-	-	19	23
600	1475	1475.9	6.0	3.9	15.4	18.8
800	1430	1430.8	8.0	5.7	19.4	23.7
1000	1434	1436.5	8.0	6.2	21.1	25.7
Tile waste-based geopolymer						
50	1736	1586	-	-	33	38
600	1583.0	1579.20	9.6	3.5	16.8	27.69
800	1569.2	1579.08	9.6	3.6	13.2	23.62
1000	1576.9	1566.24	9.9	3.6	36.6	38.19
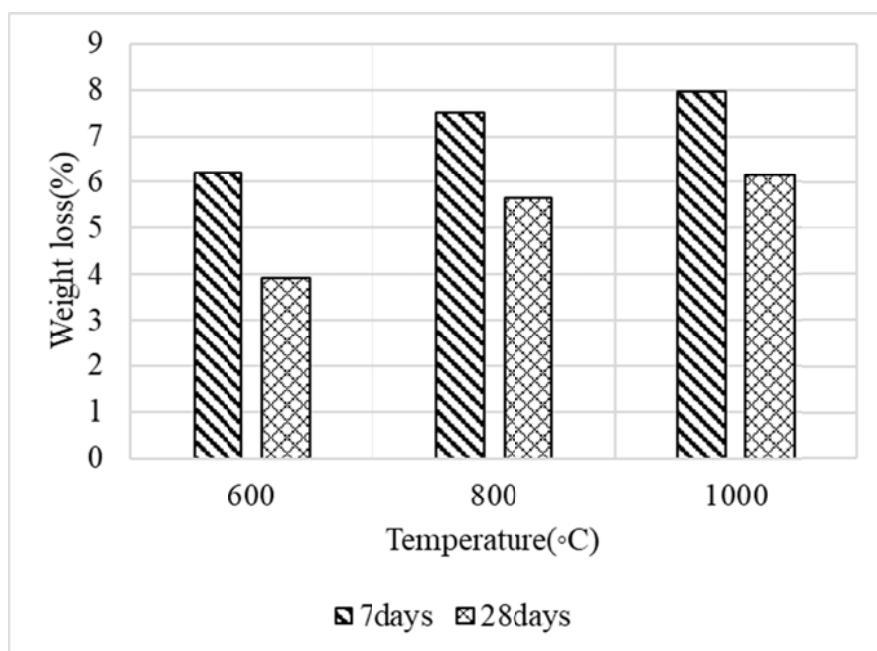
Figure 16. Weight loss of brick-based geopolymer after elevated temperature exposure.
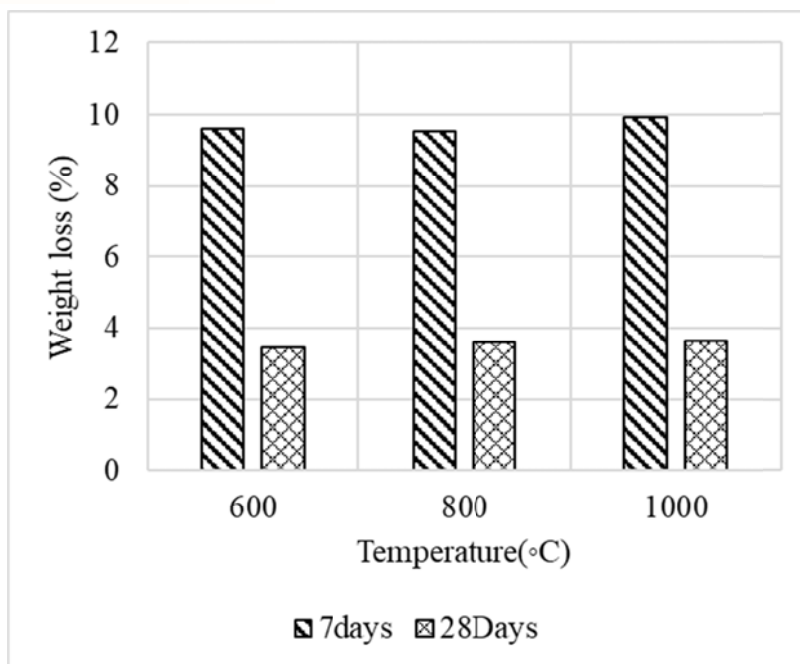
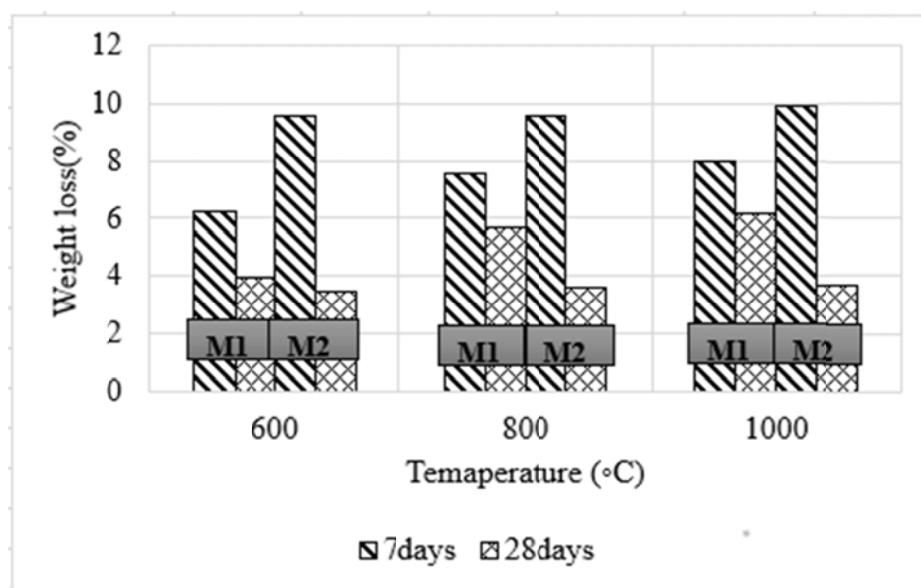**Figure 17**. Weight loss of tile-based geopolymer after elevated temperature exposure.

Figure 18. Weight loss of brick-based and tile-based geopolymer after elevated temperature exposure.

4.3. Density

The experimental results of the density test are graphically presented in Figures19 to 22. Also, the values of bulk densities are represented in Table 7. From Figures 19 to 22, it can be seen that the density of geopolymer samples decreases as increasing the temperature exposure, for both brick-based and tile-based geopolymers. With the increase in heating, a gradual plunge in the bulk density was observed for all materials related to the progressive drying process and dehydroxylation, leading to mass change. The figures demonstrate the density values at the established temperature and the density of the initial unheated material. The progressive heating of the geopolymer results in drying of matrix, as well as aggregates. The water present in the material is gradually removed from the heated matrix. With increase in temperature, the free water is removed first and then after the adsorbed water evaporated. At higher temperatures, the water-bound physically in the form of hydroxyl groups is removed. According to Duxson et al., [25], the dehydroxylation process that occur at 250°-600°C induces the shrinkage of the geopolymer binder. Nevertheless, the geopolymer binder may experience an expansion attributed to the thermal dilation of water around the temperature of 120°C. As soon as the drying process starts, intensive shrinkage begins to take place.
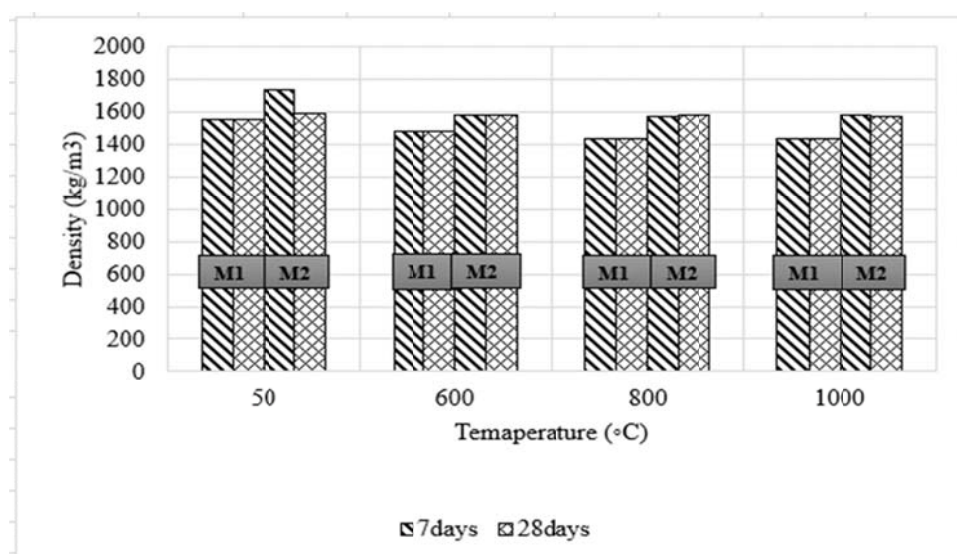

Figure 19. Density of brick-based (M1) and tile-based (M2) geopolymers, before and after temperature exposure.
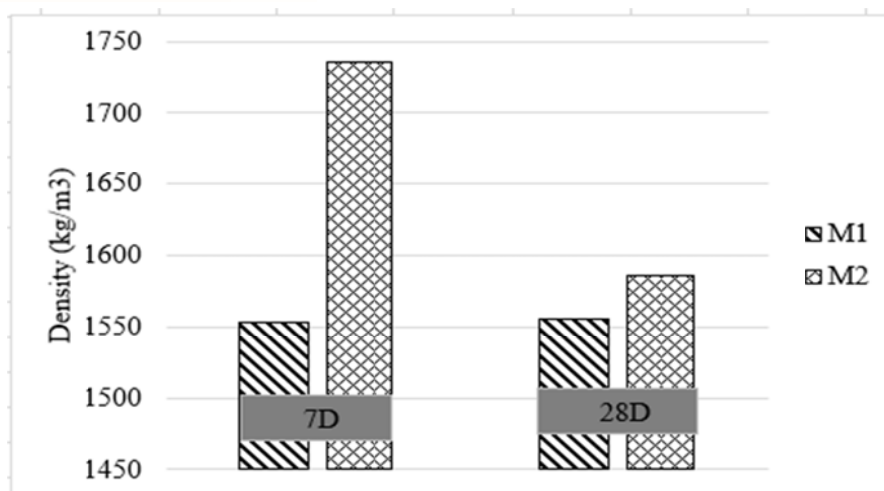
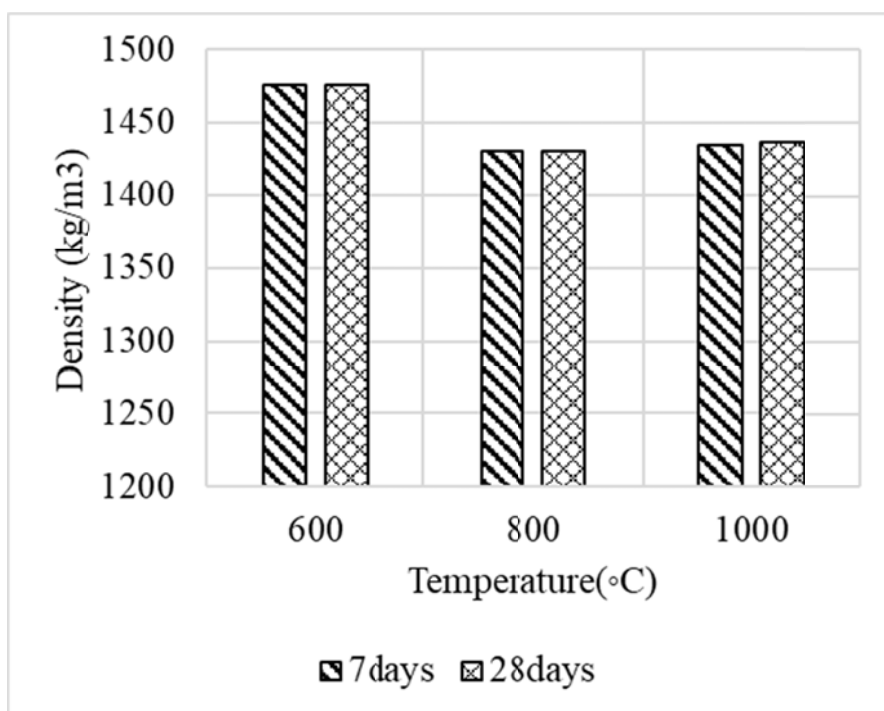**Figure 20**. Density of brick-based (M1) and tile-based (M2) geopolymer pastes at 50 .

Figure 21. Density of brick-based geopolymer after temperature exposure.
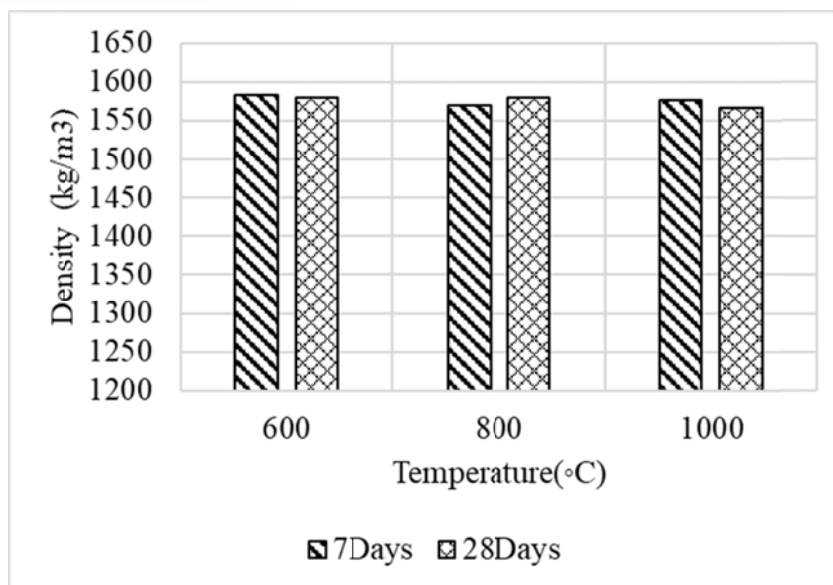
Figure 22. Density of tile-based geopolymer after temperature exposure.

4.4 Compressive Strength

4.4.1 Before Temperature Exposure

Figure 23 illustrates the development of the compressive strength of different mixtures on 7th day and 28th day. The compressive strength of all the mixes increases when an augment in the elevated temperature exposure is made. The curing at higher temperatures has a significant effect on enhancing the compressive strength of all mixtures, which can accelerate the polymerization rate. The earlier findings of the research study carried out by Akçaozoglu and Ulu [117] confirmed that the compressive strength of alkali activated slag binders developed promptly at early ages, up to 7 days. Bilim et al. [118] asserted that curing conditions had a substantial effect on the properties of alkali activated slag mortar. In this case, the heat curing noticeably accelerated the early strength development and mitigated the high drying shrinkage. Chi [119] is of the opinion that heat curing not only improved the compressive strength of alkali activated slag-concrete, but also improved its durability. Whatsoever, at the age of 28 days, the compressive strength of all mixtures was found to be increased owing to the solubility of alumina-silicate components in the alkaline solution [25]. The incorporation of CDW wastes of tiles enhanced the strength of geopolymer samples as compared to the CDW waste of brick-based geopolymer specimens on 7th day and 28th day. The compressive strength of CDW wastes of brick-based geopolymer and CDW wastes of tiles-based geopolymer samples at 50°C were recorded with 19MPa and 23MPa, as well as 33MPa and

38MPa on 7th and 28th day compressive strength, respectively. The referred temperature may cause rapid evaporation of water, reasonably rapid microstructure densification, repressed additional species diffusion, limit the headway of the reactions and then the strength development [120]. The key features of Figure 23 are that curing at a high ambient temperature has a positive effect on the compressive strength of all mixtures at the ages of 7 and 28 days. The enhancement in the compressive strength due to the incorporation of powder of waste tiles could be attributed to the packing effect of the fine particles that can fill in the voids, producing a more compact microstructure, resulting in higher compressive strength. In any case, the reasons for these differences in strength for both tiles-based and brick-based geopolymer samples could be related to the chemical composition and the particle grain size of powders of CDW waste of tiles and CDW waste of brick as well as the change in the ratio of silicon/aluminium (Si/Al). In addition, the change in the ratio of Si/Al can affect the compressive strength of the composite. It was found that Si/Al has a significant effect on alumina-silicate materials during the reaction kinetics of geopolymerization [121]. Khale and Chaudhary [122] suggested that there are limits for Si/Al ratios in order to form strong geopolymeric products. Higher or lower values than those limits led to less stable of the polymerized network.
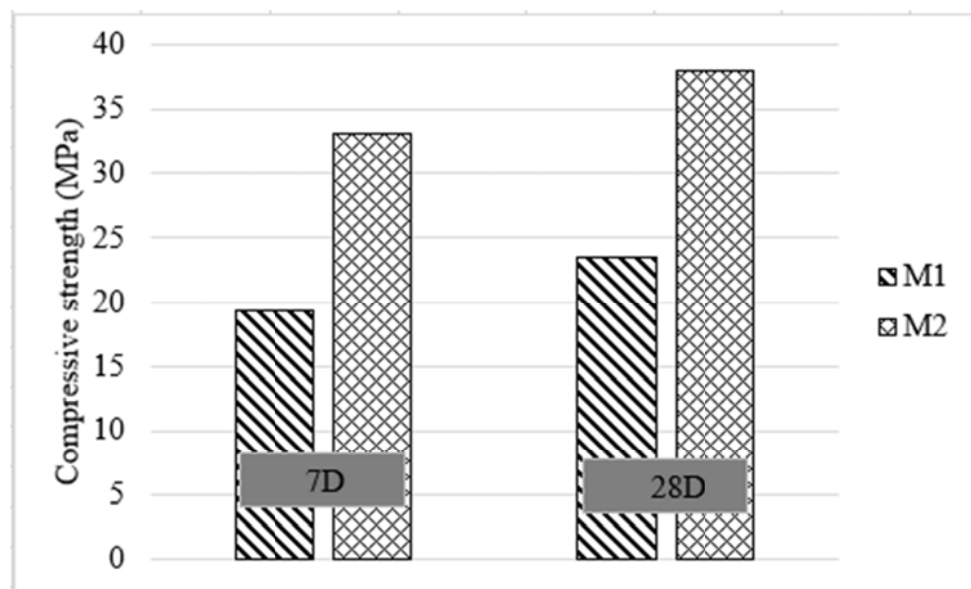

Figure 23. Compressive strength at 50[o]C.

4.4.2   After Elevated Temperature Exposure

The performance of the brick-based and tiles-based geopolymer samples exposed to elevated temperatures was evaluated by measuring the compressive strength subsequent to heating. Figures 24 to 26 depict the residual compressive strength of various hardened pastes following their exposure at 600° to 1000°C, for 2 hrs. Apparently, the residual compressive strength is directly influenced by the waste type and degree of temperature. The initial compressive strength of both the bricks-based and tiles-based geopolymer samples display a marginal reduction at 600°C. The early compressive strength of bricks-based geopolymer was reported displaying 15.4, 19.4, 21.1 MPa as well as 18.8, 23.7, 25.7 on 7 and 28 days after exposing to 600°, 800° and 1000°C, respectively. Whereas the early compressive strength of tiles-based geopolymer was found figuring as 16.8, 13.2, 36.6 MPa as well as 27.7, 23.6, 38.2 on 7 and 28 days subsequent to exposure at 600°, 800° and 1000°C, respectively as illustrated by Figure 25. At temperature of 1000°C, an essential change in the residual strength was noted down. The residual strength increases at these severe temperatures and accounts for more increases than that of the reference, as represented by Figure 26. The compressive strength of 21.1 and 25.7 MPa was observed in bricks-based geopolymer samples on 7 and 28 days, respectively, as depicted in Figure 24. Likewise, the matching trend was observed in the case of tiles-based geopolymer samples demonstrating 36.6 and 38.2 MPa on 7 and 28 days. The general improvement in the residual compressive strength, of all types of the pastes, at 1000°C is associated with melting of alkali. At temperatures higher than 800°C, alkalis with solid materials can cause partial sintering of the unreacted crystalline phases remaining from the raw materials. This phenomenon plays an essential role in enhancing the residual mechanical properties at 1000°C and helps the geopolymers to resist elevated temperatures without destruction [123]. From the above discussion, it can be confirmed that the integration of powder of tiles has a positive effect on the compressive strength after heating at all temperature regimes. It can be concluded from Table 7 that the percentage reduction in compressive strength was higher for bricks-based geopolymer than of tiles-based geopolymer, at all temperature exposures. The highest percentage reduction in compressive strength was observed for the bricks-based geopolymer at 600°C. Both the types of geopolymer reported with gain in strength beyond 800°C, due to the polymerization of initially unreacted material increasing the amorphous phase content. This phase content is less in the case of bricks-based geopolymer due to the decomposition of particles at elevated temperatures, which leads to the formation of voids in the concrete

matrix. These voids enhance the pore pressure and accelerate the cracks formed in the matrix. This causes the poor residual strength of the specimen [124]. The portrayed figures indicate that both types of geopolymer gained strength above 800°C because the amorphous content increased, due to the polymerization of unreacted crystalline material [125]. As a result, there was no further strength loss recorded in geopolymer concrete, as represented in Table 7. This particular trend of the outcomes is found consistent with the previous findings conducted by Sun et al. [126], who found a reduction in the compressive strength of geopolymer pastes prepared with ceramic, derived from municipal waste, activated with sodium silicate and potassium hydroxide solution after exposure to 100°C. The compressive strength found increased steadily with increasing temperatures and reached its highest value at 1000°C. In any case, the increase or decrease of the compressive strength after heating could be depending upon the dominant process of (1) further geopolymerization of unreacted particles or/and sintering process resulting in strength enhancement, or (2) thermal incompatibility due to non-uniform distribution of the temperature resulting in strength deterioration [127]. In the literature, there are still unsteady results about the effect of elevated temperatures on geopolymer. Rashad and Khalil [128] stated a reduction in the compressive strength of alkali activated Slag-pastes using activator of sodium silicate after exposure to 400–800°C, whilst the compressive strength started to increase at 1000°C.Wang et al. [129] declared a reduction in the compressive strength of alkali activated Slag-pastes activated with sodium silicate and NaOH solutions after exposure to 200°, 500° and 800°C. Aziz et al. [130] cured alkali activated slag-pastes using sodium silicate and NaOH solutions as activators at room temperature. After 28 curing days, the specimens were exposed to 200° to1000°C. The results revealed a reduction in the compressive strength at 200°-800°C but the compressive strength started to increase at 1000°C. Türker et al. [131] reported that there was a reduction in the compressive strength of alkali activated slag-mortars employing sodium silicate and NaOH solutions as activators, cured at 60°C for 6 hrs followed by laboratory conditions, after exposure to 200°-800°C. On the other hand, mortars cured at ambient temperature exhibited superior compressive strength after exposure to 200° and 400°C, in comparison with the control, whilst a reduction in the strength was perceived after exposure to 600° and 800°C. Rashad et al. [132] and Rashad [133] unveiled an increase in the compressive strength of alkali activated-pastes utilizing Na_2SO_4 as activator after exposure to 200°- 600°C, whilst a reduction in the strength was obtained subsequent to exposure at 800°C. Based on the above discussion, generally, it can be confirmed that the performance of the alkali activated slag

system at elevated temperatures could be affected by concentration of activator, silica modulus ratio, activator type, fineness of waste, curing conditions and chemical properties of waste used [131, 134].
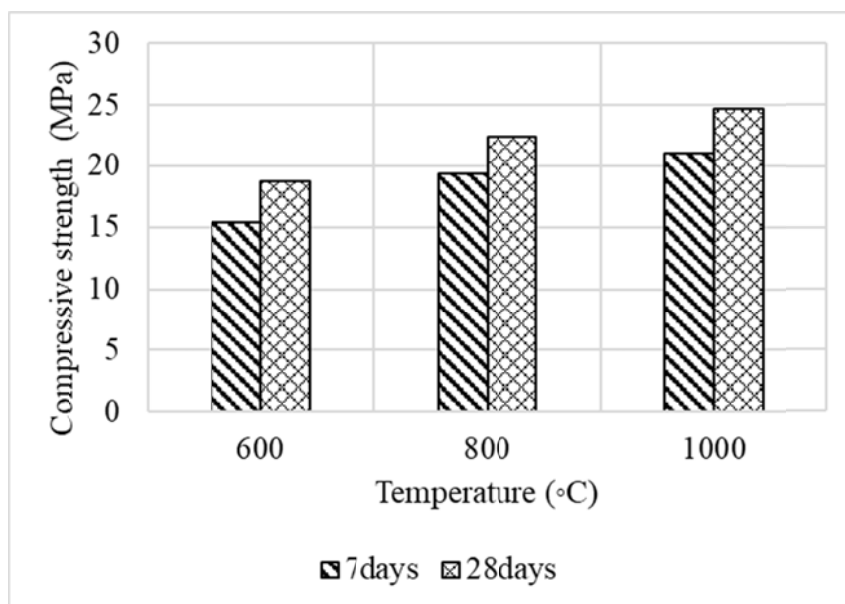

Figure 24. Compressive strength of brick-based geopolymer at elevated temperature.
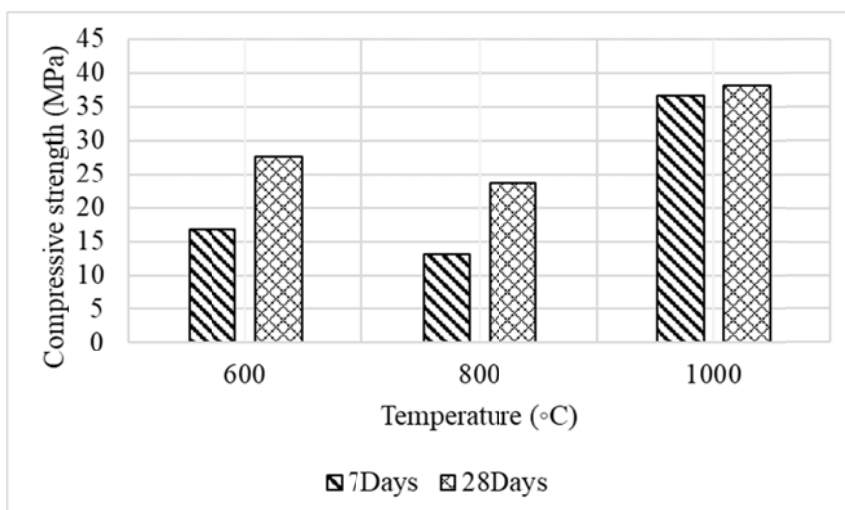

Figure 25. Compressive strength of tile-based geopolymer at elevated temperature.
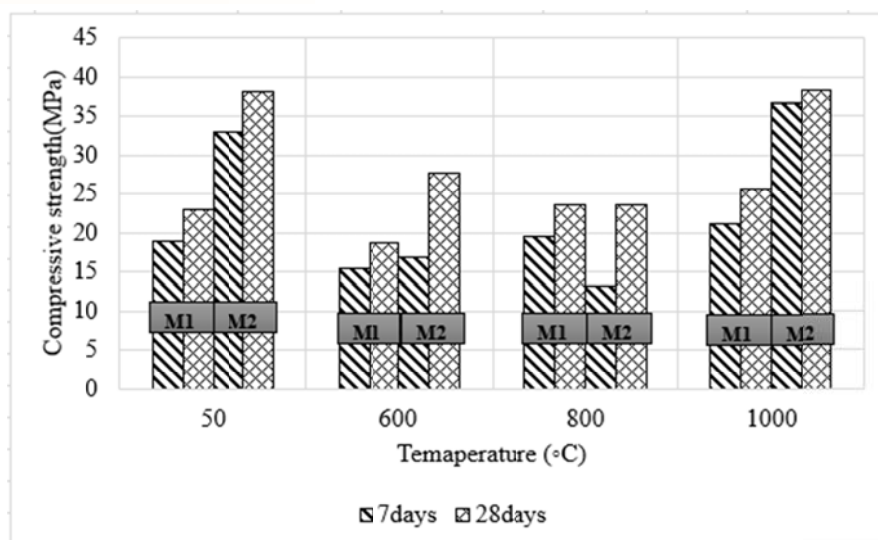
Figure 26. Compressive strength of brick-based (M1) and tile-based (M2) geopolymer.

5. THERMAL INSULATION DESIGN

Apart from the resistance to fire, the geopolymeric materials should also possess extremely low thermal conductivity and density. Such properties are achieved by controlling the materials composition through proper additions of modifiers. The reduction of the density is strongly linked to the reduction of the thermal conductivity. Thus, in the DEFEAT project the reduction of the density will be aimed to be achieved by means of two methods: a) chemically: with the addition of proper amount of the total mass of the material by Aluminium powder (Al-) or Hydrogen Peroxide (H_2O_2) and b) mechanically: with the addition of lightweight aggregates or cenospheres. The target of the specific material is a density of <400 kg/m^3 and thermal conductivity of 0.04W/m.K. Tables 8, 9 and 10 show the thermal insulation material mix design proportions. In the present research study, the CDW waste- (i.e., CDW waste of bricks, CDW waste of tiles and CDW waste of concrete) based geopolymer pastes are tested under thermal temperature, with a prime focus on the density to be less than 400 kg/m^3 and thermal conductivity of 0.04W/m.K. The 100%-CDW wastes made up of CDW waste of bricks, CDW waste of tiles and CDW waste of concrete are employed as precursors and dissimilar alkaline activators such as potassium hydroxide (KOH) and sodium silicate (Na_2SiO_3) are utilized to manufacture purely CDW-based geopolymers. The researchers investigated preliminary data (Tables 11-16 and in Figures 27-38) to develop solely CDW based thermal and fire-resistant geopolymer materials and offer a strong groundwork to conduct advance potential investigations in future.

Table 8. Thermal insulation material mix design proportions by using waste bricks.

Mix ID	Specimen #	Precursor (g)	KOH (PH) (ml)	NaOH (SH) (ml)	Na$_2$SiO$_3$ (SS) (ml)	H$_2$O$_2$ (ml)	Al (g)	H$_2$O$_2$ (%)	Al (%)	S/L	SS/ (PH or SH)	Average Density (kg/m^3)	Average Compressive Strength (MPa)
B_CDW001	1-3	380	121.2			4.4		3.5		3.0		1196.9	1.3
B_CDW002	4-6	418		99.4	99.4	4.5		2.2		2.1	1.0	1326.3	4.0
B_CDW003	7-9	380	121.0			4.4		3.5		3.0		1161.8	2.8
B_CDW004	10-12	380	180.9			4.4		2.4		2.1		840.6	0.9
B_CDW005	13-15	380	90.2		90.2	4.5	10.7	2.4	2.7	2.1	1.0	648.2	1.0
B_CDW006	16-18	420	191.0				0.8	0.0	0.2	2.2		1289.9	8.1
B_CDW007	19-21	420	191.0			6.0		3.0		2.1		765.0	0.0
B_CDW008	22-24	420	95.5		95.5		2.0	0.0	0.5	2.2	1.0	948.0	2.2
B_CDW009	25-27	380	213.6							1.8		1663.6	2.9
B_CDW010	28-30	380	142.4		142.4		0.2		0.1	1.3	1.0	1797.6	3.3
B_CDW011	31-33	380	142.4		142.4		0.2		0.1	1.3	1.0	1478.7	3.5
B_CDW012	34-36	380	142.4		142.4		0.2		0.1	1.3	1.0	1533.3	2.7
B_CDW013	37-39	380	153.2				0.5		0.1	2.5		1185.3	2.4
B_CDW014	40-42	380	63.8		63.8		0.5		0.1	3.0	1.0	1804.4	3.8
B_CDW015	43-45	760	427.2				1.0		0.1	1.8		1295.3	3.8
B_CDW016	46-48	760	106.8		146.3		1.0		0.1	3.0	1.4	1186.7	3.3
B_CDW017	49-51	380	31.9		95.7		0.5		0.1	3.0	3.0	1978.4	4.2
B_CDW018	52-54	380	95.7		31.9		0.5		0.1	3.0	0.3	1851.2	3.6

B_CDW019	55-57	380	121.2			4.4		3.5		3.0		530.7	1.9
B_CDW020	58-60	380	35.6		35.6	4.5	10.7	6.0	2.7	5.0	1.0	756.3	1.9
B_CDW021	61-63	380	30.3		90.9	5.0		4.0		3.0	3.0	1977.2	3.8
B_CDW022	64-66	380	90.9		30.3	5.0		4.0		3.0	0.3	866.0	1.1

Table 9. Thermal insulation material mix design proportions by using waste tiles.

Mix ID	Specimen #	Precursor (g)	KOH(PH) (ml)	Na$_2$SiO$_3$ (SS) (ml)	H$_2$O$_2$ (ml)	Al (g)	H$_2$O$_2$ (%)	Al (%)	S/L	SS/ (PH or SH)	Average Density (kg/m^3)	Average Compressive Strength (MPa)
T_CDW01	37-39	380	73.3	73.3		0.5	0.0	0.1	2.6	1.0	1230.9	11.2
T_CDW02	40-42	420	112.0	56.0		1.0	0.0	0.2	2.5	0.5	1144.5	6.2
T_CDW03	43-45	420	112.0	56.0	6.0		3.4	0.0	2.4	0.5	1081.1	2.9
T_CDW04	46-48	420	127.0	64.0	8.0		4.0	0.0	2.1	0.5	1099.1	3.8
T_CDW05	49-51	420	112.0	56.0		1.5	0.0	0.4	2.5	0.5	1160	5.0
T_CDW06	52-54	420	90.5	90.5	10.0		5.2		2.2	1.0	1329.6	18.1
T_CDW07	55-57	380	146.7			0.5		0.1	2.6		1028.8	2.8
T_CDW08	58-60	380	73.4	73.4		0.5		0.1	2.6	1.0	653.1	1.9
T_CDW09	61-63	380	73.4	73.4		0.5		0.1	2.6	1.0	1640.0	2.2
T_CDW10	64-66	380	36.7	110.1		0.5		0.1	2.6	3.0	1873.2	4.3
T_CDW11	67-69	380	110.1	36.7		0.5		0.1	2.6	0.3	1110.1	3.7
T_CDW12	70-72	380	22.4	67.05	4.7		5.0		4.0	3.0	1161.1	2.7
T_CDW13	73-75	380	67.1	22.35	4.7		5.0		4.0	0.3	1087.5	2.7

Table 10. Thermal insulation material mix design proportions by using waste concrete rubbles.

Mix ID	Specimen #	Precursor (g)	KOH (PH) (ml)	NaOH (SH) (ml)	Na$_2$SiO$_3$ (SS) (ml)	H$_2$O$_2$ (ml)	Al (g)	H$_2$O$_2$ (%)	Al (%)	S/L	SS/ (PH or SH)	Average Density (kg/m^3)	Average Compressive Strength (MPa)
C_CDW01	76-78	580		163.8	64.4	4.5		1.9	0.0	2.5	0.4	990.7	3.1
C_CDW02	79-81	380		81.9	37.2		0.5	0.0	0.1	3.2	0.5	1095.4	3.1
C_CDW03	82-84	483		104.0	47.4	4.5	0.5	2.9	0.1	3.1	0.5	975.9	2.4
C_CDW04	85-87	420	118.2		47.2	4.5		2.6	0.0	2.5	0.4	1188.5	3.5
C_CDW05	88-90	420	118.2		47.2		0.5	0.0	0.1	2.5	0.4	680.5	0.8
C_CDW06	91-93	420	118.2		47.2	4.5	0.5	2.6	0.1	2.5	0.4	795.0	1.8

1. **Effect of aluminum powder on density of brick waste (M1), tile waste (M2) and concrete waste (M3) based geopolymers**

Table 11. Mix design for brick waste based geopolymer (M1) with incorporation of aluminum powder.

Mix ID	Specimen #	M1 (g)	KOH (PH) (ml)	Na_2SiO_3 (SS) (ml)	H_2O_2 (ml)	Al (g)	H_2O_2 (%)	Al (%)	S/L	SS/(PH or SH)	Average Density (kg/m^3)	Average Compressive Strength (MPa)
B_CDW006	16-18	420	191.0			0.8		0.2	2.2		1289.9	8.1
B_CDW008	22-24	420	95.5	95.5		2.0		0.5	2.2	1.0	948.0	2.2
B_CDW015	43-45	760	427.2			1.0		0.1			1295.3	3.8
B_CDW016	46-48	760	106.8	146.3		1.0		0.1		1.4	1186.7	3.3
B_CDW020	58-60	380	35.6	35.6	4.5	10.7	6.0	2.7		1.0	756.3	1.9

Table 12. Mix design for tile waste based geopolymer (M2) with incorporation of aluminum powder.

Mix ID	Specimen #	M2 (g)	KOH (PH) (ml)	Na_2SiO_3 (SS) (ml)	Al (g)	Al (%)	S/L	SS/ (PH or SH)	Average Density (kg/m^3)	Average Compressive Strength (MPa)
T_CDW01	67-69	380	73.3	73.3	0.5	0.1	2.6	1.0	1230.9	11.2
T_CDW02	70-72	420	112.0	56.0	1.0	0.2	2.5	0.5	1144.5	6.2
T_CDW05	79-81	420	112.0	56.0	1.5	0.4	2.5	0.5	1160.0	5.0
T_CDW07	85-87	380	146.7		0.5	0.1	2.6		1028.8	2.8
T_CDW08	88-90	380	73.4	73.4	0.5	0.1	2.6	1.0	653.1	1.9

Table 13. Mix design for concrete waste based geopolymer (M3) with incorporation of aluminum powder.

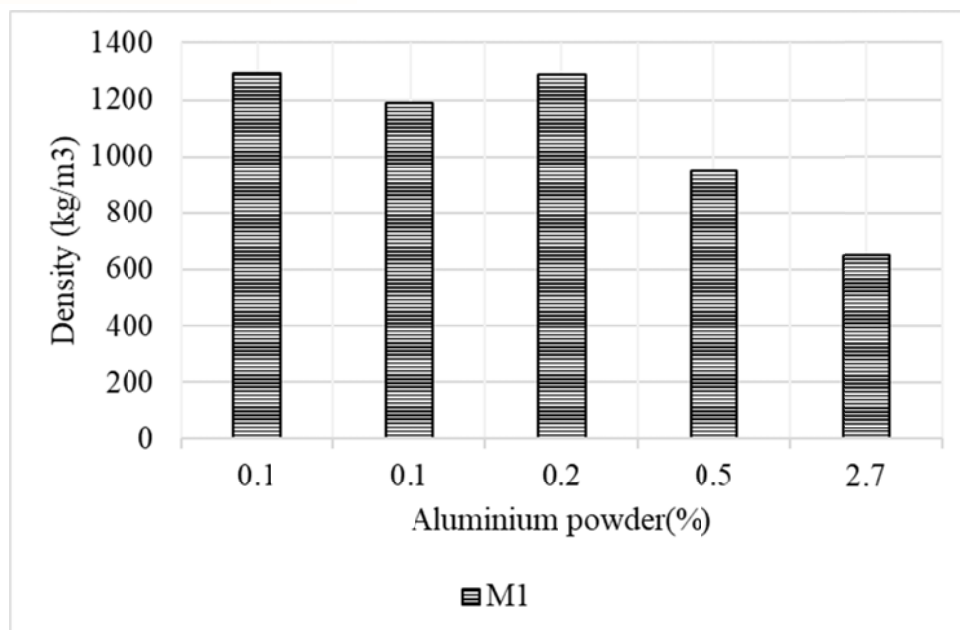| Mix ID	Specimen #	M3 (g)	KOH (PH) (ml)	NaOH (SH) (ml)	Na₂SiO₃ (SS) (ml)	H₂O₂ (ml)	Al (g)	H₂O₂ (%)	Al (%)	S/L	SS/ (PH or SH)	Average Density (kg/m³)	Average Compressive Strength (MPa)
C_CDW02	109-111	380		81.9	37.2		0.5		0.1	3.2	0.5	1095.4	3.1
C_CDW05	118-120	420	118		47.2		0.5		0.1	2.5	0.4	680.5	0.8
C_CDW09	130-133	380	71.2				0.6		0.2	5.3		1198.0	1.1
C_CDW10	134-136	380	35.6		35.6		0.6		0.2	5.3	1.0	1736.3	3.2

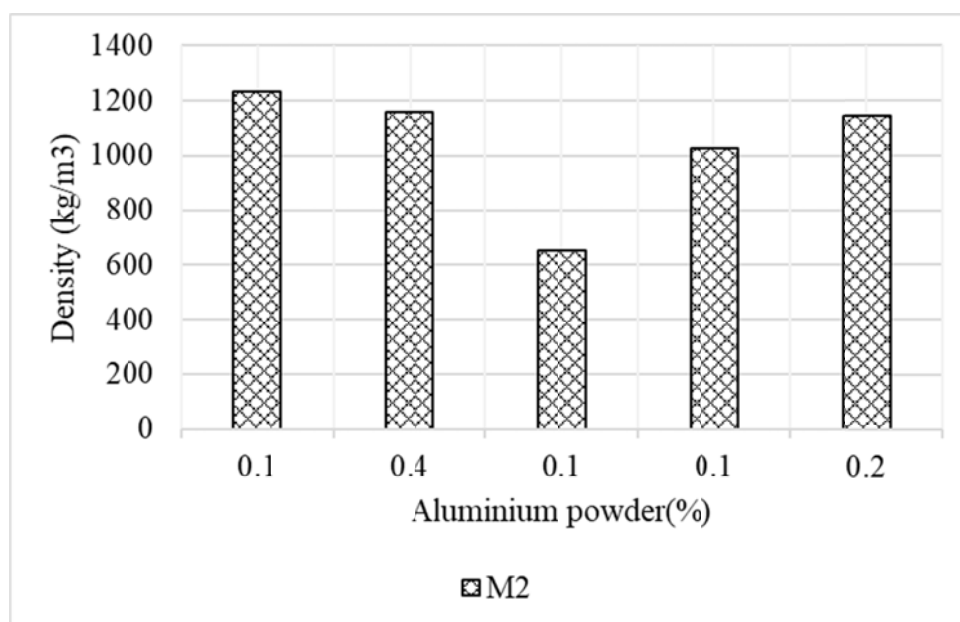**Figure 27**. Density of brick waste-based (M1) geopolymer.

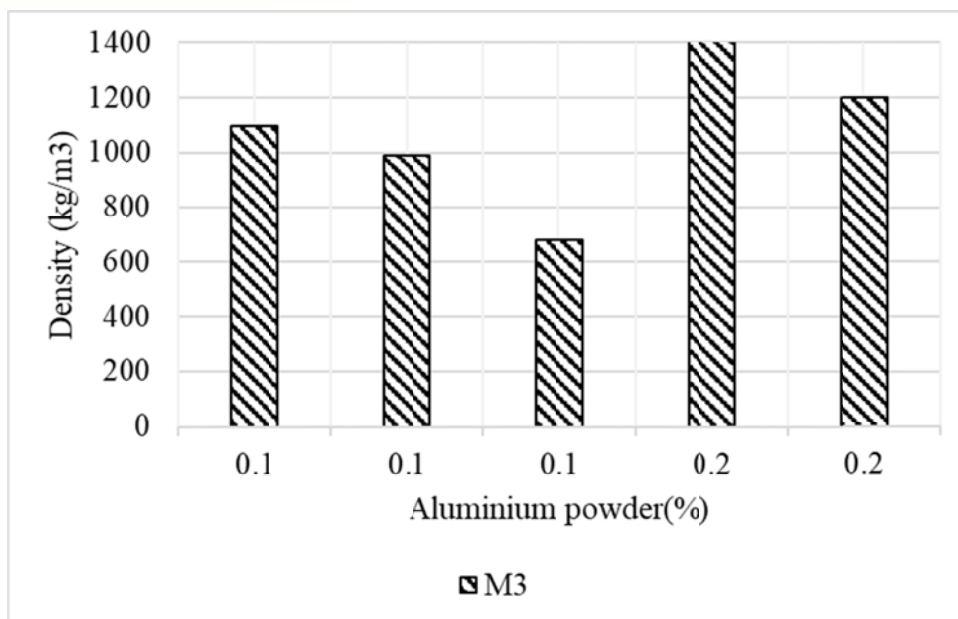**Figure 28**. Density of tile waste-based (M2) geopolymer.

Figure 29. Density of concrete waste-based (M3) geopolymer.

2. Effect of aluminum powder on compressive strength of brick waste (M1), tile waste (M2) and concrete waste (M3) based geopolymer
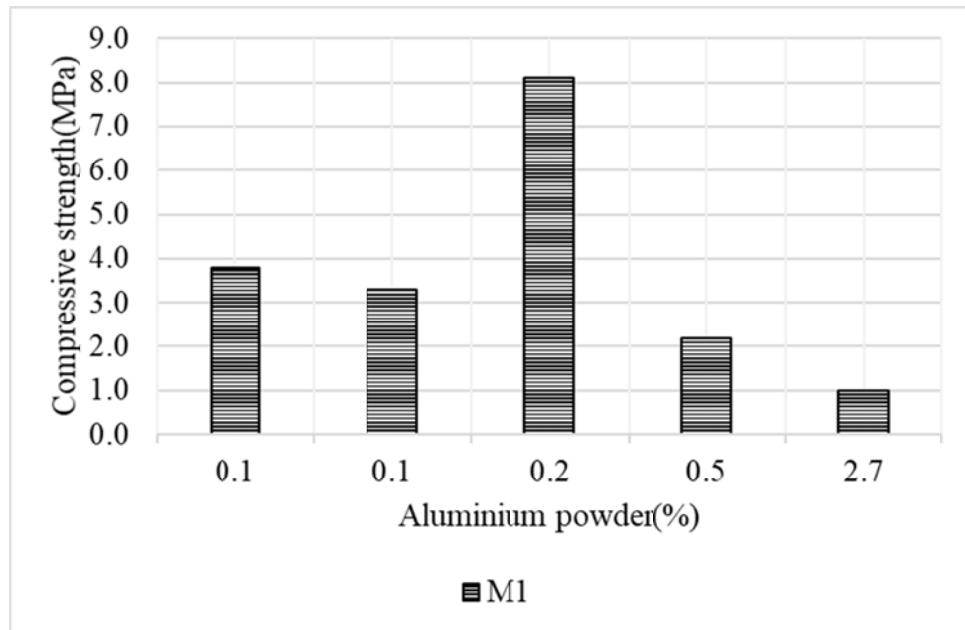

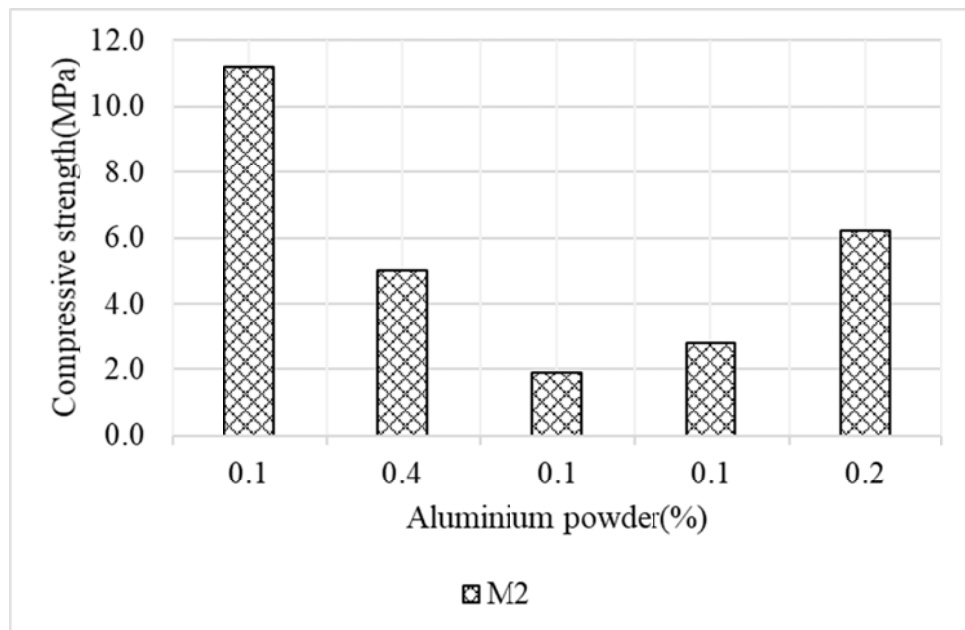**Figure 30**. Compressive strength of waste brick-based (M1) geopolymer.

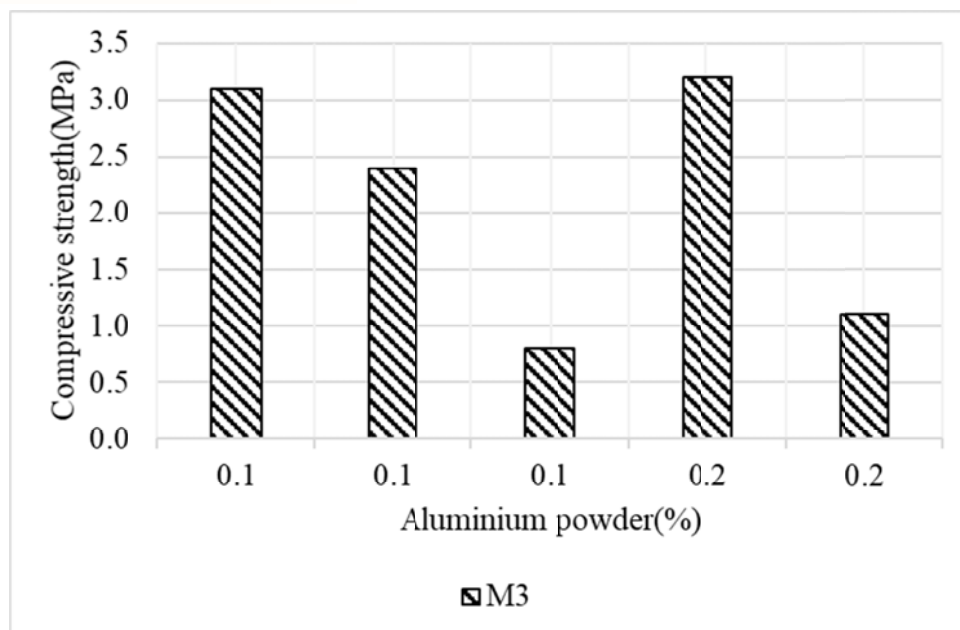**Figure 31**. Compressive strength of waste tile-based (M2) geopolymer.

Figure 32. Compressive strength of waste concrete-based (M3) geopolymer.

1. Effect of hydrogen peroxide on compressive strength of waste brick (M1), tile (M2) and concrete (M3) based geopolymers.

Table 14. Mix design for waste brick based geopolymer (M1) with incorporation of hydrogen peroxide.

Mix ID	Specimen #	M1 (g)	KOH (PH) (ml)	NaOH (SH) (ml)	Na$_2$SiO$_3$(SS) (ml)	H$_2$O$_2$ (ml)	H$_2$O$_2$ (%)	S/L	SS/(PH or SH)	Average Density (kg/m^3)	Average Compressive Strength (MPa)
B_CDW002	4-6	418		99.4	99.4	4.5	2.2	2.1	1.0	1326.3	4.0
B_CDW004	10-12	380	180.9			4.4	2.4	2.1		840.6	0.9
B_CDW007	19-21	420	191.0			6.0	3.0	2.1		765.0	0.0
B_CDW019	55-57	380	121.2			4.4	3.5			530.7	1.9
B_CDW022	64-66	380	90.9		30.3	5.0	4.0		0.3	866.0	1.1

Table 15. Mix design for waste tile based geopolymer (M2) with incorporation of hydrogen peroxide.

Mix ID	Specimen #	M2 (g)	KOH (PH) (ml)	Na$_2$SiO$_3$ (SS) (ml)	H$_2$O$_2$ (ml)	H$_2$O$_2$ (%)	S/L	SS/(PH or SH)	Average Density (kg/m^3)	Average Compressive Strength (MPa)
T_CDW03	73-75	420	112.0	56.0	6.0	3.4	2.4	0.5	1081.1	2.9
T_CDW04	76-78	420	127.0	64.0	8.0	4.0	2.1	0.5	1099.1	3.8
T_CDW06	82-84	420	90.5	90.5	10.0	5.2	2.2	1.0	1329.6	18.1
T_CDW12	100-102	380	22.4	67.1	4.7	5.0	4.0	3.0	1161.1	2.7
T_CDW13	103-105	380	67.1	22.4	4.7	5.0	4.0	0.3	1087.5	2.7

Table 16. Mix design for waste concrete based geopolymer (M3) with incorporation of hydrogen peroxide.

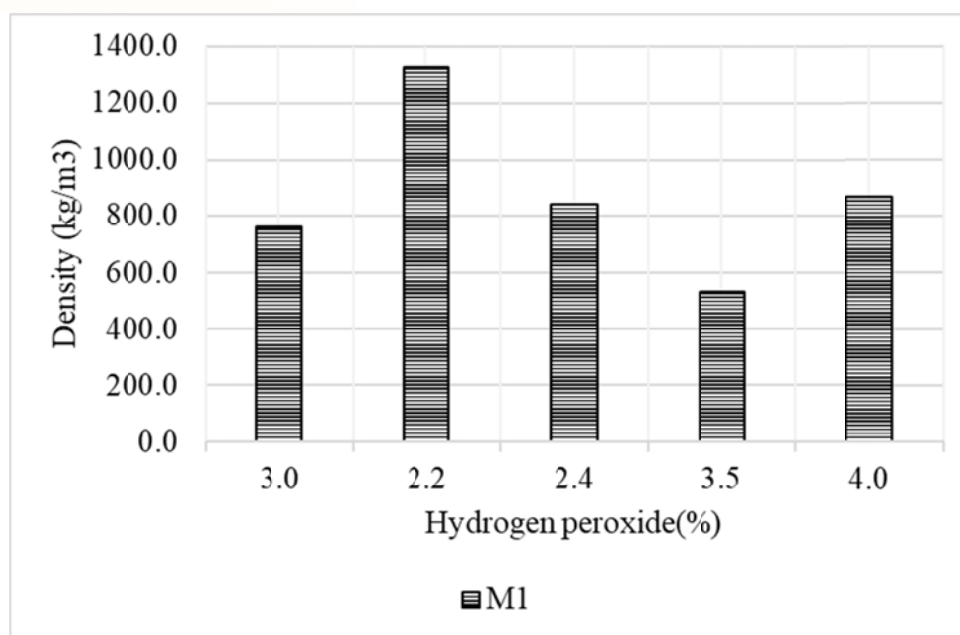| Mix ID	Specimen #	M3 (g)	KOH (PH) (ml)	NaOH (SH) (ml)	Na_2SiO_3 (SS) (ml)	H_2O_2 (ml)	Al (g)	H_2O_2 (%)	Al (%)	S/L	SS/(PH or SH)	Average density (kg/m^3)	Average compressive strength (MPa)
C_CDW01	106-108	580		163.8	64.4	4.5		1.9		2.5	0.4	990.7	3.1
C_CDW04	115-117	420	118		47.2	4.5		2.6		2.5	0.4	1188.5	3.5
C_CDW06	121-123	420	118		47.2	4.5	0.5	2.6	0.1	2.5	0.4	795.0	1.8
C_CDW11	137-139	380	71.2			4.5		5.9		5.0		1046.9	1.2
C_CDW12	140-142	380	35.6		35.6	4.5		5.9		5.0	1.0	1178.1	1.1

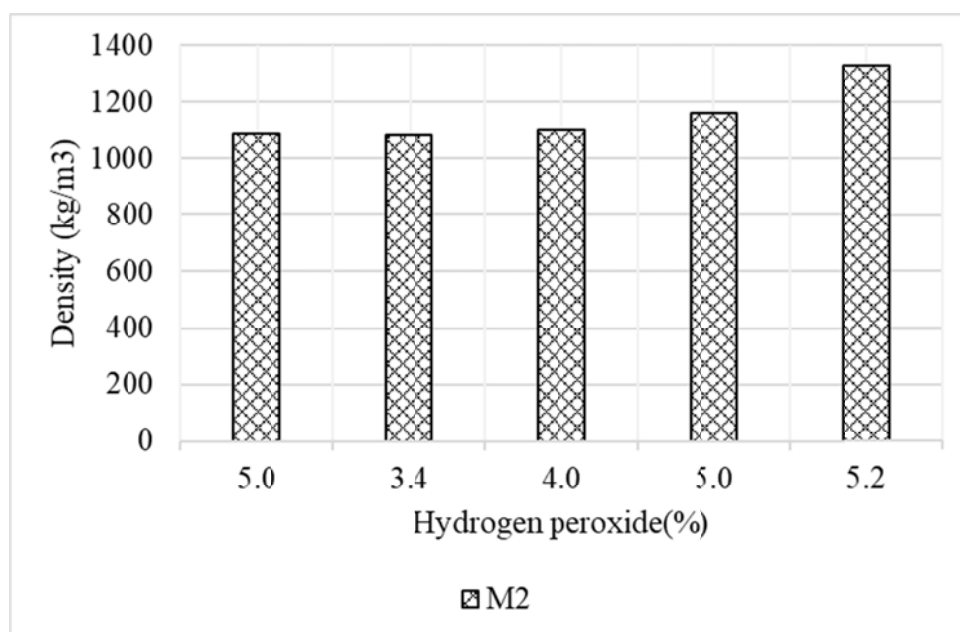**Figure 33**. Density of waste brick based (M1) geopolymer.

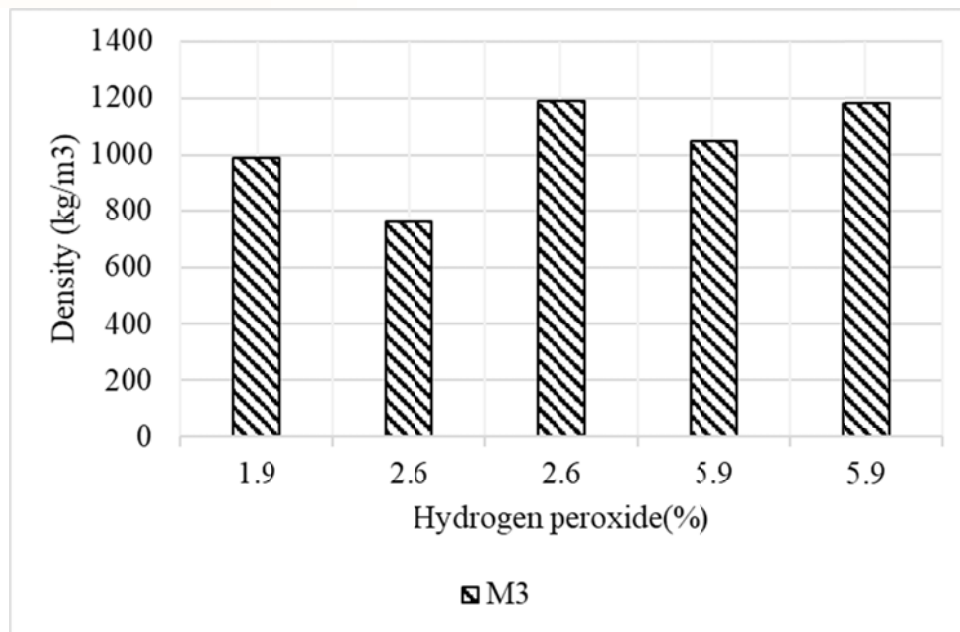**Figure 34**. Density of waste tile based (M2) geopolymer.

Figure 35. Density of waste concrete based (M3) geopolymer.

2. Effect of hydrogen peroxide on compressive strength of waste brick (M1), tile (M2) and concrete (M3) based geopolymers.
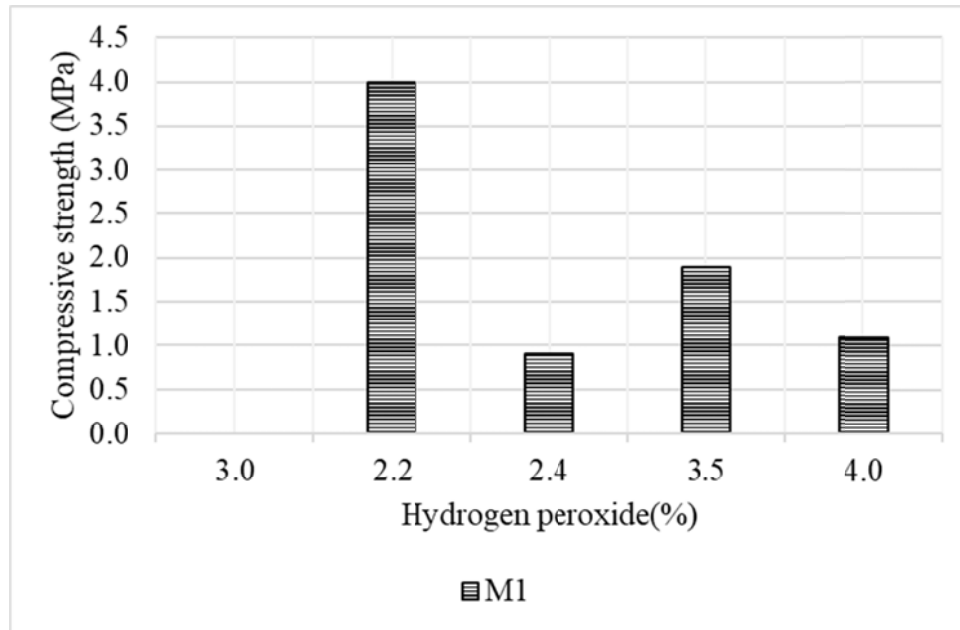

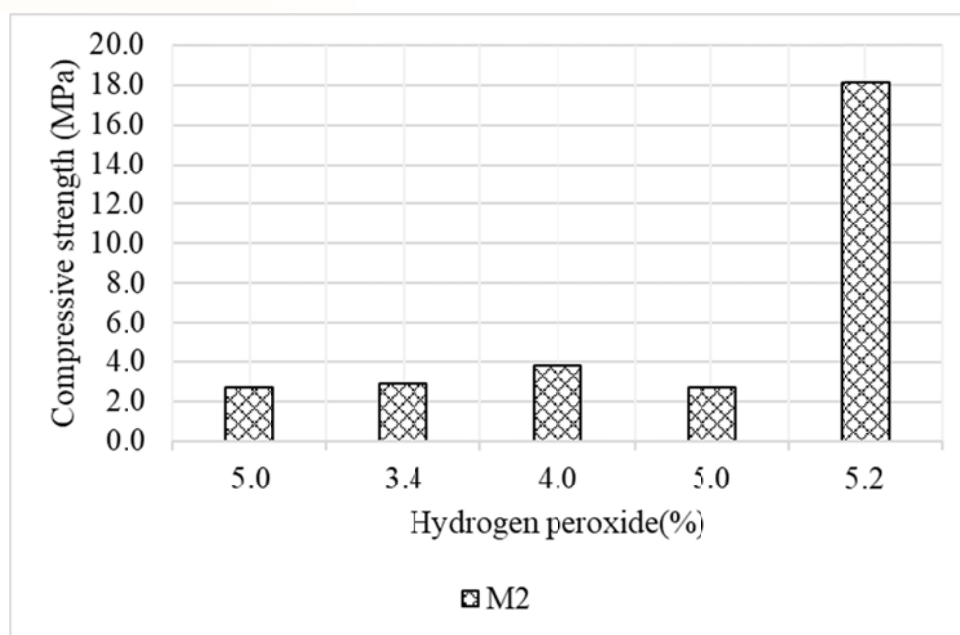**Figure 36**. Compressive strength of waste brick based (M1) geopolymers.

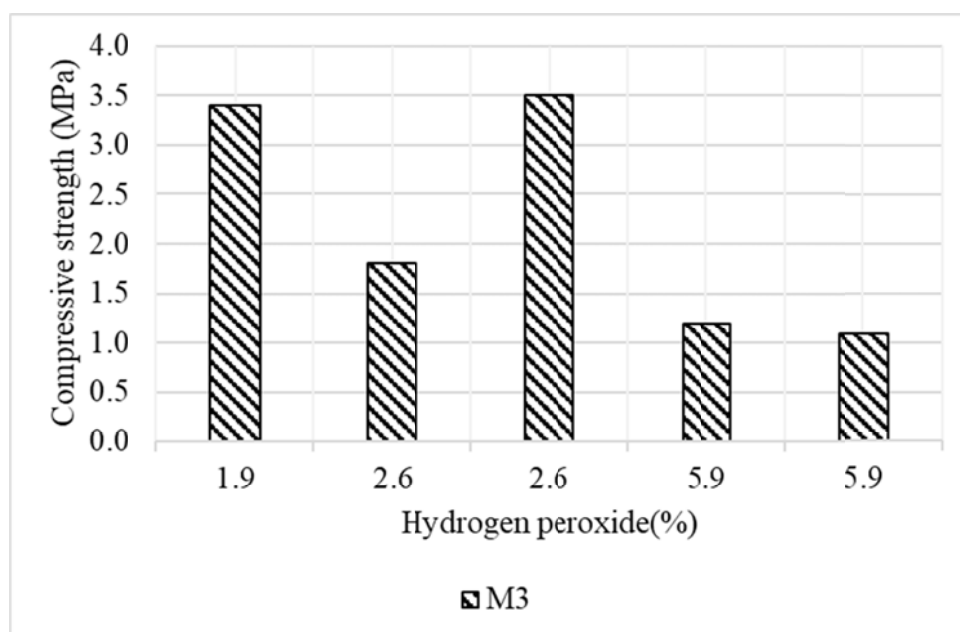**Figure 37**. Compressive strength of waste tile based (M2) geopolymers.

Figure 38. Compressive strength of waste concrete based (M3) geopolymer.

6. CONCLUSIONS

The current report summarizes the obtained experimental results related to the development of the thermal and the fire insulation materials that eventually will compose the DEFEAT composite. Despite the fact that WP5 ends in month 24 of the project, the results indicate that both materials nearly satisfy all the targeted values. The current report will be continuously updated throughout the duration of WP5 and a final version will be eventually prepared. The report also includes the results provided by the Katholieke Universiteit Leuven (KUL), which is the Foreign Organization of the DEFEAT consortium. KUL conducted a parallel experimental program to the Cyprus consortium, aiming to provide additional necessary information and/or to validate and confirm experimental results. Part of the work conducted by KUL (i.e. the part relevant to Deliverable D5.1) by the time of submission of the project's interim report is provided in Annex and is an integral part of the main report. Additional work is planned ahead, which will also be included in the final version of this report. The work by KUL will be extended in several other aspects of the DEFEAT project.

REFERENCES

1. G.J. Gluth, W.D. Rickard, S. Werner, S. Pirskawetz, Acoustic emission and microstructural changes in fly ash geopolymer concretes exposed to simulated fire, Mater. Struct. 49 (2016) 5243–5254.

2. M.W. Hussin, M.A.R. Bhutta, M. Azreen, P.J. Ramadhansyah, J. Mirza, Performance of blended ash geopolymer concrete at elevated temperatures, Mater. Struct. 48 (2015) 709–720.

3. J. Xin, C. Huang, Fire risk analysis of residential buildings based on scenario clusters and its application in fire risk management, Fire Saf. J. 62 (2013) 72–78.

4. D.L.Y. Kong, J.G. Sanjayan, Effect of elevated temperatures on geopolymer paste, mortar and concrete, Cem. Concr. Res. 40 (2010) 334–339.

5. S.J.G. Crozier, J.G. Sanjayan, Chemical and physical degradation of concrete at elevated temperature, Conc. Aust. 25 (1999) 18–20.

6.] Z. Pan, J.G. Sanjayan, B.V. Rangan, An investigation of the mechanisms for strength gain or loss geopolymer mortar after exposure to elevated temperature, J. Mater. Sci. 44 (2009) 1873–1880.

7. N. Ranjbar, M. Mehrali, U.J. Alengaram, H.S.C. Metselaar, M.Z. Jummat, Compressive strength and microstructural analysis of fly ash/ palm oil fuel ash based geopolymer mortar under elevated temperatures, Const. Build. Mater. 65 (2014) 114–121.

8. A.M. Rashad, S.R. Zeedan, The effect of activator concentration on the residual compressive strength of alkali- activated fly ash paste subjected to thermal load, Constr. Build. Mater. 25 (2011) 3098–3107.

9. K. Sakkas, P. Nomikos, A. Sofianos, D. Panias, G. Anagnostou, Slag based geopolymer for passive fire protection of tunnels underground, The Way to the Future (2013) 343–349.

10. European Commission, 2011. COM (2011) 571 Final. Communication from the Commission to the European Parliament, the Council, the European Economic and Social Committee and the Committee of the Regions: Roadmap to a Resource Efficient Europe. Brussels.

11. European Commission, 2020. COM (2020) 98 Final. Communication from the Commission to the European Parliament, the Council, the European Economic and

Social Committee and the Committee of the Regions: A New Circular Economy Action Plan for a Cleaner and More Competitive Europe. Brussels.

12. Herczeg, M., McKinnon, D., Milios, L., Bakas, I., Klaassens, E., Svatikova, K., Widerberg, O., 2014. Resource Efficiency in the Building Sector – Final Report. Ecorys - Copenhagen Resource Institute, Rotterdam.

13. European Commission, 2018. Development and Implementation of Initiatives Fostering Investment and Innovation in Construction and Demolition Waste Recycling Infrastructure. Final Report. Directorate-General for Internal Market, Industry, Entrepreneurship and SMEs; Industrial Transformation and Advanced Value Chain, ISBN 978-92-79-68097-7. IDEA Consult NV/SA.

14. Arenas, C., Luna-Galiano, Y., Leiva, C., Vilches, L.F., Arroyo, F., Villegas, R., Fern´andezPereira, C., 2017. Development of a fly ash-based geopolymeric concrete with construction and demolition wastes as aggregates in acoustic barriers. Construct. Build. Mater. 134, 433–442.

15. Robayo-Salazar, R.A., Rivera, J.G., Mejía de Guti´errez, R., 2017. Alkali-activated building materials made with recycled construction and demolition wastes. Construct. Build. Mater. 149, 130–138.

16. Robayo-Salazar, R.A., Mejía-Arcila, J.M., Mejía de Guti´errez, R., 2017. Eco-efficient alkali-activated cement based on red clay brick wastes suitable for the manufacturing of building materials. J. Clean. Prod. 166, 242–252.

17. Robayo-Salazar, R.A., Valencia-Saavedra, W., Mejía de Guti´errez, R., 2020. Construction and demolition waste (CDW) recycling—as both binder and aggregates—in alkaliactivated materials: a novel Re-use concept. Sustainability 12, 5775.

18. H. Ulugol, ¨A. Kul, G. Yıldırım, M. S¸ ahmaran, A. Aldemir, D. Figueira, A. Ashour, Mechanical and microstructural characterization of geopolymers from assorted construction and demolition waste-based masonry and glass, J. Clean. Prod. 280 (2021) 124358.

19. G. Yıldırım, A. Kul, E. Ozçelikci, ¨M. S¸ ahmaran, A. Aldemir, D. Figueira, A. Ashour, Development of alkali-activated binders from recycled mixed masonry-originated waste, J. Build. Eng. 33 (2021) 101690.

20. C.S. Poon, A.T.W. Yu, L.H. Ng, On-site sorting of construction and demolition waste in Hong Kong, Resour. Conserv. Recycl. 32 (2001) 157–172.

21. Luhar, S., Chaudhary, S., & Luhar, I. (2018). Thermal resistance of fly ash based rubberized geopolymer concrete. Journal of Building Engineering, 19, 420-428.

22. Davidovits, J. Geopolymers: Inorganic polymeric new materials. J. Therm. Anal. 1991, 37, 1633–1656.

23. Luhar, S., Nicolaides, D., & Luhar, I. (2021). Fire Resistance Behaviour of Geopolymer Concrete: An Overview. Buildings, 11(3), 82.

24. Davidovits, J. Geopolymer Chemistry and Applications; Institut Géopolymère: Saint-Quentin, France, 2008.

25. Duxson, P.; Fernandez-Jimenez, A.; Provis,, J.L.; Lukey, G.C.; Palomo, A.; van Deventer, J.S.J. Geopolymer technology: The current state of the art. J. Mater. Sci. 2007, 42, 2917–2933.

26. Duxson, P.; Lukey, G.C.; van Deventer, J.S.J. Thermal evolution of metakaolin geopolymers: Part 1—physical evolution. J. Non Cryst. Solids 2006, 352, 5541–5555.

27. Barbosa, V.F.F.; MacKenzie, K.J.D. Synthesis and thermal behaviour of potassium sialate geopolymers. Mater. Lett. 2003, 57, 1477–1482.

28. Duxson, P.; Lukey, G.C.; van Deventer, J.S.J. The thermal evolution of metakaolin geopolymers: Part 2—Phase stability and structural development. J. Non Cryst. Solids 2007, 353, 2186–2200.

29. Krivenko, P.V.; Kovalchuk, G.Y. Directed synthesis of alkaline aluminosilicate minerals in a geocement matrix. J. Mater. Sci. 2007, 42, 2944–2952.

30. Barbosa, V.F.F.; MacKenzie, K.J.D. Thermal behaviour of inorganic geopolymers and composites derived from sodium poLysialate. Mater. Res. Bull. 2003, 38, 319–331.

31. H. Ulug̈ol, A. Kul, G. Yıldırım, M. S̨ahmaran, A. Aldemir, D. Figueira, A. Ashour, Mechanical and microstructural characterization of geopolymers from assorted construction and demolition waste-based masonry and glass, J. Clean. Prod. 280 (2021) 124358.

32. G. Yıldırım, A. Kul, E. ̈Ozçelikci, M. S̨ahmaran, A. Aldemir, D. Figueira, A. Ashour, Development of alkali-activated binders from recycled mixed masonry-originated waste, J. Build. Eng. 33 (2021) 101690.

33. A. Allahverdi, E. Najafi Kani, Construction wastes as raw materials for geopolymer binders, Int. J. Civ. Eng. 7 (2009) 154–160.

34. L. Reig, M.M. Tashima, L. Soriano, M. V Borrachero, J. Monz´o, J. Pay´a, Alkaline activation of ceramic waste materials, Waste Biomass Valoriz. 4 (2013) 729–736.

35. K. Komnitsas, D. Zaharaki, A. Vlachou, G. Bartzas, M. Galetakis, Effect of synthesis parameters on the quality of construction and demolition wastes (CDW) geopolymers, Adv. Powder Technol. 26 (2015) 368–376.

36. G. Silva, D. Casta˜neda, S. Kim, A. Casta˜neda, B. Bertolotti, L. Ortega-San-Martin, J. Nakamatsu, R. Aguilar, Analysis of the production conditions of geopolymer matrices from natural pozzolana and fired clay brick wastes, Construct. Build. Mater. 215 (2019) 633–643.

37. R. Xiao, Y. Ma, X. Jiang, M. Zhang, Y. Zhang, Y. Wang, B. Huang, Q. He, Strength, microstructure, efflorescence behavior and environmental impacts of waste glass geopolymers cured at ambient temperature, J. Clean. Prod. 252 (2020) 119610.

38. M. Torres-Carrasco, F. Puertas, Waste glass in the geopolymer preparation. Mechanical and microstructural characterisation, J. Clean. Prod. 90 (2015) 397–408.

39. M. Cyr, R. Idir, T. Poinot, Properties of inorganic polymer (geopolymer) mortars made of glass cullet, J. Mater. Sci. 47 (2012) 2782–2797.

40. M. Vafaei, A. Allahverdi, High strength geopolymer binder based on waste-glass powder, Adv. Powder Technol. 28 (2017) 215–222.

41. R.A. Robayo-Salazar, J.F. Rivera, R. Mejía de Guti´errez, Alkali-activated building materials made with recycled construction and demolition wastes, Construct. Build. Mater. 149 (2017) 130–138.

42. S. Dadsetan, H. Siad, M. Lachemi, M. Sahmaran, Construction and demolition waste in geopolymer concrete technology: a review, Mag. Concr. Res. 71 (2019) 1232–1252.

43. Abdulkareem, O.A.; Al-bakri, A.M.M.; Kamarudin, H.; Nizar, I.K.; Saif, A.A. Effects of elevated temperatures on the thermal behaviour and mechanical performance of fly ash geopolymer paste, mortar and light weight concrete. Constr. Build. Mater. 2014, 50, 337–387.

44. Rickard, W.D.A.; Temuujin, J.; van-Riessen, A. Thermal analysis of geopolymer pastes synthesized from five fly ashes of variable compositions. J. Non Cryst. Solids 2012, 358, 1830–1839.

45. Ranjbar, N.;Mehrali,M.; Alengaram, U.J.;Metselaar, H.S.C.; Jumaat,M.Z. Compressive strength andmicrostructural analysis of fly ash/palmoil fuel ash based

geopolymermortar under elevated temperatures. Constr. Build. Mater. 2014, 65, 114–121.

46. Nayaka, R.R.; Alengaram, U.J.; Jumaat,M.Z.; Yusoff, S.B.; Alnahhal,M.F. High volume cement replacement by environmental friendly industrial by-product palmoil clinker powder in cement–limemasonrymortar. J. Clean. Prod. 2018, 190, 272–284.

47. Bakharev, T. Thermal behaviour of geopolymers prepared using class F fly ash and elevated temperatures curing. Cem. Concr. Res. 2006, 36, 1134–1147.

48. Kong, D.L.Y.; Sanjayan, J.G. Effect of elevated temperatures on geopolymer paste, mortar and concrete. Cem. Concr. Res. 2010, 40, 334–339.

49. Kong, D.L.Y.; Sanjayan, J.G.; Sagoe-Crentsile, K. Comparative performance of geopolymers made with metakaolin and fly ash after exposure to elevated temperatures. Cem. Concr. Res. 2007, 37, 1583–1589.

50. Guerrieri, M.; Sanjayan, J.G. Behaviour of combined fly ash/slag based geopolymers when exposed to high temperatures. Fire Mater. 2010, 34, 163–175.

51. Rickard, W.D.A.; Vickers, L.; van Riessen, A. Performance of fibre reinforced, lowdensity metakaolin geopolymers under simulated fire conditions. Appl. Clay Sci. 2013, 73, 71–77.

52. Giancaspro, J.; Balaguru, P.N.; Lyon, R.E. Use of inorganic polymer to improvethe fire response of balsa sandwich structures. J. Mater. Civ. Eng. 2006, 18, 390–397.

53. Lyon, R.E.F.; Foden, A.J.; Balaguru, P.; Davidovits, J.; Davidovits, M. Properties of geopolymer matrix in carbon fibre composites. In Proceedings of the 2nd International Conference Geopolymere, Geopolymer Institute, Saint-Quentin, France, 1–2 July 1999; pp. 67–73.

54. Davidovits, J. Fireproof geopolymeric cements. In Proceedings of the 2nd International Conference Geopolymere, Geopolymer Institute, Saint-Quentin, France, 30 June–2 July 1999; pp. 165–169.

55. Liefke, E. Industrial applications of foamed inorganic polymers. In Proceedings of the 2nd International Conference Geopolymere, Geopolymer Institute, Saint-Quentin, France, 1–2 July 1999; pp. 189–199.

56. Büchler, C. Fire safety in industrial buildings and nuclear power plants with airfilters made of geopolymer composite. In Proceedings of the 2nd International Conference Geopolymere, Geopolymer Institute, Saint-Quentin, France, 1–2 July 1999; pp.181–188.

57. Messina, F.; Ferone, C.; Colangelo, F.; Roviello, G.; Cioffi, R. Alkali activated waste fly ash as sustainable composite: Influence of curing and pozzolanic admixtures on the early-age physico-mechanical properties and residual strength after exposure at elevated temperature. Compos. Part B Eng. 2018, 132, 161–169.

58. Gourley, J.T.; Johnson, G.B. Developments in geopolymer precast concrete. In Proceedings of theWorld Congress Geopolymer, Geopolymer Institute, Saint-Quentin, France, 28 June–1 July 2005; pp. 139–143.

59. Perera, D.S.; Trautman, R.L. Geopolymers with the potential for use as refractory Castables. Adv. Technol. Mater. Mater. Process. 2005, 7, 187–190.

60. Kamseu, E.; Rizzuti, A.; Leonelli, C.; Perera, D. Enhanced thermal stability in K2O-metakaolin-based geopolymer concretes by Al2O3 and SiO2 fillers addition. J. Mater. Sci. 2010, 45, 1715–1724.

61. Temuujin, J.; Rickard, W.; Lee, M.; van Riessen,, A. Preparation and thermal properties of fire resistant metakaolin-based geopolymer-type coatings. J. Non Cryst. Solids 2011, 357, 1399–1404.

62. Rickard,W.D.A.; van Riessen, A. Performance of solid and cellular structured fly ash geopolymers exposed to a simulated fire. Cem. Concr. Compos. 2014, 48, 75–82.

63. Sakkas, K.; Nomikos, P.; Sofianos, A.; Panias, D. Inorganic polymeric materials for passive fire protection of underground constructions. Fire Mater. 2013, 37, 140–150.

64. Whittaker, E.J.W.; Muntus, R. Ionic radii for use in geochemistry. Geochim. Cosmochim. Acta 1970, 34, 945–956.

65. Huang, L.; Kieffer, J. Structural origin of negative thermal expansion in high-temperature silica polymorphs. Phys. Rev. Lett. 2005, 95, 215901.

66. Zuda, L.; Cˇ erný, R. Measurements of linear thermal expansion coefficient of alkali-activated aluminosilicate composites up to 1000 C. Cem. Concr. Compos. 2009, 31, 263–267.

67. Konon, M.Y.; Stolyar, S.V.; Dikaya, L.F.; Polyakova, I.G.; Drozdova, I.A.; Antropova, T.V. Physicochemical properties of glasses of the Na2O–B2O3–SiO2–Fe2O3 system in the 8Na2O/70SiO2 section 1. Glas. Phys. Chem. 2015, 41, 116–121.

68. He, J.; Zhang, J.; Yu, Y.; Zhang, G. The strength and microstructure of two geopolymers derived from metakaolin and red mud-fly ash admixture: A comparative study. Constr. Build. Mater. 2012, 30, 80–91.

69. Lyon, R.E.; Balaguru, P.N.; Foden, A.; Sorathia, U.; Davidovits, J.; Davidovics, M. Fire resistant aluminosilicate composites. Fire Mater. 1997, 21, 67–73.

70. Kong, D.; Sanjayan, J.; Sagoe-Crentsil, K. Factors affecting the performance of metakaolin geopolymers exposed to elevated temperatures. J. Mater. Sci. 2008, 43, 824–831.

71. Li, C.; Sun, H.; Li, L. A review: The comparison between alkali activated slag (Si+Ca) and Metakaolin (Si+Al) cement. Cem. Concr. Res. 2005, 40, 1341–1349.

72. Fernandez-Jimenez, A.; Palomo, A.; Criado, M. Microstructure development of alkali activated fly ash cement, a descriptive model. Cem. Concr. Res. 2005, 35, 120–126.

73. Park, S.M.; Jang, J.G.; Lee, N.K.; Lee, H.K. Physiochemical properties of binder gel in alkali activated fly ash/slag exposed to high temperature. Cem. Concr. Res. 2016, 89, 72–79.

74. Kong, D.L.Y.; Sanjayan, J.G. Damage behaviour of geopolymer composites exposed to elevated temperatures. Cem. Concr. Compos. 2008, 30, 986–991.

75. Bernal, S.; Rodríguez, E.; Mejía de Gutiérrez, R.; Gordillo, M.; Provis, J. Mechanical and thermal characterisation of geopolymers based on silicate-activated metakaolin/ slag blends. J. Mater. Sci. 2011, 46, 5477–5486.

76. Lahoti, M.; Yang, E.-H.; Tan, K.H. Developments in Strategic Ceramic Materials II. In Influence of Mix Design Parameters on Geopolymer Mechanical Properties and Microstructure; John Wiley & Sons: Hoboken, NJ, USA, 2017; pp. 21–33.

77. Duxson, P.; Provis, J.L.; Lukey, G.C.; Mallicoat, S.W.; Kriven, W.M.; van Deventer, J.S.J. Understanding the relationship between geopolymer composition, microstructure and mechanical properties. Colloids Surf. A Physicochem. Eng. Asp. 2005, 269, 47–58.

78. Subaer, A.; van Riessen, A. Thermo-mechanical and microstructural characteri-sation of sodium-poly(sialate-siloxo) (Na-PSS) geopolymers. J. Mater. Sci. 2007, 42, 3117–3123.

79. Lin, T.S.; Jia, D.C.; He, P.G.; Wang, M.R. Thermomechanical and microstructural characterisation of geopolymers with alpha alumina particulate filler. Int. J. Thermophys. 2009, 30, 1568–1577.

80. Bell, J.; Gordon, M.; Kriven, W.M.; Comrie, D. Graphite fiber reinforced geopolymer molds for near net shape casting of molten diferrous silicide, conferencepaper. In Proceedings of the Workshop on Geopolymers and Geopolymer Concrete, Perth, Western Australia, 28–29 September 2005; p. 12.

81. Silva, F.J.; Mathias, A.F.; Thaumaturgo, C. Evaluation of the fracture toughness in poly(sialate-siloxo) composite matrix, conference paper. Geopolymer 1999, 99, 97–106.

82. Duxson, P.; Lukey, G.C.; van Deventer, J.S.J. Physical evolution of Na-geopolymer derived from metakaolin up to 1000C. J. Mater. Sci. 2007, 42, 3044–3054.

83. He, P.; Jia, D.; Wang, M.; Zhou, Y. Thermal evolution and crystallization kinetics of potassium-based geopolymer. Ceram. Int. 2011, 37, 59–63.

84. Vidal, L.; Joussein, E.; Colas, M.; Absi, J.; Rossignol, S. Effect of the addition of ammonium molybdate on metakaolin-based geopolymer formation: Shrinkage and crystallization. Powder Technol. 2015, 275, 211–219.

85. Kuenzel, C.; Li, L.; Vandeperre, L.; Boccaccini, A.R.; Cheeseman, C.R. Influence of sand on the mechanical propeties of metakaolin geopolymers. Constr. Build. Mater. 2014, 66, 442–446.

86. Duan, P.; Yan, C.J.; Zhou,W.; Luo,W.J.; Shen, C.H. An investigation of the microstructure and durability of a fluidized bed fly ash-metakaolin geopolymer after heat and acid exposure. Mater. Des. 2015, 74, 125–137.

87. Samal, S.; Thanh, N.P.; Petríková, I.; Marvalová, B. Improved mechanical properties of various fabric-reinforced geocomposites at elevated temperature. J. Met. 2015, 67, 1478–1485.

88. Sarker, P.K.; Kelly, S.; Yao, Z.T. Effect of fire exposure on cracking, spalling and residual strength of fly ash geopolymer concrete. Mater. Des. 2014, 63, 584–592.

89. Tugnoli, A.; Moricone, R.; Scarponi, G.E.; Cozzani, V. Effective thermal conductivity of fibrous fireproofing materials. Int. J. Therm. Sci. 2019, 136, 107–120.

90. Suvorov, S.A.; Skurikhin, V.V. Vermiculite—A promising material for high-temperature heat insulators. Refract. Ind. Ceram. 2003,44, 186–193.

91. Murri, N.A.; Rickard,W.D.A.; Bignozzi, M.C.; van Riessen, A. High temperature behaviour of ambient cured alkali-activated materials based on ladle slag. Cem. Concr. Res. 2013, 43, 51–61.

92. Mohamedbhai, G.T.G. Effect of exposure time and rates of heating and cooling on residual strength of heated concrete. Mag. Concr. Res. 1986, 38, 151–158.

93. Heikal, M. Effect of temperature on the physico- mechanical and mineralogical properties of homra pozzolanic cement pastes. Cem. Concr. Res. 2000, 30, 1835–1839.

94. Khoury, G.A.; Grainger, B.N.; Sullivan, P.J.E. Strain of concrete during fast cooling form 600 C under load. Mag. Concr. Res. 1986, 38, 3–12.

95. Li, Z.; Xu, J.; Bai, E. Static and dynamic mechanical properties of concrete after high temperature exposure. Mater. Sci. Eng. A 2012, 544, 27–32.

96. Kong, D.L.Y.; Sanjayan, J.G. Damage due to elevated temperatures in metakaolinite-based geopolymer pastes. In Proceedings of the International Workshop on Geopolymer and Geopolymer Concrete, Perth, Australia, 28–29 September 2005.

97. Papayianna, I.; Valliasis, T. Heat deformations of fly ash concrete. Cem. Concr. Comp. 2005, 27, 249–254.

98. Poon, C.S.; Azhar, S.; Anson, M.;Wong, Y.L. Performance of metakaolin concrete at elevated temperatures. Cem. Concr. Comp. 2003, 25, 83–89.

99. Pan, Z.; Sanjayan, J.; Rangan, B. An investigation of the mechanisms for strength gain or loss of geopolymer mortar after exposure to elevated temperature. J. Mater. Sci. 2009, 44, 1873–1880.

100. Khoury, G.A. Effect of fire on concrete and concrete structures. Fire Concr. 2000, 2, 429–447.

101. Wang, H.; Li, H.; Wang, Y.; Yan, F. Preparation of macroporous ceramic from metakaolinite-based geopolymer by calcination. Ceram. Int. 2015, 41, 11177–11183.

102. Temuujin, J.; Rickard,W.; Van Riessen, A. Characterization of various fly ashes for preparation of geopolymers with advanced applications. Adv. Powder Technol. 2013, 24, 495–498.

103. Zhang, H.; Kodur, V.; Bo, W.U.; Wang, C.F. Thermal behaviour and mechanical properties of geopolymer mortar after exposure to elevated temperatures. Constr. Build. Mater. 2016, 109, 17–24.

104. Temuujin, J.;Williams, R.P.; Van Riessen, A. Effect of mechanical activation of fly ash on the properties of geopolymer cured at ambient temperature. J. Mater. Process. Technol. 2009, 209, 5276–5280.

105. Fan, F.; Guoji, X.U.; Peng, H.; Cai, C.S. Mechanical and thermal properties of fly ash based geopolymers. Constr. Build. Mater. 2018, 160, 66–81.

106. Demirel, B.; Kelestemur, O. Effect of elevated temperature on the mechanical properties of concrete produced with finely ground pumice and silica fume. Fire Saf. J. 2010, 45, 385–391.

107. Hosan, A.; Haque, S.; Shaikh, F. Compressive behaviour of sodium and potassium activators synthetized fly ash geopolymer at elevated temperatures: A comparative study. J. Build. Eng. 2016, 8, 123–130.

108. Duan, P.; Yan, C.; Zhou,W. Compressive strength and microstructure of fly ash based geopolymer blended with silica fume under thermal cycle. Cem. Concr. Compos. 2017, 78, 108–119.

109. Zhang, H.Y.; Kodur, V.; Qi, S.L.; Cao, L.; Wua, B. Development of metakaolin–fly ash based geopolymers for fire resistance applications. Constr. Build. Mater. 2014, 55, 38–45.

110. Lahoti, M.; Wong, K.K.; Tan, K.H.; Yang, E.-H. Effect of alkali cation type on strength endurance of fly ash geopolymers subject to high temperature exposure. Mater. Des. 2018, 154, 8–19.

111. Samal, S. Effect of high temperature on the microstructural evolution of fiber reinforced geopolymer composite. Heliyon 2019, 5, e01779.

112. Pan, Z.; Sanjayan, G.J.; Collins, F. Effect of transient creep on compressive strength of geopolymer concrete for elevated temperature exposure. Cem. Concr. Res. 2014, 56, 182–189.

113. Lahoti, L.; Wong, K.K.; Yang, E.-H.; Tan, K.H. Effects of Si/Al molar ratio on strength endurance and volume stability of metakaolin geopolymers subject to elevated temperature. Ceram. Int. 2018, 44, 5726–5734.

114. Mathewa, G.; Joseph, B. Flexural behaviour of geopolymer concrete beams exposed to elevated temperatures. J. Build. Eng. 2018, 15, 311–317.

115. Kljajevi´c, L.M.; Nenadovi´c, S.S.; Nenadovi´c, M.T.; Bundaleski, N.K.; Todorovi´c, B.Ž.; Pavlovi´c, V.B.; Rakoˇcevi´c, Z.L. Structural and chemical properties of thermally treated geopolymer samples. Ceram. Int. 2017, 43, 6700–6708.

116. Sivasakthi, M.; Jeyalakshmi, R.; Rajamane, N.P.; Rinu, J. Thermal and structural micro analysis of micro silica blended fly ash based geopolymer composites. J. Non Cryst. Solids 2018, 499, 117–130.

117. Akçaozoglu Semiha, Ulu Cüneyt, Recycling of waste PET granules as aggregate in alkali-activated blast furnace slag/metakaolin blends, Construct. Build. Mater. 58 (2014) 31–37.

118. Bilim Cahit, Karahan Okan, Cengiz Duran Atiş, Ilkentapar Serhan, Influence of admixtures on the properties of alkali-activated slag mortars subjected to different curing conditions, Mater. Des. 44 (2013) 540–547.

119. Chi Maochieh, Effects of dosage of alkali-activated solution and curing conditions on the properties and durability of alkali-activated slag concrete, Construct. Build.Mater. 35 (2012) 240–245.

120. Oswaldo Burciaga-Díaz, Y. Gomez-Zamorano Lauren, Jose Ivan Escalante-García, Influence of the long term curing temperature on the hydration of alkaline binders of blast furnace slag-metakaolin, Construct. Build. Mater. 113 (2016) 917–926.

121. P. De Silva, K. Sagoe-Crenstil, V. Sirivivatnanon, Kinetics of geopolymerization: role of Al2O3 and SiO2, Cement Concr. Res. 37 (2007) 512–518.

122. Khale Divya, Chaudhary Rubina, Mechanism of geopolymerization and factors influencing its development a review, J. Mater. Sci. 42 (2007) 728–746.

123. Bajare Diana, Vitola Laura, Dembovska Laura, Bumanis Girts, Waste steamporous

7. alkali activated materials for high temperature application", Frontiers in Materials 6 (92) (2019) 1–13.

124. Tran Tai Thanh, Hyug-Moon Kwon, Influence of activator Na2O concentration on residual strengths of alkali-activated slag mortar upon exposure to elevated temperatures, Materials 11 (1296) (2018) 1–19.

125. Chithambaram S. Jeeva, Sanjay Kumar, M.M. Prasad, Thermo-mechanical characteristics of geopolymer mortar, Construct. Build. Mater. 213 (2019) 100–108.

126. Sun Zengqing, Cui Hao, An Hao, Tao Dejing, Xu Yan, Zhai Jianping and Li Qin, "Synthesis and thermal behavior of geopolymer-type material from waste ceramic" Construct. Build. Mater., 49, 281-287.

127. Zhu Pan, G. Sanjayan Jan, B.V. Rangan, An investigation of the mechanism for strength gain or loss of geopolymer mortar after exposure to elevated temperature 44 (2009) 1873–1880.

128. M. Rashad Alaa, H. Khalil Mervat, A preliminary study of alkali-activated slag blended with silica fume under the effect of thermal loads and thermal shock cycles, Construct. Build. Mater. 40 (2013) 522–532.

129. Wei-Chien Wang, Her-Yung Wang, Lo Ming-Hung, The engineering properties of alkali-activated slag pastes exposed to high temperatures, Construct. Build. Mater. 68 (2014) 409–415.

130. Ikmal Hakem Aziz, Cheng-Yong Heah, Moh Mustafa Al Bakri Abdullah, Liew Yun Ming, Behaviour changes of ground granulated blast furnace slag geopolymer at high temperature, Adv. Cement Res. (2019).

131. Hakan Tacettin Türker, Balçikanli Müzeyyen,Ibrahim Halil Durmus¸ Ozbay Erdogan, Erdemir Mustafa, Microstructural alteration of alkali activated slag mortars depend on exposed high temperature level, Construct. Build. Mater. 104 (2016) 169–180.

132. A.M. Rashad, Y. Bai, P.A.M. Basheer, N.C. Collier, N.B. Milestone, Chemical and mechanical stability of sodium sulfate activated slag after exposure to elevated temperature, Cement Concr. Res. 42 (2012) 333–343.

133. M. Rashad Alaa, An exploratory study on sodium sulphate-activated slag blended with Portland cement under the effect of thermal loads, J. Therm. Anal. Calorim. 119 (2015) 1535–1545.

134. T.W. Cheng, J.P. Chiu, Fire-resistant geopolymer produced by granulated blast furnace slag, Miner. Eng. 16 (2003) 205–210.

ACKNOWLEDGEMENTS

The Project DEFEAT (INTEGRATED/0918/0052) has been co-funded by the European Regional Development Fund (ERDF) and the Cyprus Government, through the RESTART 2016-20 framework program of the Cyprus Research & Innovation.Foundation.

ANNEX: REPORT OF THE KATHOLIEKE UNIVERSITEIT LEUVEN (KUL) ON FIRE RESISTANCE DESIGN OF CDW BASED GEOPOLYMER

The Katholieke Universiteit Leuven (KUL) is the Foreign Organisation of the DEFEAT consortium, with great expertise on the development of fire resistant geopolymeric materials. KUL conducted a parallel experimental program to the Cyprus consortium, aiming to provide additional necessary information and/or to validate and confirm experimental results. Part of the work conducted by KUL (i.e. the part relevant to Deliverable D5.1) by the time of submission of the project's interim report is summarized below. The work by KUL will be extended in several other aspects of the DEFEAT project.

Development of an Innovative Insulation Fire Resistant Façade from the Construction and Demolition Waste

DEFEAT

INTEGRATED/0918/0052

Report of The Katholieke Universiteit Leuven (KUL)
on Fire Resistance Design of CDW Based Geopolymer

Dr. L. Kriskova

Prof. Y. Pontikes

1 Introduction and objective

The aim of this work was to characterize the as-received construction and demolition wastes (i.e. tiles and bricks) and to investigate their potential for usage as an innovative insulation and/or fire-resistant façade materials.

2 Materials and methods

Two types of construction and demolition waste (CDW), i.e. tiles and bricks were obtained. Both materials were crushed using a hammer and milled using a Fritsch Pulverisette 13-disc mill. Afterwards, the slags were milled using an attritor ball mill (Wiener 1S) for 6h. The resulting powders were characterized with respect to their density by means of using a Quantachrome Multipycnometer. The air permeability specific surface area of the powders was measured using the Blaine method according to EN 196-6. Chemical compositions of the materials were determined by WD-XRF (PW 2400, Philips). Mineralogy was determined by X-ray powder diffraction analysis (XRPD, Bruker D2 Phaser). Diffraction patterns were measured in 2θ range of $5°$-$70°$ using CuK_α radiation at 30 kV and 10 mA. The diffractometer was operated with a step increment of $0.02°$ 2θ and step time of 0.6 s. An anti-scatter slit (1 mm) was used. FTIR was performed on powder samples using the ATR-FTIR alpha Bruker setup.

The reactivity of the materials was determined by means of a dissolution test and isothermal calorimetry. The dissolution of Si and Al was in focus, while other elements, such as S, Ca, Fe and Ti were also followed. For the purpose of dissolution test, the powders were mixed with a 4M and 10M NaOH or KOH solution, respectively, in a ratio of 50 g solution to 0.2 g of powder, followed by shaking with 186 r/min for 1 and 24 h in 50 ml polypropylene bottles at 25 ± 0.5 °C. After designated time the suspensions were filtered using a 0.45 µm filter and diluted with a solution of 3% HNO_3 for up to 50 times. The dissolved elements were measured using ICP-OES (720 E, Varian).

The reaction kinetics was determined using the isothermal calorimetry (TAM Air) on pastes samples. For this purpose, the milled powders, i.e. bricks and tiles, were mixed with water or

activating solution by keeping the solid to solution mass ratio 0.5. As alkali activating solution, the potassium silicate solution with the SiO_2/K_2O molar ratio of 1.6 and water content of 65 wt.% was used (1.6KS65). The pastes were homogenized for 2 minutes by hand mixing and placed in calorimeter. The signal recording started 40 minutes after mixing was initialized.

Paste samples were also prepared to follow up the mechanical properties development and to follow up the reactions. For this purpose, 2 types of samples, blended cement and alkali activated pastes, were prepared. The blended cements were synthetized by blending 70 wt.% of CEM II 32.5 and 30 wt.% of CDW (tiles or bricks) and mixing the powders with water, keeping the powder to water mass ratio 0.5. Alkali activated materials were synthetized in the same way as samples for isothermal calorimetry. All paste samples were homogenized for 2 minutes using a hand mixer, casted in (2x2x2) cm^3 molds, wrapped in plastic foil and cured at RT (21 +/-1 °C). All samples, accept for alkali activated tiles, which did not set in 24h, were demoulded after one day and split in 2 groups, whereas one group was further cured at room temperature (RT samples) in a close plastic box and the other group was placed in autoclave and hydrothermally treated in saturated water vapor at 200 °C for 24h (HT samples) prior storing them in close plastic containers.

After designated time (7 and 28 days) the samples were tested for compressive strength by means of Instron 5985 Tensile test machine. From each sample type one crushed cube was placed in a plastic container with 100 ml isopropanol to stop the reaction. Dried samples were then used for analyses, e.g. XRPD, FTIR and SEM. The SEM pictures obtained on broken surfaces of dried Au-plated samples using a XL30 FEG microscope.

The fire-resistance potential of the paste samples was investigated by heating up the samples to 1100 °C for with the heating rate of 5 °C/min and letting them at the high temperature for 2 hours after which the samples were cooled to RT in the oven (cooling rate 5-10 °C/min). The resulted materials were subjected to same investigation as listed above.

Porous alkali activated samples were synthetized from both wastes' materials using the mechanical and chemical foaming methods. The later was done by means of fine Al powder, while the former was achieved by means of dry foam.

3 Results

3.1 Materials characterization

The as-received materials were subjected to same milling procedure, which resulted in fine powders with Blaine surface area of ~6500 cm^2/g and ~5500 cm^2/g for bricks and tiles, respectively. The density of the tile powder was 2.49 g/cm^3 and the density of brick powder equaled to 2.82 g/cm^3. Chemical compositions of powders are listed in Table 1.

Table 1: Chemical composition of the as-received tiles and bricks.

Chemical Formula	Bricks Wt (%)	Tiles Wt (%)
SiO$_2$	40.9	56.2
CaO	13.2	4.4
Al$_2$O$_3$	12.1	15.1
Fe$_2$O$_3$	9.9	1.0
MgO	5.4	0.5
Na$_2$O	2.1	2.3
K$_2$O	0.9	3.1
TiO$_2$	0.7	0.5
SO$_3$	0.7	-
MnO	0.1	-
P$_2$O$_5$	0.1	0.2
ZrO$_2$	-	0.2
ZnO	-	0.1
Sum	86.0	83.7

Regarding the mineralogy, Table 2, both materials are highly crystalline, mainly consisting of feldspar phases and quartz. These phases are considered to be of limited or no hydraulic activity without activation.

Table 2: Mineralogical composition of the as-received tiles and bricks wastes.

Mineral	Chemical Formula	Bricks Wt (%)	Tiles Wt (%)
Quartz	SiO_2	14	58
Hematite	Fe_2O_3	< 1	-
Albite	$Na(AlSi_3O_8)$	4	6
Orthoclase	$K(AlSi_3O_8)$	3	10
Anorthite	$Ca(Al_2Si_2O_8)$	39	-
Diopside	$Ca(Al_2Si_2O_8)$	13	-
Andesine	$(Na.Ca)[Al(Si.Al)Si_2O_8]$	19	-
Muscovite	$KAl_2(AlSi_3O_{10})(OH)_2$	7	-
Mullite	$Al_{4+2x}Si_{2-2x}O_{10-x}$	-	25

3.2 Reactivity

Dissolution of the two powders, tiles and bricks, presented a similar trend, Fig. 1. They dissolved significantly more of both Si and Al as the experiment lasted longer and as the molarity of the solution increased. Regarding the solution molarity, this showed to affect equally the initial dissolution as well as the dissolution after 24 hours for Al, while for Si, the initial dissolution seemed not to be affected significantly, if at all. Overall, the dissolution was being developed between the first 24 hours of reaction as the amount of Al increased about 3 times for bricks- and about 4 times for tiles- samples, while higher increase were always observed for NaOH based solutions. Regarding Si amounts, here, the relationships seemed to be more complex, as the type of alkali ion played a significant role. While in both powders, at least some Si was determined after 1h, when activated with KOH solutions, no or only very limited amount of Si was dissolved after 1h, when NaOH based solutions were used, regardless its molarity. Interestingly, higher Si values were determined after 24h in NaOH solutions. Overall, the dissolution of SI and Al initiated faster in KOH solutions but after 24h was more pronounced in NaOH solutions.

Rather different behavior was observed in case of Sulphur, where rather high amounts were determined already after 1h reaction. The S amounts varied between 78 and 230 ppm/g of powder for tiles, depending on type and molarity of the solution. In case of bricks samples, the S content stayed relatively constant ~170 ppm/g of powder. In both materials, it was observed that when 10M NaOH solution was used, the amount of S decreased over time, which could indicate a precipitation of some S-containing phases. The decreasing amount of S over time was observed in bricks sample also for the 10M KOH solution.
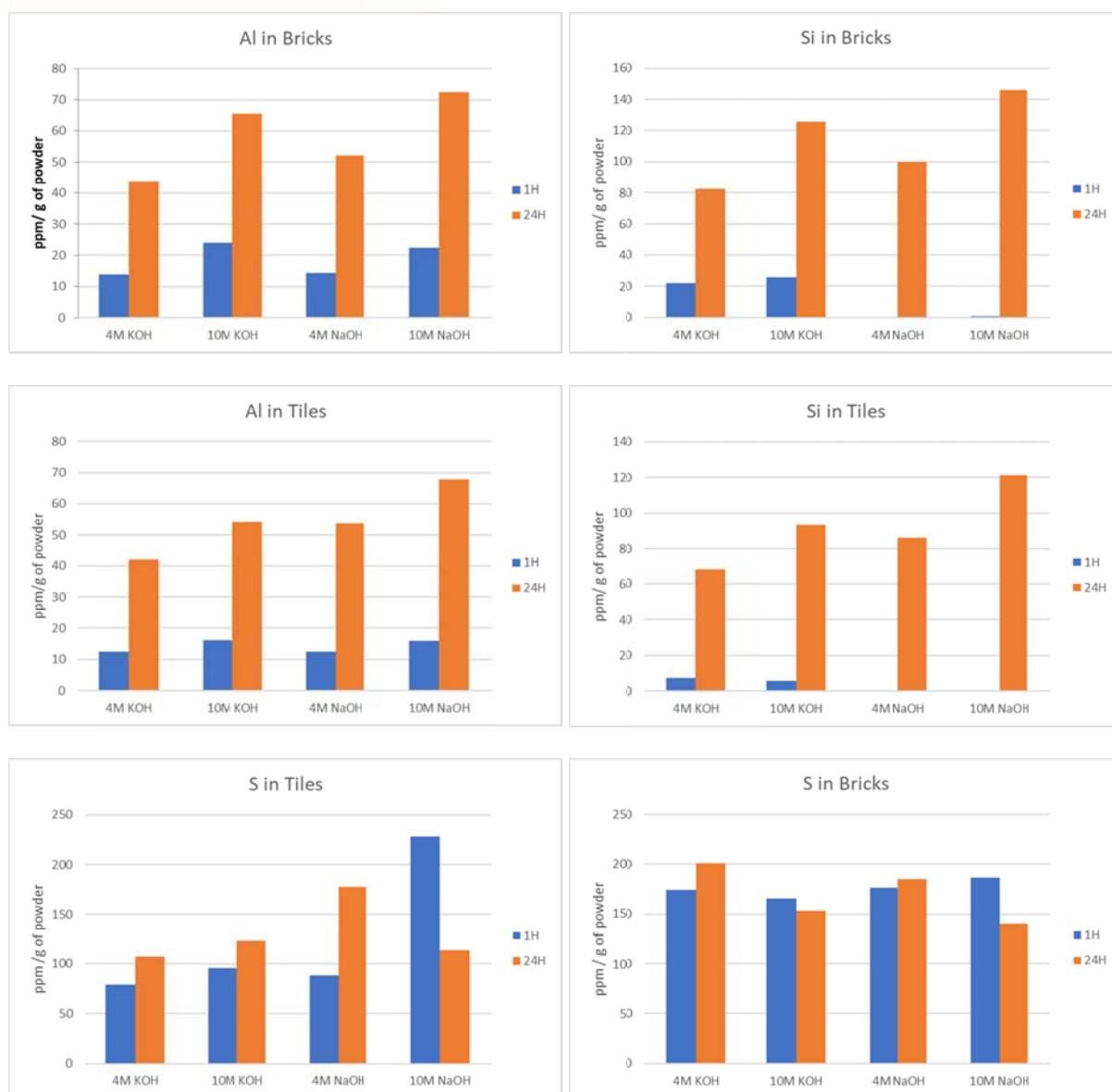
Figure 1: Dissolution of Al, Si and S from tiles and bricks in NaOH and KOH based solutions.

Isothermal calorimetry curves, Fig. 2, show low heat release of tiles and bricks powder when mixed with both water (top) and alkali solution (bottom). Regarding the water samples, here a small hump is observed between 5-30 hours for tiles sample, no hump is observed in bricks sample during the whole period. Nevertheless, in both samples a small amount of heat is

generated over the time, however this is very low and the overall heat release does only reach 5 J/g and 1 J/g after 90 hours of reaction for tiles and bricks, respectively.

Samples activated with 1.6KS65 activating solution showed a peak within the first 20 hours. The heat release gradually decreases up to 60 – 80 h of reaction. The cumulative heat release curves, demonstrate that the heat release is more pronounced in the bricks sample, however after 110 h it seems to be equal for both materials and extrapolating the results beyond the measured period indicates that the tiles remain releasing more heat. Assuming that the heat release is associated to the binder formation reaction the above points to the fact that although the bricks are reacting faster, the overall activation potential of tiles seems to be higher.
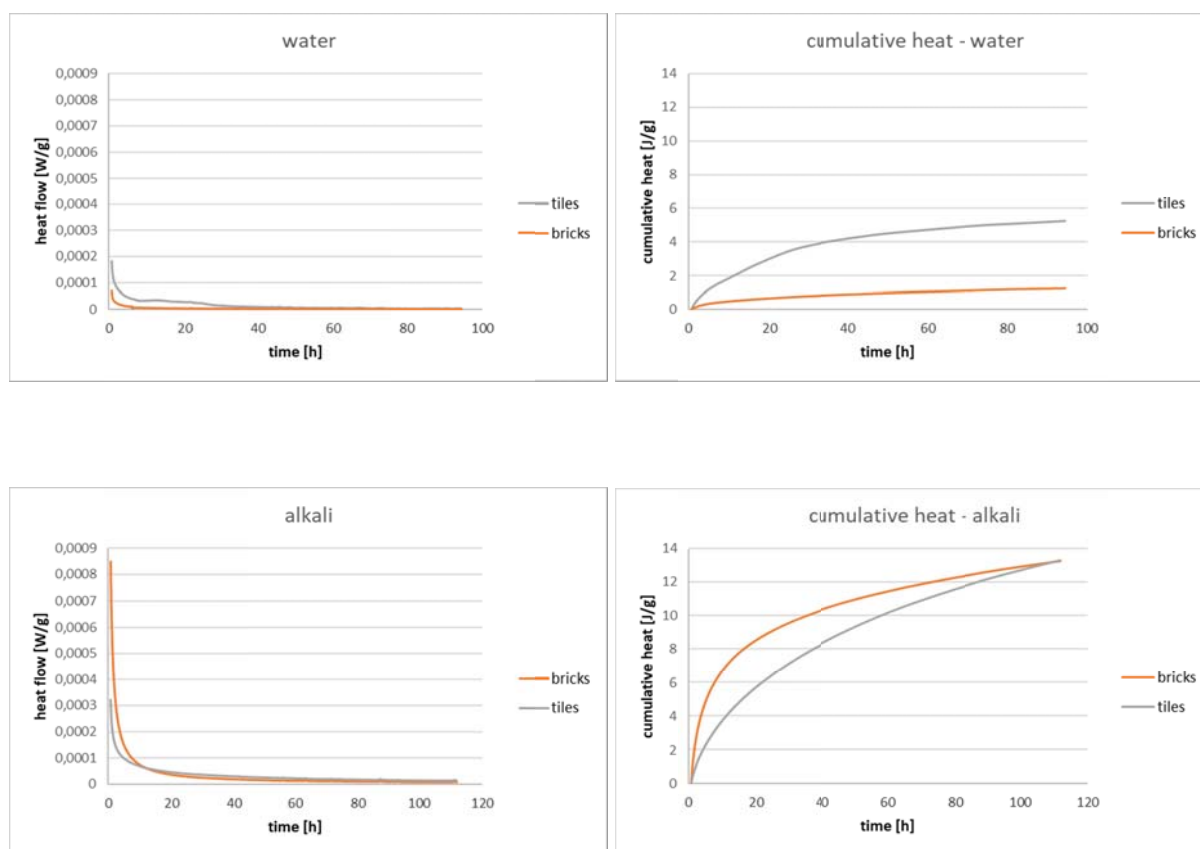
Figure 2: Isothermal calorimetry curves for material mixed with water (top) and with alkali solution (bottom).

3.3 Binder properties

Microstructure

Despite the relatively low heat release the, both materials showed a developed gel structure, resembling the inorganic polymer gel, already after 7 days of reaction. The tile IP is presented in Fig. 3, was rather porous with unreacted grains present in the structure. A significant cracking appears along the unreacted grains. The detail view however suggests that the gel in between the particles is well developed and covered with shapeless plate like clusters.
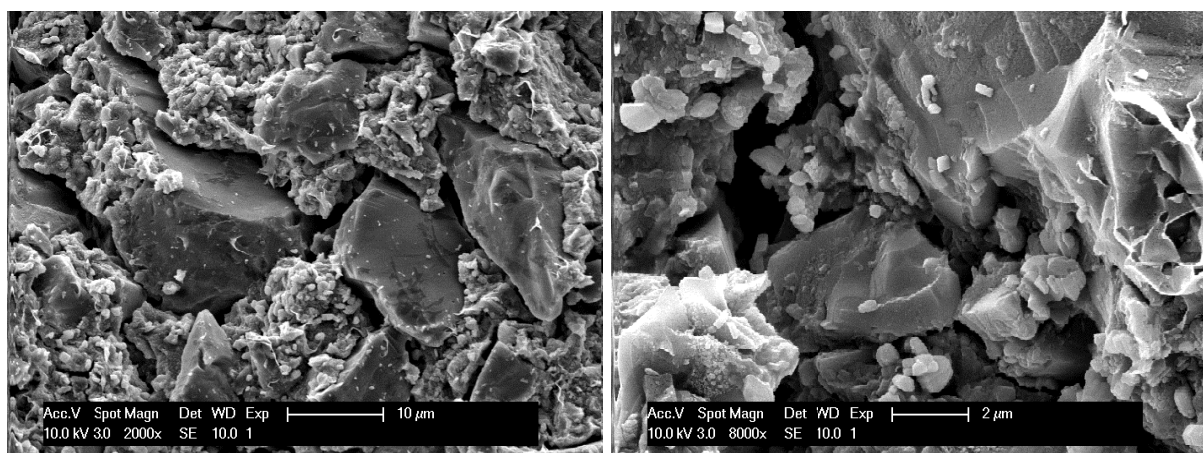

Figure 3: Structure of the alkali activated tiles after 7 days. Overall view in left, detail view on gel in right photo.

The brick IP gel, Fig. 4, seemed to be rather dense with few cracks. The detail view revealed formation of rectangular crystal-like clusters. Very dense IP gel without cracks can also be seen in sample subjected to hydrothermal curing. Here, the above-mentioned clusters are even more pronounced and their structure seems to be very well defined. Any obvious unreacted particles were observed in any of the IP brick samples.
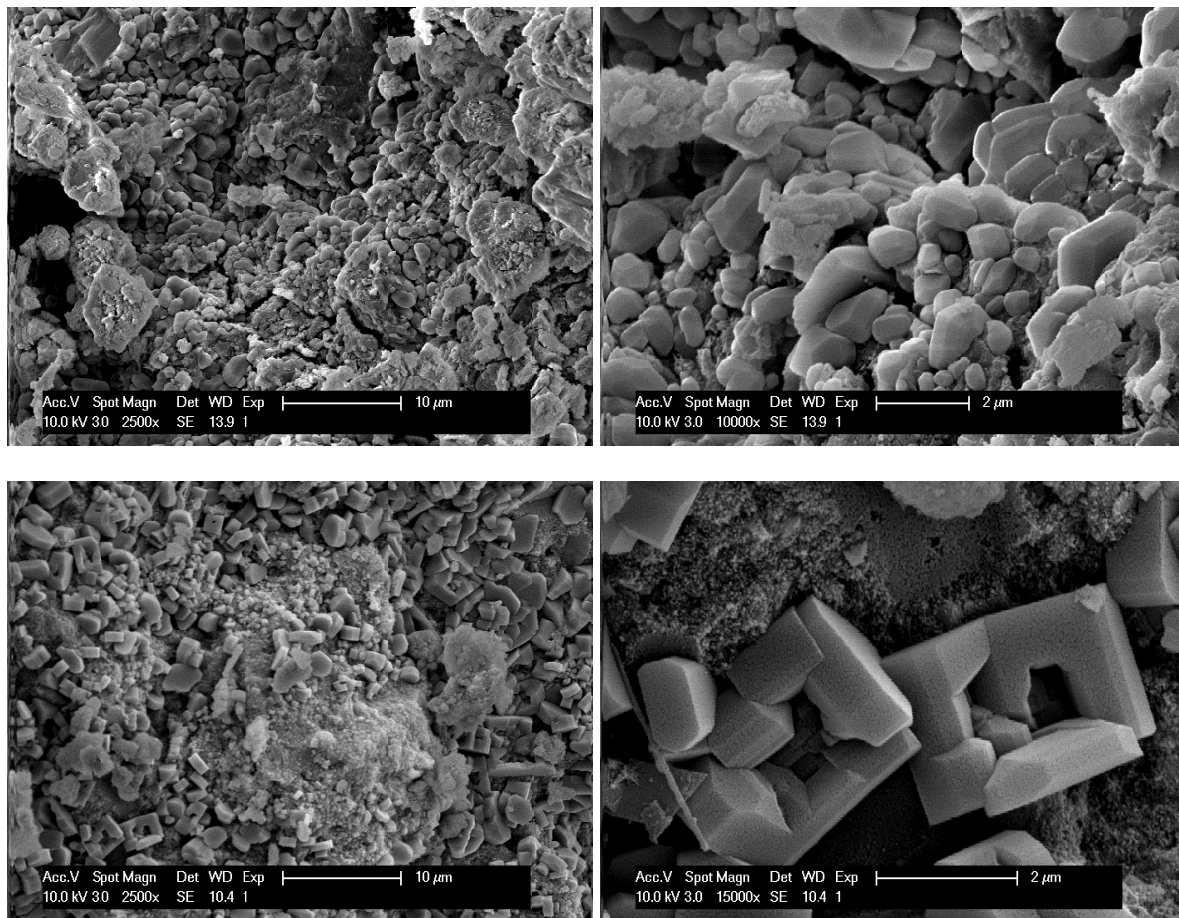
Figure 4: Structure of the alkali activated bricks. Top: IP after 7 day reaction, bottom: hydrothermally cured IP. Overall view in left, detail view on gel in right photo.

The microstructure of the blended cements was very similar, thus only SEM for blended cement with tiles will be showed. On Fig. 5 below, the structure of a typical cement binder is formed. Needle – like C-S-H gel is well formed and detail view also reveals formation of long needles, resembling ettringite and plate like hexagonal crystals, resembling portlandite, which are the 2 common structure formed in OPC based binders. Yet, the formed binder is rather porous, which could be related to the slower reaction rate of the used CEM II and/or the 30% replacement with slowly or not reactive CDW.
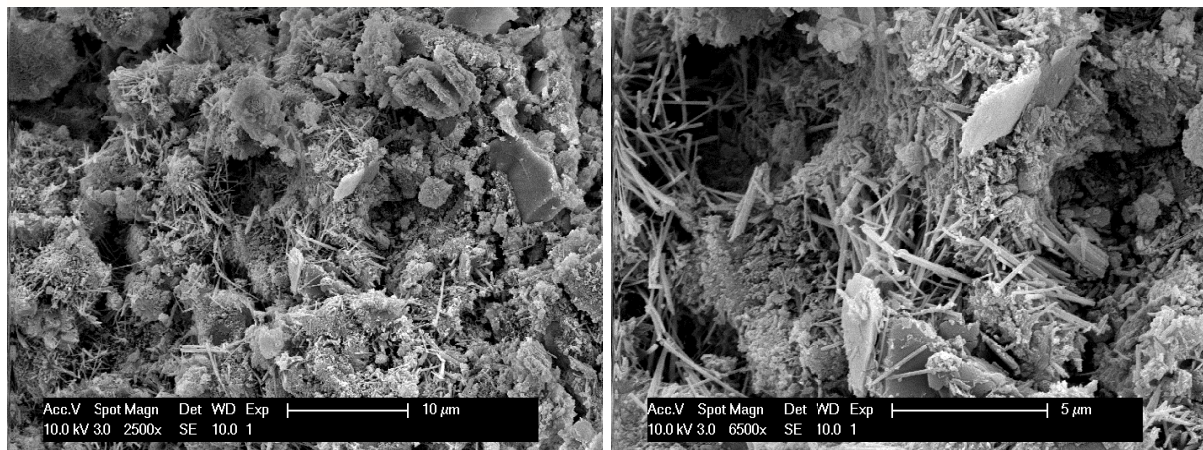
Figure 5: Structure of the blended cement synthetized from tiles. Overall view in left, detail view on gel in right photo.

XRD

To better understand the reaction mechanism of the IP samples XRD analyses was performed and spectra were compared with the ones of the as-received materials. The graphs below, Fig. 6 top, shows the comparison of the tiles- powder and the IP synthetized from it. Two phenomena can be seen: a) a formation of an amorphous hump between 20° and 40° 2θ and occurrence of new peaks, which resembles position of C-A-S-H and/or N-A-S-H. Both phenomena were also visible in binder made from bricks. Additionally, hydrothermal curing (HT) resulted in dissolution of quartz, which most probably participated in the formation of the IP gel. No zeolitic structure was identified in the HT cured sample. The above supports the findings of SEM, that the alkali activation lead to an inorganic gel formation in both received materials.
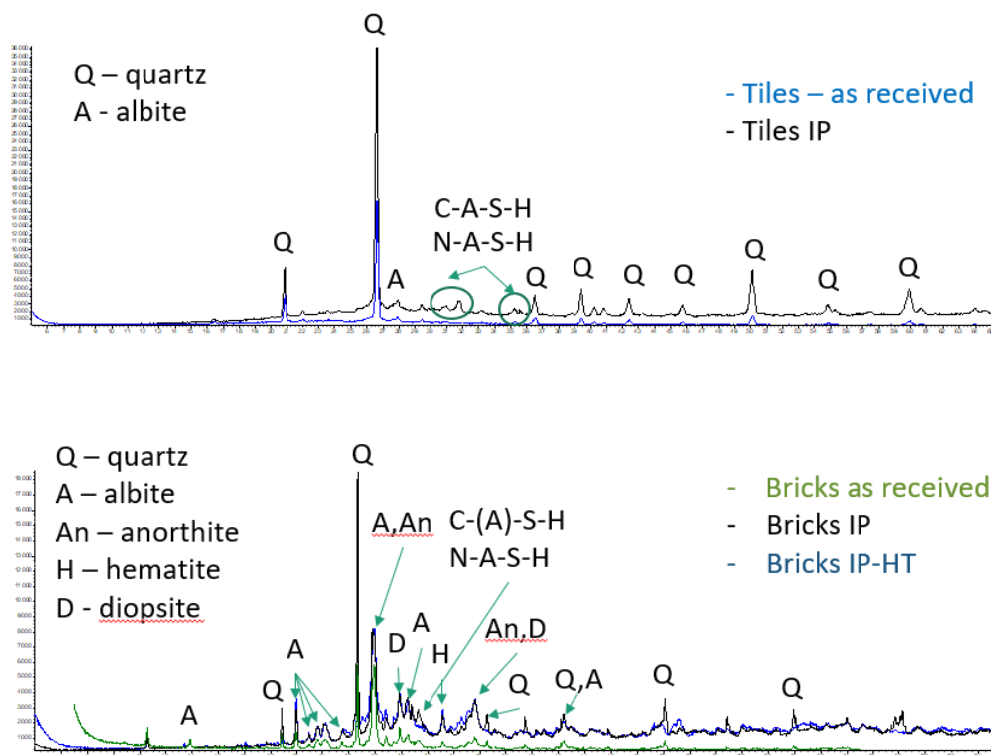
Figure 6: XRD patterns of: (top) as received tiles powder and alkali activated binder and (bottom) as received brick powder, alkali activated binder cured at RT and HT.

FTIR

Four groups of absorption bands are visible in FTIR spectra, Fig. 7. A band between ± 800 and 1200 cm^{-1} resembling the Si-O stretching bands, a band at ±400-500 cm^{-1} resembling the Si-O and rocking bands, an in-plane bending band at ±700-800 cm^{-1}. Eventually, the band assigned to the presence of carbonates appearing at ±1500 cm^{-1}. The main changes are happening in the ± 800 and 1200 cm^{-1} region, thus this band will be discussed here. Regarding tiles, this band is rather broad with some local peaks at about 850, 1050, 1100 and 1170 cm^{-1}, which can be assigned to Si-O in different crystalline phases present in the structure. Even more complex band is visible for brick sample, where the local peak scan be identified at 870, 960, 1050, 1100 and 1170 cm^{-1}. This in agreement with the XRD results, that indicated more complex mineralogical composition of bricks.

After mixing with alkalis, the local maxima's became less pronounce and/ or disappeared indicating their participation in the reaction. A slight wavenumber shift of the Si-O stretching band to lower wavenumbers is visible. This phenomenon could be related to the dissolution and polymerization reaction of formed inorganic polymers. The phenomena is more pronounced in tile sample, where the peak shifted from about 1050 down to about 960 cm^{-1}. In brick sample, the actual peak maxima remained at the same position, i.e. 960 cm-1, however shifts towards lower wavenumbers are visible on the local peak at 1050, which is moved to about 1000 cm^{-1}. Additionally, a clear hump at 870 cm^{-1} is being formed. All above mentioned changes are visible and even more pronounced in the brick sample subjected to hydrothermal (HT) curing. The above is in good agreement with XRD and SEM finding, that support the formation of inorganic polymer gel.
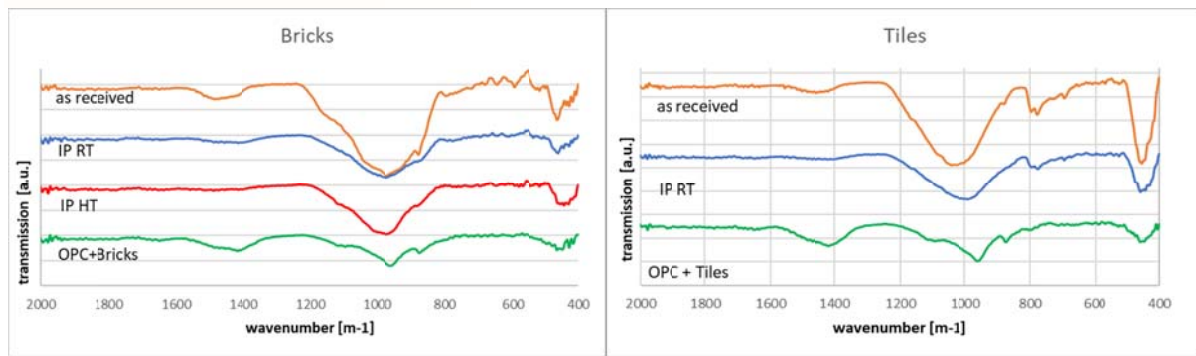
Figure 7: FTIR spectra of original bricks and tiles powder and of the synthetized IP and blended cement binders after 7d of reaction.

The spectra of the two blended cements are almost identical. This is due to the majority of the material (70 wt%) in both blends in the same type of OPC. The main peaks are located at 875, 950 and 1100 cm^{-1}, which can be assigned to C-S-H gel, C_2S phase and portlandite, respectively.

Compressive Strength

Compressive strength was measured after 7 and 28 days of reaction on both blended cement as IP samples, Fig. 7. No obvious strength difference was observed between brick and tile-based IP after 7 days, however, at later state, tile-based IP performed significantly better, but still only reached about 19 MPa. Hydrothermal curing significantly affected the compressive strength as this increased from about 9 MPa reached at 28 days in brick sample up to 45 MPa. Regarding the blended cements, addition of any of the 2 investigated material to OPC resulted in drop of strength. The used CEM II 32.5 cement should reach > 32 MPa in 28 days, which was not the case for any of the two materials, when RT curing was applied. Hydrothermal curing resulted in increase of the 7 days strength for both bricks and tiles and late strength for tile containing blends. Interestingly, HT curing resulted in drop of strength for brick containing blend. This cause of the strength drop is unclear and needs to be further investigated.
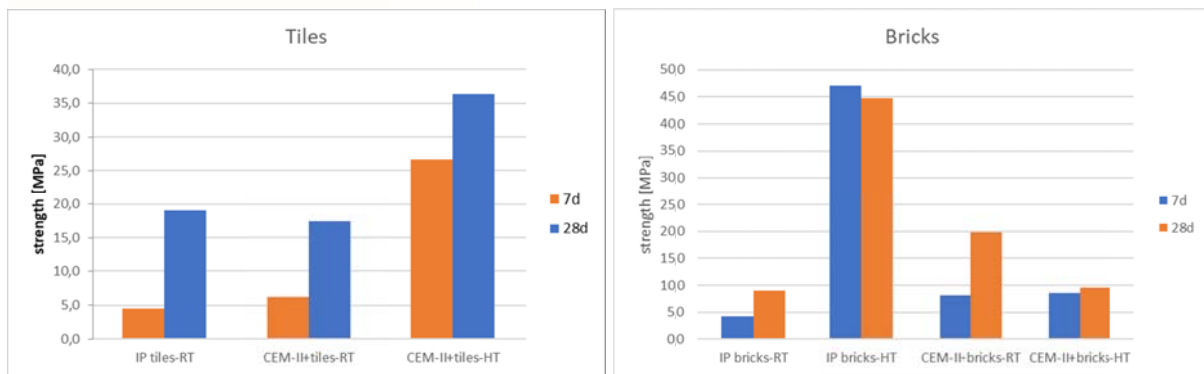
Figure 8: Compressive strength of binders cure at RT and HT.

3.4 Fire resistance

As one of the project goals is to develop a façade material that shows fire resistance, the behavior of binders expose to high temperature was investigated. Both, blended cements as well as IP binders were heated up to 1100 °C and as showed below, the samples remained visually stable after the 2-hour long exposure, Fig. 9.

Figure 9: Binder samples after 2 h exposure to 1100 °C. From left: IP tiles, IP bricks, blended cements tiles, blended cement bricks.

SEM

Microstructural analyses revealed severe changes in the microstructures of all binders. Regarding the IP binders, here a massive formation of pores was observed. While the structure of the fired tile-based IP (Fig. 10 top) resembles the Emmental cheese with many pores in the range of 10 -30 microns, the porosity in the brick-based IP (Fig. 10 bottom) was less obvious. In both IP samples the gel underwent obvious changes and partial melting and/or sintering probably occurred during the exposure to the high temperature.
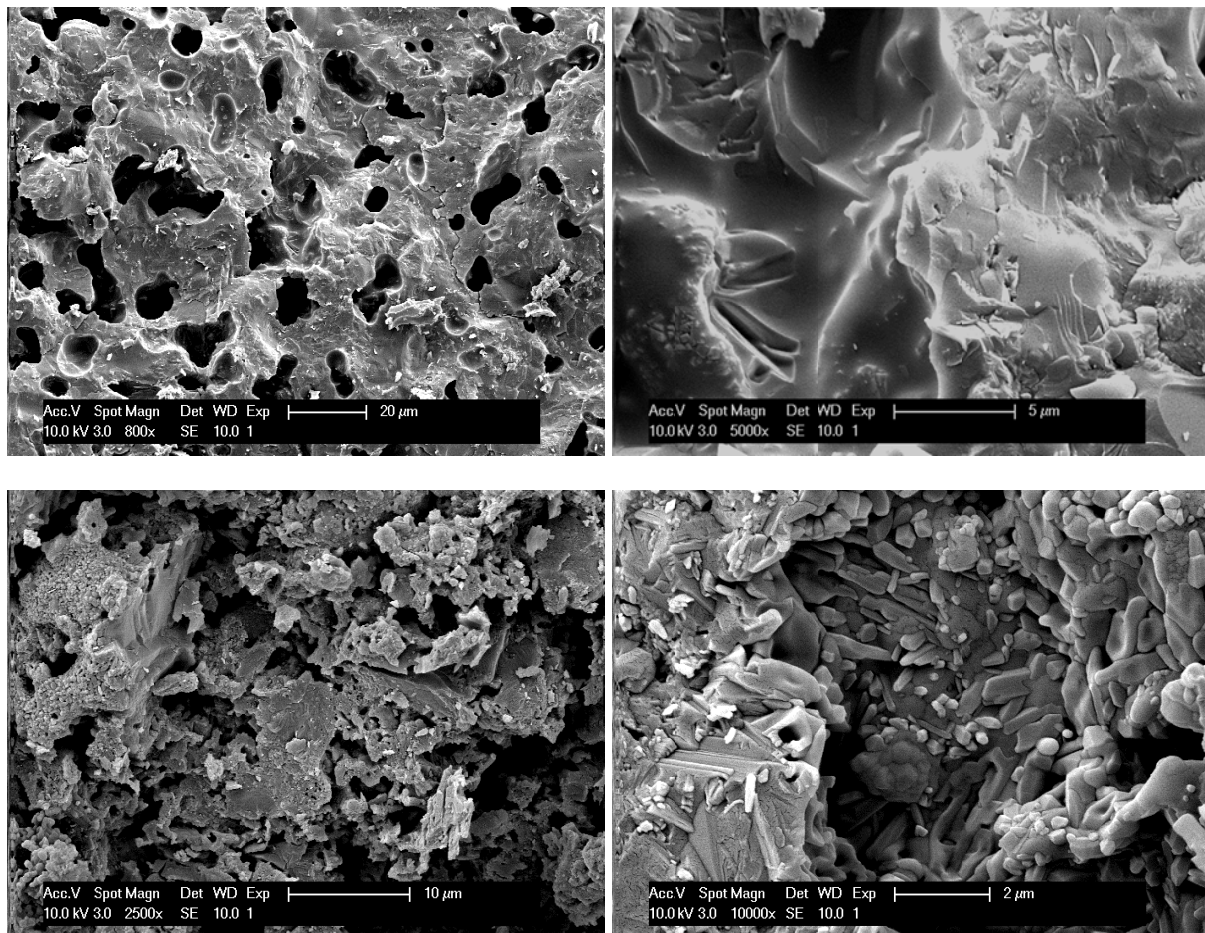
Figure 10: Microstructure of the fired IP binders. Top) tile-based IP, bottom) brick-based binder.

Microstructure of the fired blended cements was very similar and thus only tile containing blended cement will be discussed, Fig. 11. The cement-based binder after firing appeared

very rather destroyed. The originally present fiber crystals changed to small globules and/ or appeared very dried out. Some hexagonal plate crystals, most probably of portlandite, were still present however the plate structure was very porous and was formed of small nano-crystalline clusters. At several places previously, molten structures were visible. The overall porosity of the blended cements was rather high and the original gel appear to be without structural integrity and / or rigidity.
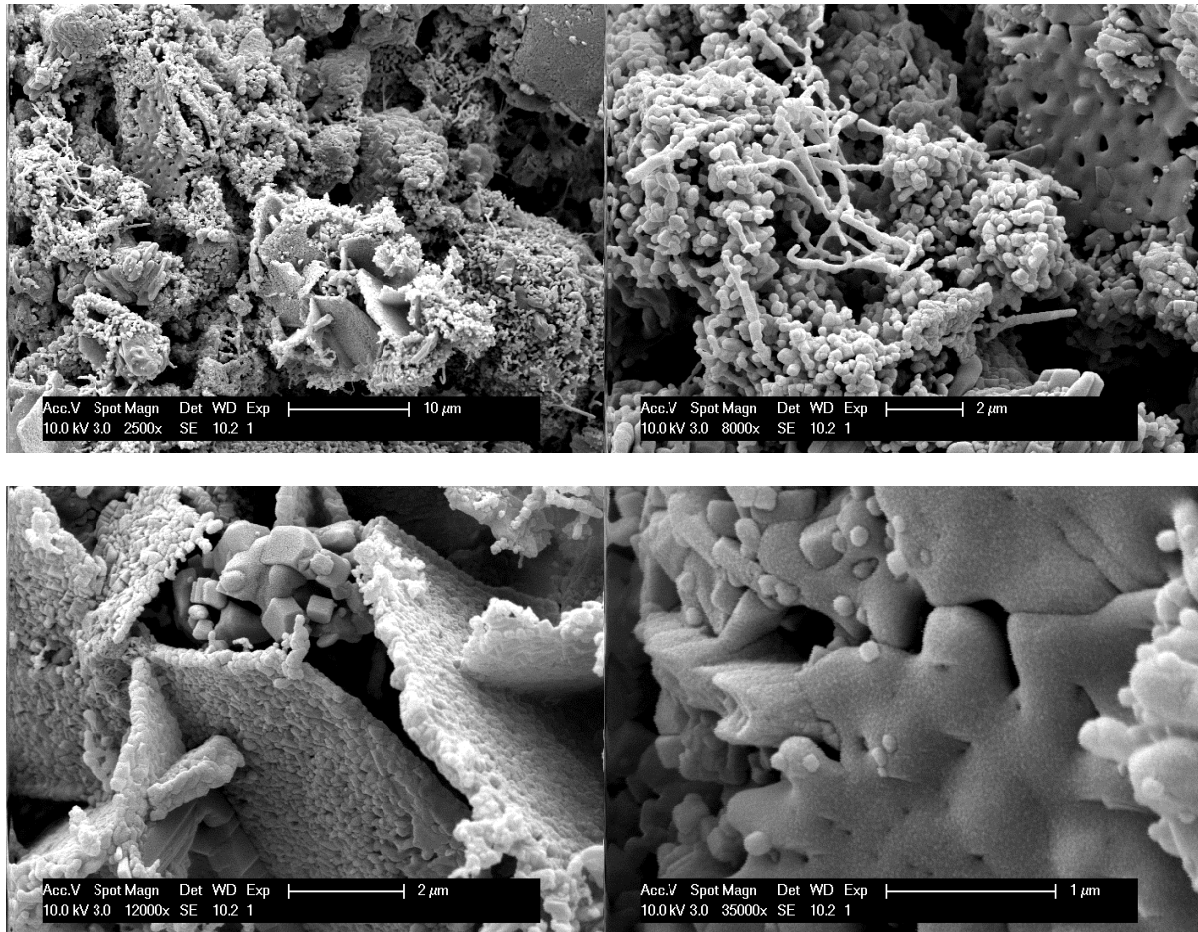

Figure 11: Microstructure of the fired blended cement containing tile powder.

The above is also reflected in the mechanical properties determined after firing, Fig. 12. The compressive strength of both fired IP increased dramatically and reached almost 70 MPa for tile based inorganic polymer. The IP made from brick reached after firing > 30 MPa. Only

very low strength (~2 MPa) was determined in both blended cement samples. This is in good agreement with the observation of the structure destruction.
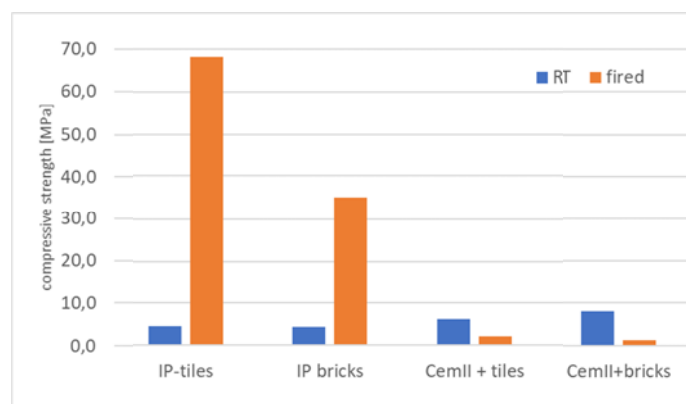

Figure 12: Compressive strength of binders before and after firing.

FTIR

The FTIR spectra listed below, Fig. 13, demonstrated that the firing had a significant effect on all binders. In blended cements the firing resulted in the shift of the main peak maxima from 960 cm^{-1} down to 890 cm^{-1}, and appearance of sharp peaks at about 500 cm-1, indicating the re-formation of the original cement phases, e.g. β-C2S.

Regarding the IP samples, here the effect firing differed per sample. For Tiles IP, firing resulted in slight shift of the main peak maxima from 960 up to 1000 cm^{-1}, and appearance of and hump at about 900 cm^{-1} and a new peak at about 700 cm^{-1}. The latest could be assigned to Si-O-Si or Si-O-Al bending vibration. Even more complex changes were observed in fired IP sample made from bricks. Here the peak maxima did not shift, but became very pronounces, which sharp peak tip, which indicated crystallization of phase(s). Similar to tiles IP sample, the hump at 870 cm-1 became more visible and a new peak appeared at about 700 cm^{-1}. All the above indicate significant changes in the materials structure possibly due to melting and sintering of the IP materials during the high temperature exposure. The formation of new phases needs to be confirmed by an XRD analyses.
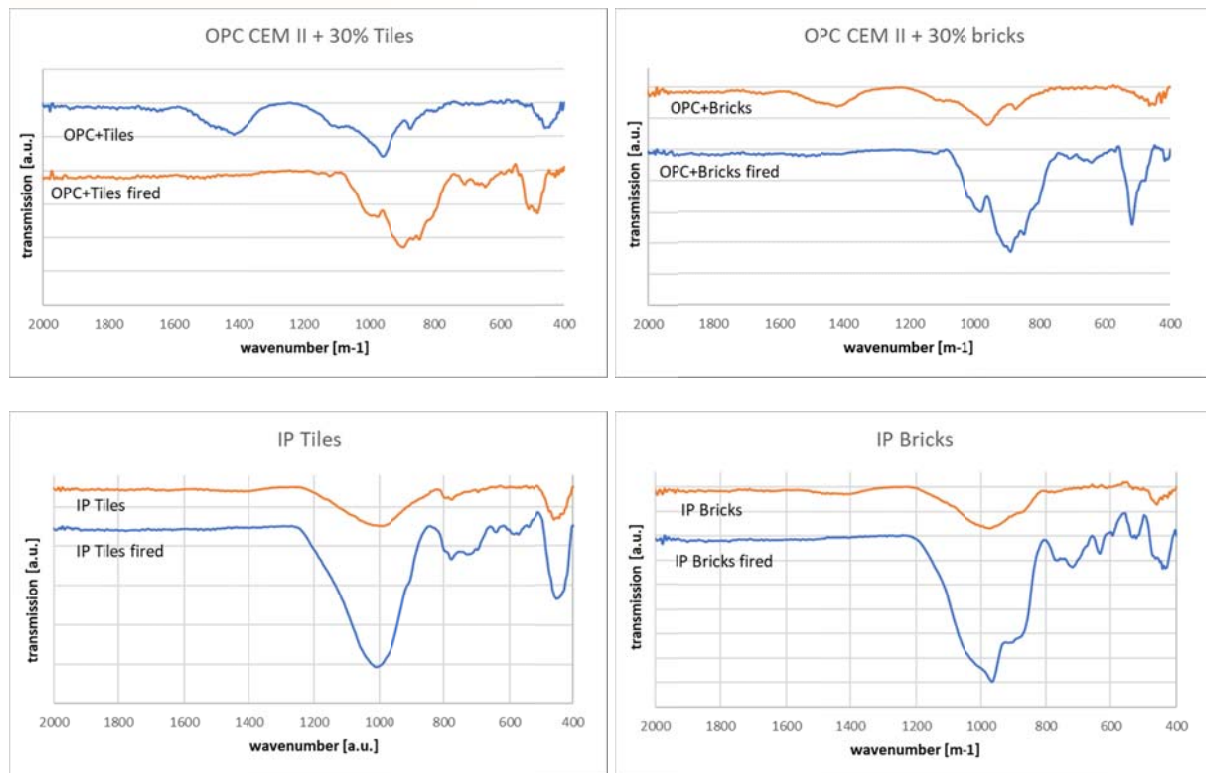
Figure 13: FTIR spectra of the original and fired binders. Top) blended cements; bottom) IP binders.

3.5 Porous materials

Mechanical and chemical foaming was applied to inorganic polymer binders from tiles and bricks in order to produced lightweight material. Synthesis of porous binders can be challenging and each foaming method has its advantages and disadvantages. In general, foaming is a complex process in which foam stability and binder setting time need to be properly aligned. Too fast setting of the binder can result in hardening of the material before the foaming has been finished. On the other hand, too slow setting would result in collapsing of the foamed material. Additionally, the liquid to solid ratio needs to be adjusted in order to increase/ fully use the foaming capacity of the binder. Too solid material would most probably harden before it would foam, while too liquid material would result in bubble coagulation and in homogenous foam formation. With respect to the above, the mix design has to be carefully adjusted for each material type, fineness, etc.

In order to understand which foaming method would deliver most suitable results both mechanical and chemical foaming was applied. The produced IP foamed were cured at 40 °C prior testing. The mechanical and physical properties of the produced foams are listed in Table 3, below.

Table 3: Mechanical and physical properties of synthetized IP foams. M= mechanically foamed; C=chemically foamed.

	Density (kg/m^3)	Compressive strength (MPa)	Flexural strength (MPa)
Porous IP-bricks-M	1243	7.1 +/- 1.1	5.4 +/-0.9
Porous IP-bricks-C	1315	7.4 +/- 1.1	2.6 +/- 1
Porous IP-tiles-M	919	1.3 +/- 0.01	-
Porous IP-tiles-C	624	1.0 +/- 0.3	0.9 +/- 0.3

Microstructure of the produced IP foams can be seen below, Fig. 14 and Fig. 15. Overall, it can be seen a homogeneous porosity and pore size distribution in all samples, but chemically foamed tiles. In all samples also small cracks are present, probably cause by drying shrinkage. However, the produced samples shown potential of using both materials in synthesis of porous IP based materials and the obtained properties could even be increase with some process optimization.
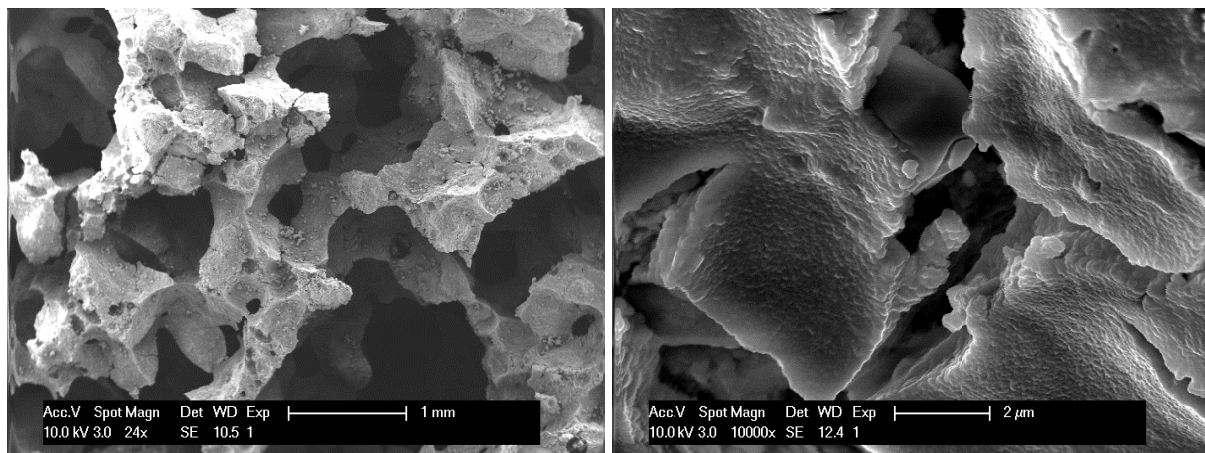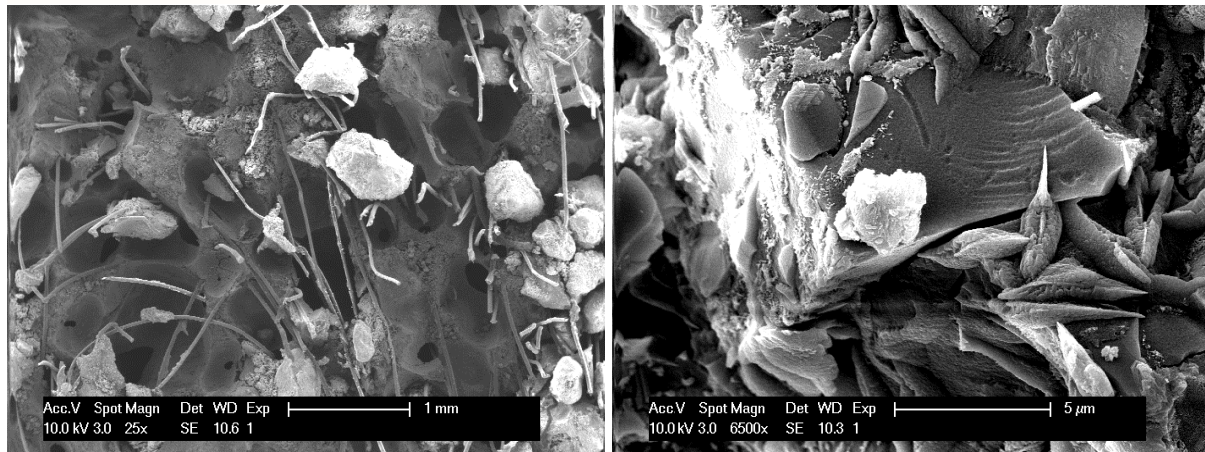
Figure 14: Microstructure of the porous IP binders from tiles. Top) chemically foamed, bottom) mechanically foamed.
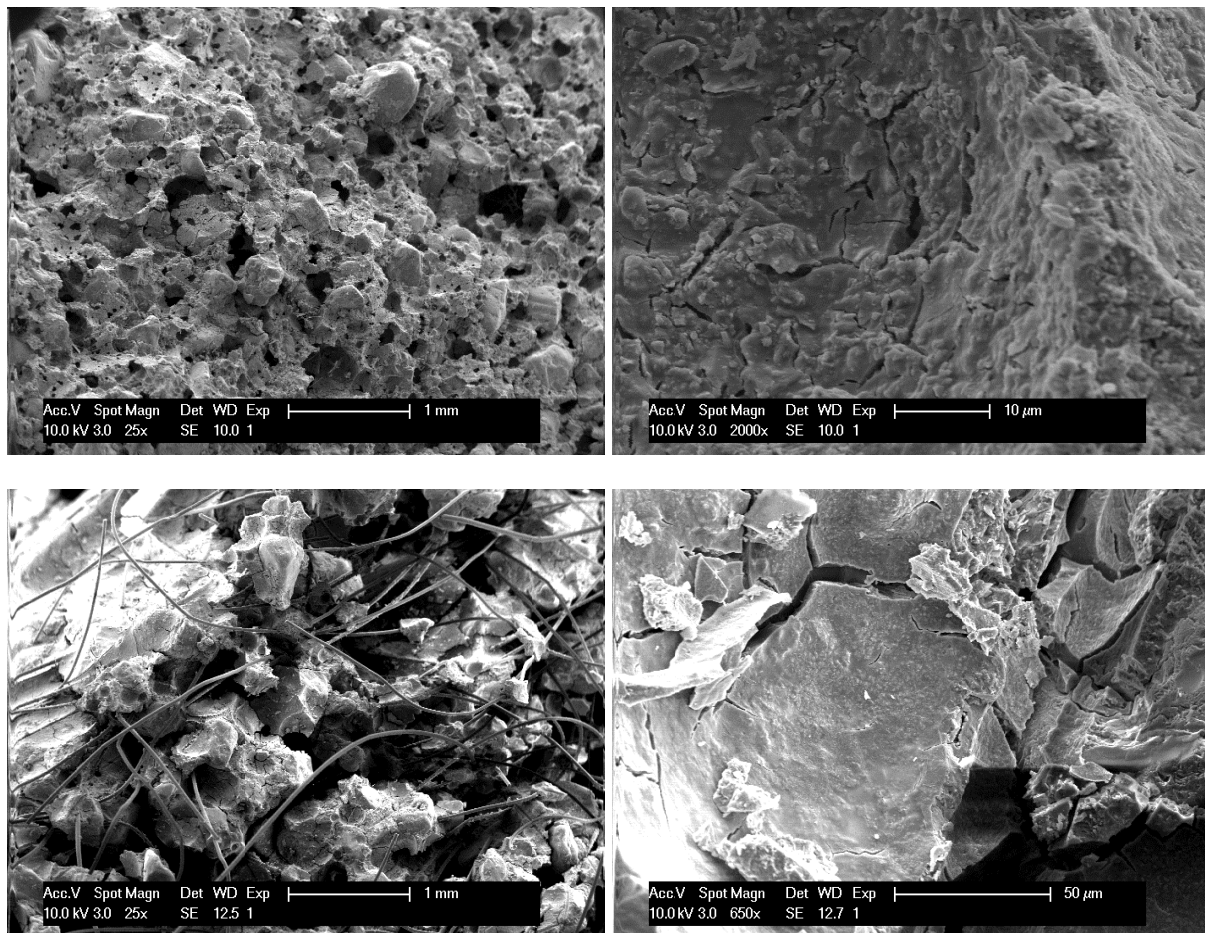

Figure 15: Microstructure of the porous IP binders from bricks. Top) chemically foamed, bottom) mechanically foamed.

4 Conclusions

Two types of CDW, bricks and tiles, were investigated for their potential to be used as unique lightweight fire-resistant building material. For this purpose blended cement and alkali activated binder were synthetized from both materials and further analyzed for their mechanical, physical properties and fire resistance. Porous IP based blocks were also made to proof de concept that these materials, could be used in production of lightweight materials.

The results demonstrated that addition of both CDWs has negative effect on mechanical properties of blended cement, only reaching up to 20 MPa after 28 days (unless hydrothermally cured). Additionally, firing at 1100 °C resulted in destruction of the binder and complete loss of mechanical properties. For this purpose, the further focus was on IP binders. Despite the relative low reactivity demonstrated by isothermal calorimetry, both precursors were able to for IP when mixed with alkalis. Mechanical strength after HT curing reached almost 45 MPa. Firing at 1100 °C gave rise to in some structural changes and possible remelting and/or sintering of phases. Additionally, it resulted in further strength increase up to 68 MPa. Porous IP were synthetized by means of mechanical and chemical foaming and acceptable result of density and compressive strength were achieved. The future research will be focused on further optimization of mix design to achieve higher strength / density ratio of porous IP.

Acknowledgements